# THIN-FILM MOLECULARLY IMPRINTED POLYMERS FOR DETECTION SYSTEMS FOR POLYCYCLIC AROMATIC HYDROCARBONS IN WATER

by

© Stefana Nicoleta Egli

A Thesis submitted to the

School of Graduate Studies

in partial fulfillment of the requirements for the degree of

**Doctor of Philosophy**

**Department of Chemistry**

Memorial University of Newfoundland

**May 2014**

St. John's, Newfoundland

## ABSTRACT

Thin-film molecularly imprinted polymers (MIPs) are smart materials that selectively uptake specific compounds from complex matrices based on molecular recognition principles. These materials can be applied for monitoring of organic pollutants such as polycyclic aromatic hydrocarbons (PAHs) in water as an early indicator of oil spills. MIPs are sometimes prepared in presence of a template that resembles the analyte (not the actual analyte), also referred to as a pseudo-template, to avoid issues with template bleed and associated false-positive results. This thesis describes the first account of thin-film MIPs for light PAHs using toluene as a pseudo-template. The procedure is very simple, fast and uses low-tech equipment. Detection is carried out offline using gas chromatography-mass spectrometry and fluorescence. As the role of each component in the MIP is discussed and recognized, various compositions were tested for sensitivity and selectivity. Several types of MIPs using toluene and phenanthrene-$d_{10}$ as pseudo-templates, and toluene as a pseudo-template and solvent (porogen) have been further characterized and validated. The composition has been optimized for each MIP; this involved experimental design at earlier stages. The selectivity and sensitivity of the various PAHs are discussed in terms of binding interactions, and the different chemistries of the targeted PAHs. Most characterization and validation tests were carried out in pure water; though high selectivity and remarkable sensitivity were determined in complex wastewater and seawater matrices with no prior sample treatment. Calibration was shown to be possible in seawater matrices such that the MIPs could readily be used for accurate quantification measurements of PAHs.

The thin-film MIP format has the potential for easy integration into a microfluidic device for on-site on-line monitoring. Such a device would be easily used even by an in-experienced operator. In preliminary work to fabricate such a device, prototyping work was carried out and included patterning channels and reservoir features in polydimethylsiloxane (PDMS) using various soft lithography low-tech methods, and etching electrodes on indium tin oxide (ITO) coated glass slides to create electrode pads. This is necessary to induce current flow, which would ensure continuous sample exposure to the MIP surface, with separation by electrokinetic chromatography with spectroscopic detection or by mass spectrometry, e.g. electrospray ionization- or desorption electrospray ionization-mass spectrometry.

## ACKNOWLEDGEMENTS

I would like to express my gratitude to my supervisor, Dr. Christina S. Bottaro for guiding my first steps as an independent researcher. Her patience, enthusiasm and great knowledge were highly appreciated.

I thank the two supervisory committee members, Drs. C. Kozak and S. Pansare for reviewing a draft of my thesis.

Advice given by Dr. E. Merschrod has been of great help in understanding microfabrication processes and in acquiring these techniques.

Assistance provided by Ms. L. Windsor, Ms. J. Collins and Dr. B. Myron in using the C-CART instruments is appreciated.

The following companies and agencies are acknowledged for their financial assistance: Petroleum Research Newfoundland and Labrador (PRNL), Atlantic Innovation Fund (AIF), School of Graduate Studies-Memorial University (SGS-MUN), Natural Sciences and Engineering Research Council of Canada (NSERC), Ocean Industries Student Research Award, OISRA.

Finally, I wish to thank my son for unknowingly being so motivating and to the family I found here in St. John's that has provided me with moral support and encouragement.

## TABLE OF CONTENTS

## LIST OF TABLES

## LIST OF FIGURES

## LIST OF SYMBOLS, NOMENCLATURE OR ABBREVIATIONS

AA – acrylic acid

ACN – acetonitrile

AIBN – azobisisobutyronitrile

AFM – atomic force microscopy

APCI – atmospheric pressure chemical ionization

APPI – atmospheric pressure photoionization

ATR-FTIR – attenuated total reflectance-Fourier transform infrared spectroscopy

B – concentration of bound analyte

BaP – benzo(a)pyrene

BET – Brunauer-Emmett-Teller

CCD – central composite design

CE – capillary electrophoresis

COC – cyclic olefin copolymer

CP – control polymers

DC – direct current

DCM – dichloromethane

DESI – desorption electrospray ionization

DMPA – 2,2-dimethoxy-2-phenylacetophenone

DVB – divinyl benzene

EI – electron ionization

ESI – electrospray ionization

EGDMA – ethylene glycol dimethacrylate

IF – impact factor

F – concentration of free analyte

FLD – spectrofluorometric detector

FTIR – Fourier transform infrared spectroscopy

ITO – indium tin oxide

GC-MS – gas chromatography- mass spectrometry

HEMA – 2-hydroxyethyl methacrylate

HF – hydrofluoric acid

LC – liquid chromatography

LLME – liquid-liquid microextraction

KOH – potassium hydroxide

MAA – methacrylic acid

MBAA – N,N-methylenebisacrylamide

MD – Molecular dynamics

MeOH – methanol

MIP – molecularly imprinted polymers

NIP – non-imprinted polymer

NMR – nuclear magnetic resonance

QCM – quartz crystal microbalance

QMB – quartz microbalance

PAH – polycyclic aromatic hydrocarbons

PDMS – polydimethylsiloxane

PMMA – polymethylmethacrylate

rf – radio frequency

SAW – surface acoustic wave

SEM – scan electron microscopy

SIM – selected ion monitoring

SPE – solid phase extraction

SPME – solid phase microextraction

TLC – thin-layer chromatography

TRIM – trimethylol-propane trimethacrylate

UHPLC – ultra high performance liquid chromatography

US-EPA – United States Environmental Protection Agency

UV – ultraviolet

2,4-D – 2,4-dichlorophenoxyacetic acid

4-VP – 4-vinyl pyridine

2-VP – 2-vinyl pyridine

# List of Appendices

# Chapter 1. Introduction and Literature Survey

## 1.1. Introduction

Over the past decades, urbanization and an ever-growing rate of industrialization have increased the amount of pollutants released into the environment, with the soil and oceans as the ultimate waste pools [1]. We rely on clean water and soil to maintain life as we know it, thus concern about maintaining a clean environment has been expressed globally by broader and stricter regulatory policies and safety guidelines. In addition, efforts have been made to increase environmental awareness and enable research towards cleaner technologies, efficient remediation processes and development of renewable resources [2]. To comply with these regulations and to mitigate accidents, environmental monitoring technologies and methods are constantly being developed. Continuous improvements in accuracy, speed, safety and cost of analysis are being made to increase the efficiency of these measurements and make informed decisions in case of accidental spills [3].

The oceans are the largest global habitat and home to a diverse and vast number of species and a valuable resource particularly for food and recreation. Analysis of marine samples can be a difficult task because of the complexity of the samples. Nevertheless, a wide range of water quality indicators have already been established, although many are for bulk properties, such as pH, "oil in water" or temperature [2, 4]. These do not offer enough information to adequately assess the impact, transport or fate of pollution in a

marine environment. Moreover, detection and quantitation of water pollutants by on-line or in-situ methods is limited, especially in off-shore oil and gas operations or remote water treatment facilities, since periodic sampling and shipping to an off-site facility must be done routinely [4]. In this context, the current trend is to create and implement simple, rapid, affordable, on-site routine monitoring devices. These devices should be capable of detecting trace level concentrations of mostly organic compounds in a complex matrix. Inevitably, determination of trace amounts of these types of contaminants in real samples requires some degree of sample pretreatment. A technique used routinely is solid phase extraction, which is used to remove a range of compounds from liquid matrices. Classic solid phase extraction (SPE) sorbents retain analytes by non-selective hydrophobic interactions, which can also retain other similar compounds, thus a more selective material would be suitable. A solution for this is the use of MIPs, a simple polymer capable of selective enrichment.

This section aims at giving a general description and a literature overview of the concepts described in the following research chapters. Thus it is not meant to be comprehensive but would give enough details to position this research with respect to current ongoing research and major trends in the analytical and environmental chemistry fields.

### 1.2. Molecularly imprinted polymers (MIPs)

MIPs are smart synthetic materials with molecular recognition properties based on complementary shape, size and functionality. Their retention mechanism is similar to the

lock and key mechanism in biological receptors, such as antibodies or enzymes, [5]. For this reason, MIPs are sometimes referred to as synthetic antibodies. But as opposed to their biological counterparts, in MIPs the selectivity can be tuned to specific compounds.

Their remarkable capacity to be selective comes from polymerization around a template in a rigid network. The principle of MIP formation is illustrated in Figure 1.1. In solution, the template forms an initial complex with the monomer to form a pre-polymerization complex based on a range of interactions that can vary from very strong covalent ones to electrostatic interactions. An initiator is included to activate a chain polymerization reaction. A crosslinker present in excess co-polymerizes around the template-monomer complex to consolidate the polymer structure. Upon removal of the template, a network with cavities that match in size, structure and functionality for a target analyte results.

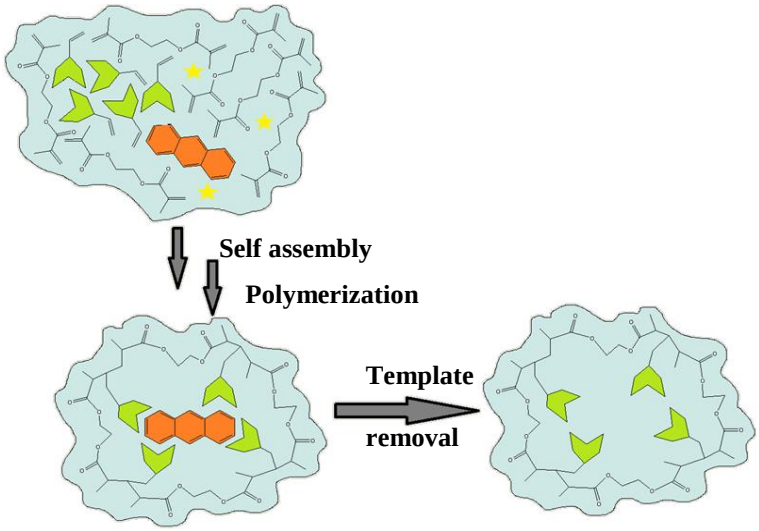


**Fig. 1.1. Schematic principle of MIPs**

### 1.2.1. A brief history of molecular imprinting

The principles of molecular imprinting were first recorded in 1931, when M. V. Polyakov observed that preparation of silica gel from silicic acid would yield polymers with different pore structures for the different solvents used, namely benzene, toluene and xylene [6]. Later in 1949, Frank Dicks made similar observations about silica that polymerized in presence of a dye and would preferentially bind that dye over others after removal of the template [6].

The beginning of the molecular imprinting field could be attributed to the research done by Günter Wulff and his co-workers in 1972. They prepared a MIP using a covalent template monomer approach for selective uptake of enantiomers of glyceric acid. This raised interest in the research community, such that later, in 1981, Klaus Mosbach and Reza Arshady reported on the preparation of MIPs using a non-covalent approach. In this approach the type of template-monomer and analyte-cavity interactions are weaker than covalent ones [7]. The simplicity of this technique and the wider range of possible materials earned it a great interest and an expansion of the research into imprinted polymers. In 1995, Whitcombe *et al*. combined the two approaches to prepare a MIP using covalent bonding formation of the cavities and non-covalent binding during analyte uptake. A template monomer was used for this purpose, and cleavage of carbon dioxide ($CO_2$) resulted in cavities with phenolic residues that could selectively uptake cholesterol via hydrogen bonding [8]. The non-covalent approach has still remained one of the most popular.

The interest in this research area has been growing exponentially as can be seen in Figure 1.2. Extensive reviews and research articles tracking the progress of MIP research

towards better understanding of the interactions occurring during upload, use of novel templates in new applications and in sensors have been periodically published [9, 10]. This trend recognizes the interest and potential of shifting the MIP research and applications from a purely academic research subject to economically sound applications.

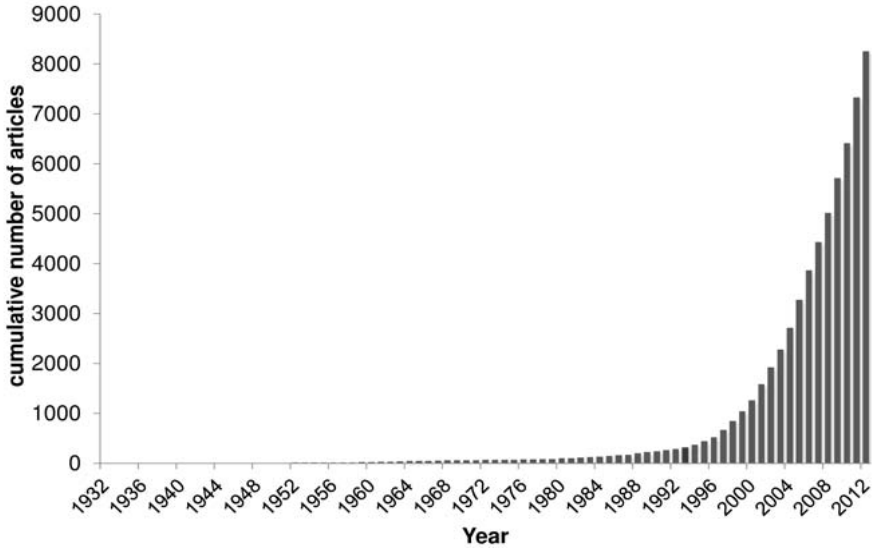


**Fig. 1.2 Number of MIP articles published since 1932, adapted with permission from [9]**

When compared to antibodies, MIPs present a number of advantages with respect to their ease, cost and time of preparation and tolerance to chemical, pressure or temperature changes [6]. Moreover, their high binding capacity indicates a significant potential for miniaturization into sensors and use in environmental applications in complex matrices, where the analyte concentrations can be in the lower μg $L^{-1}$ and ng $L^{-1}$ ranges. The most common uses of MIPs are in SPE of environmental, food and pharmaceutical samples [6, 11-14]. Applications in sample clean-up and enrichment, [13, 15, 16] and in sensing and

monitoring [13] were also reported over the years. However, there have been few commercial applications of these MIPs, although interest in commercialization is also obvious from the number of MIP patents filed over the past few years [17] and the companies that market these products (Sigma Aldrich with SupelMIP and Biotage/MIP Technologies, Sweden). Lieberzeit and Dickert, argue in a 2009 paper, [18] that the complexity of these materials compared to other physical sensors that measure temperature, pressure or conductivity, and the trade-off between sensitivity and ruggedness have slowed down the economical development in this area. Most MIP studies and environmental sensor applications reported so far are done in laboratories under ideal conditions and few are used in natural matrices, such as soil or water [18]. Other interesting areas for development of MIPs have been for medical applications, in organic synthesis and biological sensors to detect or deliver drugs in biological fluids [8, 15], analytical separations for generation of chiral chromatographic stationary phase [6, 19, 20] and catalysis [12].

### 1.2.2. MIP composition

As mentioned previously, a template-monomer complex forms in solution and is then immobilized into a polymer matrix by copolymerization with a high concentration of cross linking monomers. Once the template is removed, a structure with cavities selective for a certain target analyte results. Another polymer is prepared using the same composition as for the MIP but in absence of a template and is referred to as a control polymer (CP) or as a non-imprinted polymer (NIP) [21]. This is used to carry out the binding experiment in similar experimental conditions with the MIPs and assist to

characterize the selectivity of the imprinted materials. When exposed to a sample, the targeted molecules bind to MIPs and potentially to NIPs via a binding mechanism that relies on the potential for π- π interactions with the polymer network. A higher target analyte binding should be recorded by the MIPs because of the shape and size selectivity interactions, in addition to the matching functionalities [22]. To measure the shape selectivity of the MIPs, an imprinting factor, IF can be used. The IF is calculated as the ratio of the concentration of MIP bound analyte to the concentration of NIP bound analyte. High IFs are associated with highly selective materials. It has become apparent that the number and quality of the MIP recognition sites directly affects the nature and extent of the monomer-template interactions. Even more informative would be to determine the actual structure of the binding sites. However, this is not possible because of the amorphous nature of the polymer. Thus, X-ray or microscopy techniques are not possible, which limits the capacity to understand, predict or fully control the mechanisms involved in binding [22].

Although NIPs lack the selective cavities created through incorporation of the template in the polymer network, the presence of the monomer in the composition of the NIP increases surface functionality and the capacity of the polymer to bind the target analyte. This network functionality is not as high as the MIPs, but it is superior to the results obtained when using other solid sorption materials and can account for the relatively small IFs that have been observed in many instances in literature [21, 23]. This statement is supported by the research of Bagianni *et al.* in non-covalent bulk polymerization of small templates [21]. To focus on the MIP selectivity, additives such as 1% MeOH were added

in one instance to inhibit non-specific electrostatic interactions; however, this is not particularly favorable in environmental applications [12].

(a) *Monomers*

The functional monomer interacts with the template to form a complex before polymerization is initiated [24]. Identifying the optimal monomer in a MIP for a selected target is one of the most important steps taken towards designing these materials. Depending on the functionality it carries, the monomer interacts covalently, non-covalently or through metal complexation. These interactions are discussed in much more detail in Section 1.2.4. A strong interaction results in a more stable monomer-template complex and a higher affinity material [10]. The type of bond established is important for template removal and analyte uptake, but also the number of functional groups on the monomer that can interact with the template is a factor. These ensure binding points with the template, such that an imprinted cavity, with 4 binding points can provide an increased selectivity and affinity to a target analyte [25].

In the case of weak template-monomer interactions, an excess of monomer should be used to drive the equilibrium towards complete use of the template to form template-monomer complex as per Le Châtelier's principle [10]. However, it has also been suggested that the non-complexed monomer units form adducts at the surface of the polymer, which accounts for some of the non-selective binding common to imprinted and non-imprinted materials [26]. Overall, this would decrease the selectivity of the MIP. If the equilibrium was driven towards complete use of the monomer by adding excess template then fewer binding sites would be created [10].

Various monomers with different chemical properties are available and many more can be synthesized by rational design. Some common monomers used for preparation of MIPs for smaller molecules are methacrylic acid (MAA), acrylic acid (AA), 2-vinyl pyridine (2-VP), 4-vinyl pyridine (4-VP) and 2-hydroxyethyl methacrylate (HEMA) [10].

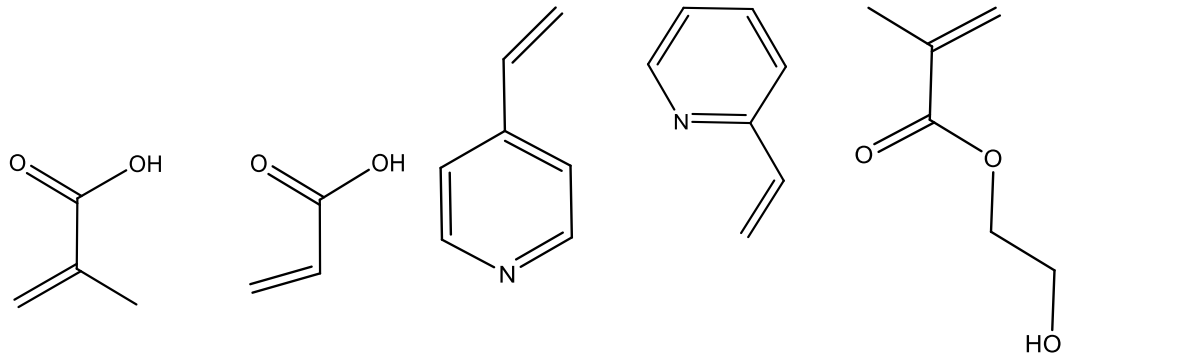


| methacrylic acid | acrylic acid | 4-vinylpyridine | 2-vinylpyridine | 2-hydroxyethyl methacrylate |
|---|---|---|---|---|
| MAA | AA | 4-VP | 2-VP | HEMA |

**Fig. 1.3. Monomers commonly used for molecular imprinting, [27]**

MIPs that target larger biomolecules such as polyphenols or polyurethanes have been prepared using β-cyclodextrins although they have shown limited use due to a restricted choice of a functional monomer [10, 28]. In preparing imprinted materials for polycyclic aromatic hydrocarbons, 4-VP and MAA have often been mentioned [16, 29-31]. 4-VP is a basic compound capable of H bonding or π-π stacking, due to the lone electron pair of the nitrogen and the aromatic heterocycle respectively [24]. MAA is capable of hydrogen bonding with the template as donor through the hydroxyl group and as acceptor through the carbonyl group. In addition, MAA has been shown to be suitable for ionic interactions [10, 27].

(b) *Crosslinker*

The crosslinker co-polymerizes around the template-monomer complex connecting the linear polymer chains into a 3-dimensional network. Addition of the crosslinker is meant to stabilize the whole structure even after template or analyte removal, when the polymer relaxes. This is important for achieving a good binding selectivity, because template removal and analyte extraction steps can subject the polymer cavities to stress either through extensive washings in organic solvents or temperature and pressure treatments. Thus the amount of crosslinker used plays an important role in preserving the morphology of the polymer and its capacity to retain the complimentary size, shape and functionality of the template [24]. It is generally agreed that a 50-80% crosslinker in the total pre-polymerization mixture is necessary to obtain a rigid network. A lower degree of crosslinking could result in a gel type MIP where cavities can undergo changes in morphology [26, 32]. This can be particularly useful in drug delivery applications. A higher crosslinking degree could decrease the number of recognition sites per unit mass of MIP, by decreasing the ratios of template and monomer [10, 27].

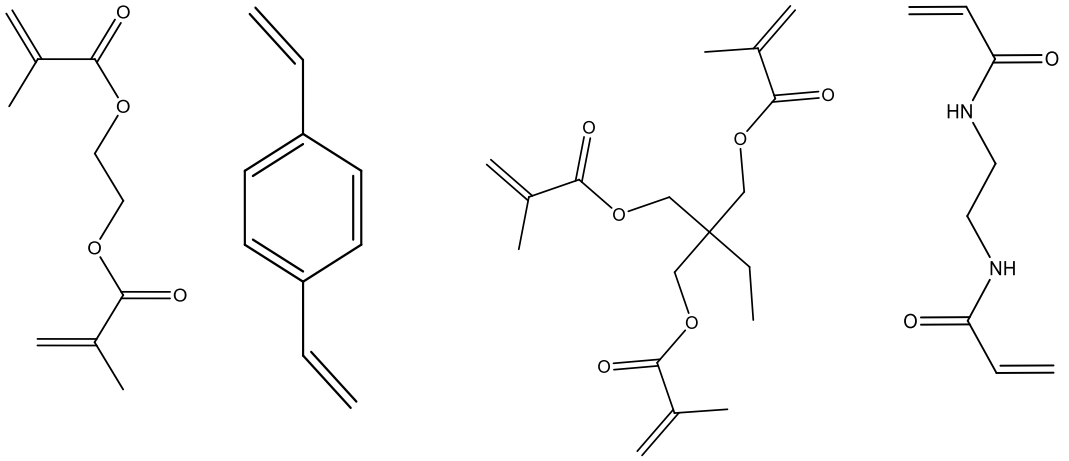


ethylene-glycol dimethacrylate EGDMA

1,4-divinylbenzene DVB

trimethylol-propane trimethacrylate TRIM

N,N′-ethylene bisacrylamide EBAA

**Fig 1.4. Crosslinking agents commonly used for molecular imprinting, [27]**

Common crosslinkers are ethylene glycol dimethacrylate (EGDMA), divinyl benzene (DVB), trimethylol-propane trimethacrylate (TRIM) or N,N`-ethylenebisacrylamide (MBAA) [8]. EGDMA is a slightly polar crosslinking agent while DVB is a non-polar compound.

(c) *Initiators*

Polymerization is activated by an initiator that decomposes into highly reactive free radical monomers with unpaired electrons when exposed to energy in the form of heat or UV light. These radicals find the nearest source of electrons, such as a covalent carbon-carbon double bond to scavenge an electron. A single bond is formed and the radical center is transferred. The reaction propagates to form the polymer structure. Temperature induced initiators are used mostly for bulk polymer imprinting while photo-initiators are better

suited for thin-film imprinting. In a study, a higher degree of crosslinking and better specificity were observed for photo initiated polymerizations [33].

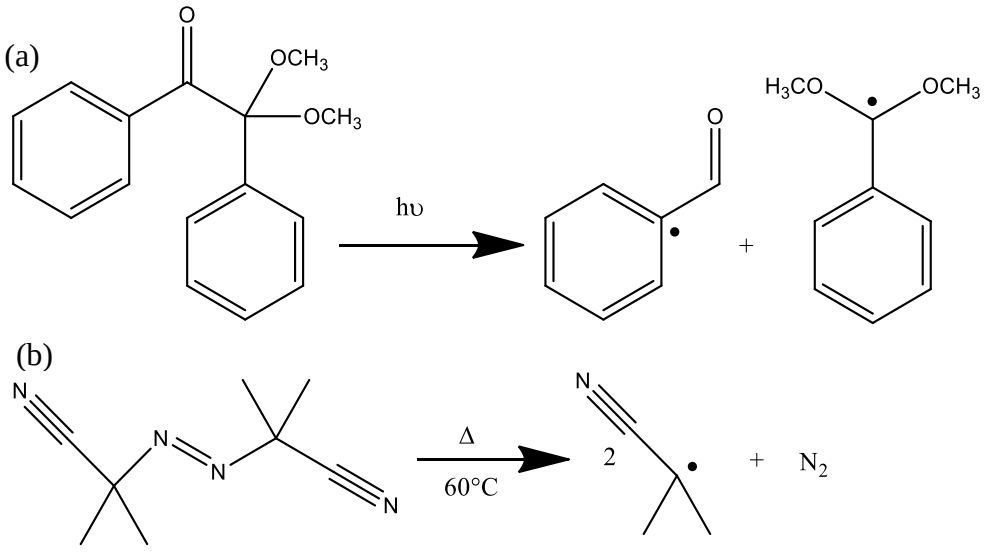


**Fig. 1.5. The decomposition reactions of (a) DMPA and (b) AIBN**

The most commonly used radical initiators in MIP synthesis are azobisisobutyronitrile (AIBN) and 2,2-dimethoxy-2-phenylacetophenone (DMPA) and the reactions to form radicals are shown schematically in Figure 1.5.

(d) *Templates*

The template is in most cases the targeted analyte, which can be representative of a class of environmental pollutants, endocrine disrupting compounds, pesticides or other health threatening compounds [10]. When considering a template for use in preparation of a MIP, certain criteria are considered. Some important aspects in choosing the template are the cost or possibility for recovery, the stability during polymerization or the functional compatibility with the monomers [10, 20]. If the template is unstable, then an analogue

could be used [13]. Most templates are small molecules. There are fewer reports of large macromolecule imprints [6, 13, 20]. Large bulky templates, such as proteins, bacteria or living cells reduce the capacity of the polymer [6]. In addition, the large complex structures with multiple functionalities enable an increased number of binding points to the monomer. This results in poor template removal and fragile cavity structures that minimize the overall selective binding capacity per unit mass of polymer [6, 34, 35]. A more recent concept is a template capable of "group selective recognition" of a restricted range of compounds from the same class, such as it could be the case for a group of polycyclic aromatic hydrocarbons [11]. Also, the ratio of the template to monomer has to be considered in the preparation of a selective robust material. In the case of weak template monomer interactions, the monomer is added in excess as discussed previously to drive complete complex formation. When the template is used in small quantities fewer template-monomer complexes form, which impacts directly on the total binding capacity. However, increasing the concentration of the template does not automatically ensure a proportional increase in the number of binding sites. Template clusters formed by self-association have been reported for large template concentrations [21, 32, 36]. This can be problematic when working with fluorescence detection, since quenching could occur.

Once the template-monomer complex has been polymerized, the next logical step is removal of the template. Complete template removal is necessary to ensure a maximum number of available binding sites, thus an optimum selectivity. However, the residual template may remain trapped in the polymer network either because of strong template-monomer interactions, poor accessibility by the extraction solvent to various regions in a

bulk polymer or binding site heterogeneity, which implies formation of template-monomer and template-template adducts [13, 15]. Thus, the template may leach further in the upload process and be detected in subsequent analysis creating false positives that can be particularly problematic when trying to achieve precise and accurate determination of target analytes present at trace levels, as is the case of actual environmental samples [15, 37]. Considering the importance of effective template removal to the overall MIP performance, research reported in this area has not been extensive [38]. The template removal methods can range from very harsh extraction conditions, such as Soxhlet extraction or heating under pressure to centrifugation or washing in organic solvents [15]. Lorenzo *et al.*, [38] provides a comprehensive review of the methods available for template removal focusing on the resources required, the environmental friendliness and the effects on maintaining the fidelity of the imprinting cavities. One of the conclusions of this review is that harsh extraction conditions can potentially damage, collapse or distort the structure of the binding sites reducing the selectivity of the imprinted materials [38]. The options to overcome the potential for false positives are either the use of a pseudo template, parallel extraction on blank samples or post-polymerization treatments [10, 38]. The pseudo template can be an isotope labeled template or a structural and functional analogue of the target analyte. The use of the pseudo template ensures that leakage of the template will not interfere with identification and quantification of the target compound.

(e) *Solvents/Porogens*

The solvent dissolves all the components of the pre-polymerization solution into one phase, thus enabling and increasing the probability of interaction between the monomer and the template. The solvent's chemistry should not affect the character or strength of the interactions that occur in the pre-polymerization complex such that during polymerization, a solid network formed by the template, monomer and crosslinker linkages grows out of the liquid phase into a solid phase. At this point, the solvent separates from the rest of the complex by phase separation and forms pores. For this reason, the solvent is often referred to as a porogen [25]. A good porogen usually separates relatively late during polymerization and leaves small surface pores. Depending on the size range, these pores account for some of the non-specific binding observed in the non-imprinted and the imprinted polymers. The polarity or hydrogen bonding capacity of the porogen can affect the properties and morphology of the imprinted cavities [10, 34]. For example an organic solvent would be ideal to dissolve all the pre-polymerization components, however it could disrupt hydrogen bonding interactions between template and monomer prior to polymerization and could decrease the number of selective sites formed [27]. As reported by some studies, [13, 27] the selectivity of the polymer could be enhanced if the analyte to be extracted was dissolved in the same solvent used for MIP preparation since swelling effects could be avoided.

### 1.2.3. Optimization of polymer fabrication

Optimization is a crucial step that considers all the factors involved in generating a MIP to achieve a material with a highly selective molecular recognition capacity [21]. These factors range from the selection of each component and their stoichiometry to polymerization conditions such as duration, temperature, and pressure and any treatment steps carried out before or after polymerization [15, 33, 39]. After identifying the optimum monomer and crosslinking agent, the variables considered essential in the development of a particular MIP are determined. For example, the polymerization temperature or duration was recognized to influence the uptake capacities of an MIP [33]. Polymerization carried out at lower temperatures yields imprinted polymers with increased binding selectivity likely because compounds typically spend more time in a stable conformation at lower temperature [26, 34]. More homogeneous cavities are generated which enhances the binding activity especially if uptake occurs at the same temperature. Even the polymerization time has an effect where longer exposure time increases the extent of polymerization which can increase the rigidity of the imprinted cavities [33]. Although it may improve the fidelity of the imprinted cavities, this could be unfavorable in terms of stability during template removal steps that involve soaking and swelling in organic solvents or mechanical shock.

To evaluate whether the optimization is successful, binding assays are undertaken where typically one factor is varied while the others are kept constant in a so called trial and error approach. Since this tactic is tedious and can miss important interactions other strategies have been used. Semi-automated procedures, where small quantities of MIPs

with different compositions are synthesized in parallel, offer similar results in a more timely fashion [12, 21]. One such example involved preparation of 80 polymers in min amounts on a plate followed by binding experiments to evaluate for their imprinting characteristics [40]. Other alternatives are the use of chemometrics (i.e. design of experiment) of monomers and crosslinkers libraries, molecular modeling software, molecular dynamics simulations or quantum mechanical calculations [32, 41]. Chemometrics can greatly reduce the number of experiments by identifying a small number of essential factors and the limits of the levels of interest and can provide details in understanding the main interactions. The libraries of monomers and crosslinkers help in identifying a range of optimal components or ratios based on the functionalities of the template and the expected binding interactions as well as the characteristics of the matrix. Computational models are not able to reproduce the recognition process in its full complexity. However they can assist in identifying suitable monomers or other components [39, 41].

### 1.2.4. Types of MIPs: covalent *vs.* non-covalent imprinting

A successful MIP, in terms of binding capacity, depends on the monomer structure and the type of binding interaction. In the liquid phase prior to polymerization, the monomer prearranges around the template covalently or non-covalently, function of the matching functionalities. The non-covalent imprinting resembles the mechanism of molecular recognition in nature and relies on interactions such as ionic, hydrogen bonding, hydrophobic and electrostatic interactions [6, 34]. Each approach to imprinting presents a number of advantages and limitations and may be suitable for a specific application. Thus a parallel comparison presented in Table 1.1 could give in-depth understanding. Although

the approaches discussed below are the main ones being employed, semi-covalent and metal coordination interactions have also been reported.

Table 1.1 Comparison of non-covalent imprinting and covalent imprinting, [6, 42, 43]

| Non-covalent imprinting | Covalent imprinting |
|---|---|
| ○ weaker interactions | ○ stronger interactions |
| ○ more non-selective uptake | ○ higher selectivity |
| ○ heterogenous surface with various binding affinity pores | ○ uniform binding sites |
| ○ monomer is used in excess to ensure complete use of the template | ○ stable interactions and predetermined stoichiometry |
| ○ straightforward method | ○ requires method development |
| ○ more choice of template, monomer, etc. | ○ limited selection of templates and monomers |
| ○ 15% of the free cavities show re-uptake of the template | ○ irreversible: release of substrate is difficult |
| ○ the template can be removed quantitatively | ○ template removal can be difficult to achieve |
| ○ fast equilibration times | ○ long equilibration times |
| | ○ used for compounds that lack functionality |

The semi-covalent approach aims to use the advantages of both covalent and non-covalent imprinting. Thus, polymerization follows covalent principles, while binding of the target analyte follows a non-covalent approach. In the metal coordinated imprinting, the template is a complex with a metal center. Prior to polymerization, the formation of the pre-polymerization complex between the template and the monomer is governed by non covalent interactions. During template removal, ligands are removed and the metal-ligand

coordinative bond is used as a highly specific binding mechanism. Hart and Shea, [44] used this approach to generate imprinted polymers containing a Ni(II) metal center that would selectively bind to the N-terminal histidine residue of small peptides.

The experimental work reported in this thesis focuses mainly on non-covalent MIPs, thus an emphasis on the characteristics of this approach will be discussed in the following sections.

### 1.2.5. Imprinted polymer formats

MIPs can be polymerized in various formats depending on the application sought.

The most common approach is bulk polymerization. The initial preparative steps of a bulk MIP seem straightforward, although grinding and sieving to reach certain particle sizes can deem it not only time consuming, but also inefficient because of the small usable polymer yield with suitable particles estimated at only 30 to 40% of the total mass of the MIP [10]. However, this approach gives best results when smaller templates are used, since removal of the template can be done more effectively and re-usability can be foreseen [10]. In terms of performance, in bulk MIPs the mass transfer is slower which reduces template removal as well as the binding capacity [10]. These limitations have not reduced the interest in using this format in preparation of monolithic stationary phases or extraction sorbent. Continued interest in MIPs led to development of various formats that do not require further preparative steps and could directly match different applications [28, 45].

Other polymerization techniques reported are suspension, emulsion and precipitation [6, 12, 14, 46]. Suspension and emulsion polymerization are heterogeneous-type polymerizations where two non-miscible phases are present: a continuous aqueous

phase and a dispersed organic phase. Polymerization is activated in the dispersed phase containing the template, initiator, monomer and crosslinker, and solid beads are generated in the continuous aqueous phase. Precipitation polymerization is a homogenous type of polymerization that occurs over time as the MIP grows, until it precipitates out of the porogen [46]. This type of polymerization is very slow and uses large volumes of porogen and template, but yields polymers with a higher selectivity and a better size control [47]. A particular type of polymerization suitable for generation of MIP films for biosensors uses conductive species such as polypyrroles for electro-deposition [46].

An MIP format of interest to environmental monitoring is thin-film imprinting because of the potential for integration into sensors. Thin-film imprinted coatings can be prepared with thickness in the lower μm range by spin coating or drop coating on various supports: mica, glass, silica beads, gold [43, 45]. Spin coating can ensure more control over the thickness of the thin-film; however it is best done in an inert atmosphere. Most thin-film MIPs are prepared using a non-covalent approach based on organic polymers [43]. Thin-film MIPs enable a better accessibility to the pores and a better mass transfer since most binding occurs at and near the surface. Large biomacromolecules can be used as templates and target analytes since removal steps allow for faster mass transfer kinetics on the MIP surface [48]. Thin-film MIPs have found applications in sensor development, sample purification and enantiomer separation. Their importance for use in forensic applications for common monitoring and detection of explosives or drugs has been recognized, although not fully established given that sensitivity is limited by the relatively small active surface area [46].

### 1.2.6. Heterogeneity in binding – short review of causes and effects

Preliminary studies suggest that surface diffusion plays the main role in analyte uptake. Easy access of the analyte to the selective cavities increases mass transfer kinetics; however the upload with increase in concentration is not constant for imprinted polymers, but constant for non-imprinted materials [48, 49]. The difference is caused by variations in morphology and functionalities of the imprinted cavities, as well as other functionalities present on the surface. The size of the pores varies from 2 to 100 nm for macropores and mesopores and below 2 nm for micropores, as shown in Figure 1.6. [26].

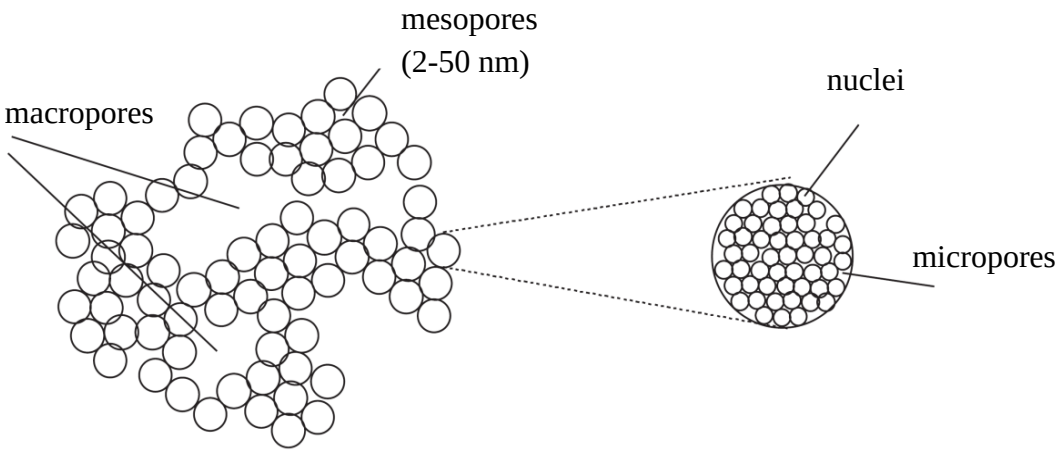


**Fig. 1.6. Pore size distribution in an MIP, adapted with permission from [26]**

This characteristic of imprinted materials, referred to as heterogeneity, is most prevalent in non-covalent imprinted polymers [25]. The range of pore size can be easily evaluated through nitrogen adsorption studies [29, 50]. In terms of functionalities and binding during upload, some interactions are specific and some are less specific, which can

cause a variation in the binding affinity, non-linear responses in sensors and broad asymmetric peaks in chromatographic separations, [48, 50]. Understanding of the binding interactions occurring prior and during polymerization could give an in-depth understanding of what causes heterogeneity in MIPs and how it can be minimized when developing a rational design for selective MIPs [36].

The template-monomer interactions expected in non-covalent MIPs were discussed in Section 1.2.4. These interactions range from ionic to electrostatic interactions, which cause low functional monomer-template association constants [28]. More complex associations occur between the components of the pre-polymerization solution, some of which are present in excess. For example, Nicholls *et al.*, [36] used molecular dynamics (MD) simulations to show formation of template-monomer complexes in various ratios and template-template self-association in a 1:1 ratio in the pre-polymerization complex. In this particular case, hydrogen bonding between amine and amide functional groups of phenylalanine anilide was at the basis of template dimer formation and accounted for some of the target analyte uptake as illustrated in Figure 1.7.

The template self-association has been observed mainly in cases of weak binding interactions [51, 52]. The same study suggests the formation of template-crosslinker complexes, an association less stable but likely to occur because of the large excess of crosslinker [36].

(a) (b)

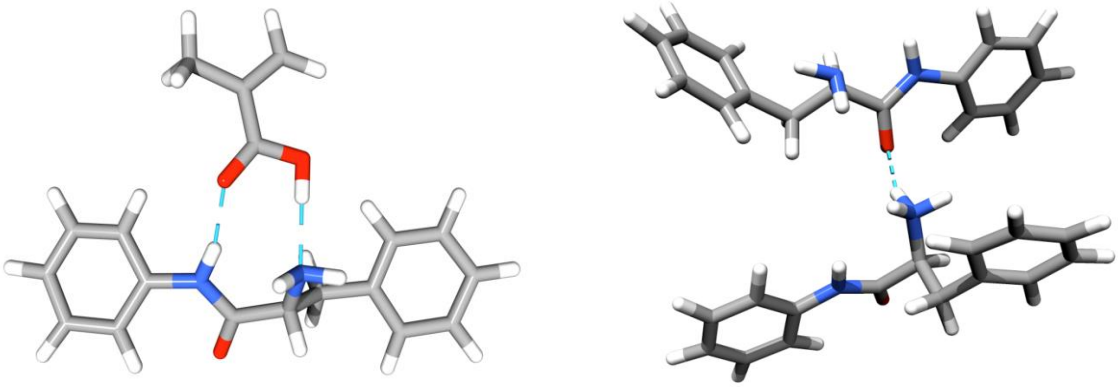

template-monomer interaction template self-association

**Fig. 1.7. The most stable interactions as calculated from MD simulations, adapted with permission from [36]. Color coding: white, hydrogen; blue, nitrogen; red, oxygen; grey, carbon**

The methods available for bonding and functional groups identification post-polymerization are limited because the polymer is amorphous. Thus, most of the studies are based on analysis of binding in the liquid pre-polymerization solution in conjunction with computational modeling. Direct techniques successfully employed so far are nuclear magnetic resonance spectroscopy (NMR), Fourier transform infrared spectroscopy (FTIR) or ultraviolet (UV) spectroscopy [19, 27, 52, 53].

These studies support the general idea that when weak electrostatic interactions govern polymer formation, the excess of components will be randomly incorporated in the polymer structure and might associate or self-associate in various ratios depending on the composition of the MIP [28, 51]. These adducts along with any template molecules trapped in the polymer network generate cavities with different degrees of affinity to the target analyte. Thus, the concentration of bound analyte with respect to the amount of free analyte

in solution or the initial upload concentration will not vary linearly for the MIPs as is the case with the NIPs [16, 25, 26, 29, 36]. As described in Figure 1.8, the experiments also referred to as batch binding tests show that the response of the MIPs resembles a curve that levels off after a certain saturation level, similarly to that of an adsorption isotherm. Figure 1.8(a) illustrates the shape of common response curves of ethyl adenine 9-acetate in acetonitrile uptake by MIPs and NIPs, where the interactions rely on hydrogen bonding [50]. Figure 1.8(b) shows similar response trends as before for the uptake of PAHs in deionized samples based on π-π interactions [16].

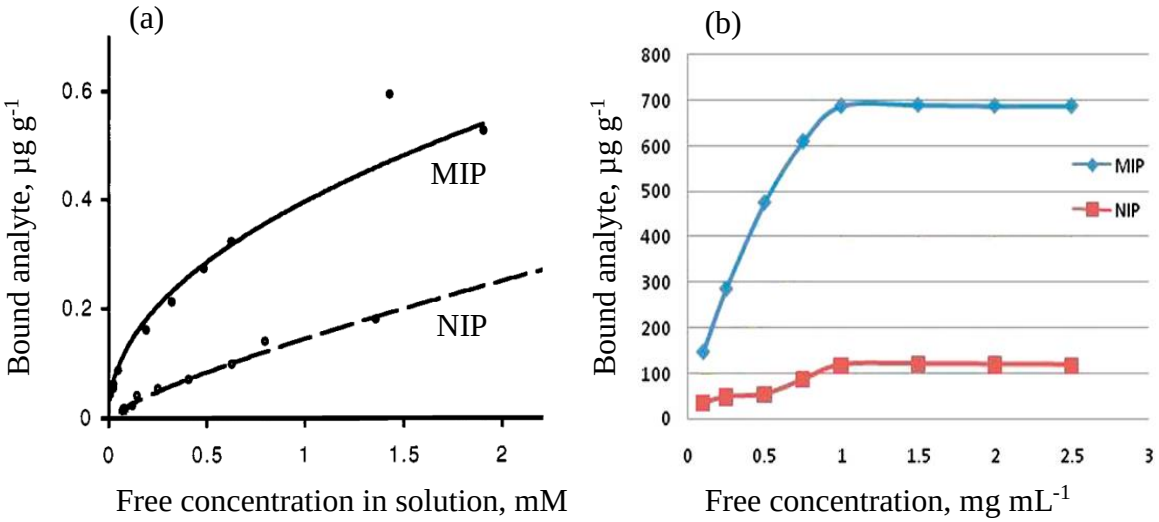


**Fig. 1.8. Binding curves for imprinted and non-imprinted polymers based on (a) overall trends and (b) observations of PAHs upload from deionized water, adapted with permission from [16, 50]**

Studies to assess which type of adsorption isotherm best describes the response of a MIP have been reported in several scientific papers [25, 50, 51]. Some authors consider

MIPs as homogeneous surfaces and use Langmuir or bi-Langmuir isotherms, while others either suggest a combination of Langmuir and Freundlich isotherms or a Freundlich isotherm fit [25, 50].

Heterogeneity is an inherent issue in non-covalent imprinting and can be at most reduced. The steps taken towards minimizing this issue involved using stoichiometric amounts of each component and chemical treatment of the surface to avoid or reduce non-specific binding. Chemical treatment involves an extra step after polymerization, when the low affinity binding sites are blocked by interaction with a suitable compound [28, 50, 54]. Either of these two steps is specific to each MIP composition and can require additional optimization steps which can reflect in a higher overall manufacturing cost.

### 1.2.7. MIP characterization and performance parameters

A successful MIP is capable of high selectivity based on the molecular recognition effect. To evaluate this property some approaches focus on the functionality of the pores and others on the pore morphology. All experiments are carried out in parallel with non-imprinted polymers, which are used as a control.

Pore functionality is directly related to the template-monomer and analyte-monomer interactions [32]. Binding assays are carried out at different polymerization and upload conditions to generate binding isotherms, calibration curves and a Scatchard plot [26, 54]. Calibration curves are graphs of binding capacity, or total concentration of imprinted analyte varying over distinct upload periods or distinct increasing analyte concentrations. In a Scatchard plot the ratio of the concentration of bound analyte to the concentration of free analyte in solution (B/F) is plotted against the concentration of bound

analyte (B) when the analyte concentrations are in equilibrium with the solid and the liquid phases. A typical Scatchard plot for the uptake of ethyl adenine 9-acetate is shown in Figure 1.9 [54]. In this case, the two slopes were calculated using linear regression and indicate two categories of binding cavities with higher affinity for the steeper slope [54].

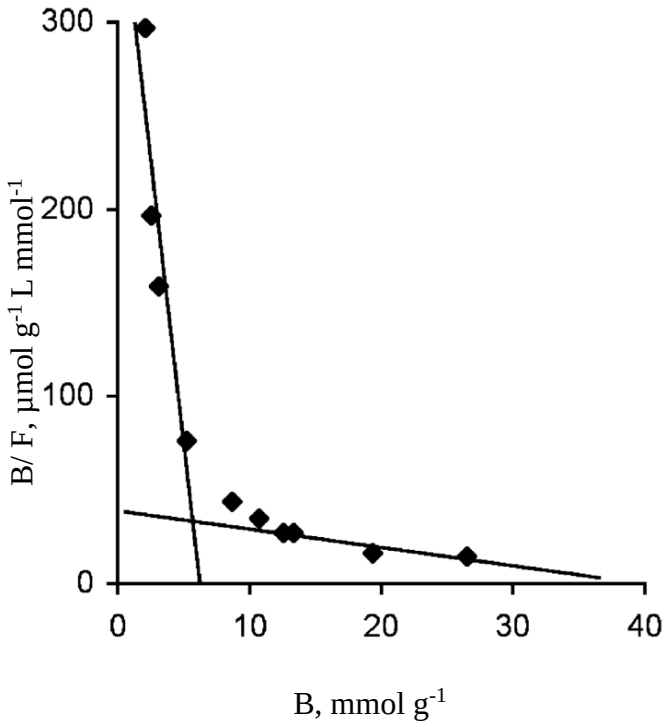


**Fig. 1.9. Typical Scatchard plot, adapted with permission from [54]**

The equation of the slope in Figure 1.9 shown in Equation 1.1. assists in determining the affinity constant, K from the slope and N, the total number of binding sites [54] where:

$$\frac{B}{F} = KN - KB \qquad \textbf{Equation 1.1.}$$

K is a measure of the analyte molecule held onto the surface of the MIP and can be expressed with respect to the mass of the polymer or time taken for the uptake [39]. However, it has been shown that a Scatchard plot will change for different upload concentration ranges. Thus, K and N cannot be reliably used to compare the performance of different or similar MIPs [50]. The Scatchard plot would be more suitable to assess binding heterogeneity of bulk polymers where the amount of analyte is expressed relative to the mass of polymer. Thus to describe the binding heterogeneity of thin-film MIPs where the analyte uptake depends on the surface exposed, the use of a Scatchard plot would find limited applicability. Another parameter used to describe MIPs is the imprinting factor, IF. The IF relates to the selectivity of the imprinted polymer over the non-imprinted material as illustrated in Equation 1.2, where $C_{MIP}$ is the concentration of analyte bound to the MIP and the $C_{NIP}$ is the concentration of analyte bound to the NIP [39]

$$IF = \frac{C_{MIP}}{C_{NIP}} \qquad \textbf{Equation 1.2.}$$

Selectivity can be evaluated by carrying out batch assay studies where the sample is spiked with compounds within the same polarity range as the analytes. If these compounds are not retained, then the material and the method are selective only towards the target analytes.

A MIP characterization would not be complete without a description of the MIP surface and pore morphology. Although such morphology does not fully reflect the selectivity potential of a material, studies are carried out to determine the size of the imprinted cavities and to evaluate their influence on the overall binding selectivity [34]. Microscopic techniques can assist in evaluating the morphology of the pores but are limited [42]. Surface characterization techniques include nitrogen sorption measurements such as

BET to determine surface area, pore size distribution or swelling; solid state NMR to determine the dissociation constants [10]; atomic force microscopy (AFM) and scanning electron microscopy (SEM) for surface morphology [45]; and FTIR and surface enhanced Raman for identification of functional groups and quantification [45, 53]. In this context, little is known about the interactions responsible for selective uptake during and after polymerization and most of the information reported is a result of computational modeling calculations [25].

### 1.2.8. Challenges and future prospects for MIPs

The rising number of research reports of new developments and applications with MIPs, indicate their great potential for real life applications. However, many articles limit themselves to laboratory based experiments run in ideal conditions and in pure matrices; few venture into exploring the sensitivity and selectivity in complex matrices ranging from environmental samples to body fluids. These reports are insufficient to raise investors' interest for transition to a wide market and large scale commercialization. The identified challenges vary significantly with the target or the interactions involved and include imprinting of biological macromolecules, template bleed, low binding capacity caused by high heterogeneity and incompatibility with aqueous media [35, 49]. Solutions to these problems were discussed in previous sections and include the use of microgels or epitomes for proteins, semi-covalent imprinting to minimize heterogeneity, surface imprinting and use of analogue templates to reduce fake positives and optimization to determine the best polymerization and upload conditions [13, 49]. Other general issues related to the use of MIPs for wide scale measurements are: recalibration when the MIP is used on site, the long-

term stability, the cost of such a device, the tradeoff between ruggedness and sensitivity and a low consumption of energy [9, 41]. These can be at most reduced slightly by thorough optimization steps. The cost of integrating a sensor to regularly calibrate the MIPs can be reduced by generating disposable polymers or labs-on-chips [55]. In terms of stability, for non-covalent imprinting, the weak binding interactions that govern the upload of analyte are affected more by changes in the upload environment and this is reflected in the output signal and the overall performance of the sensor. This can be reduced by adopting semi-covalent imprinting approaches. Improvements in the ruggedness are possible but these are done to the detriment of sensitivity.

If integrated into microchips and coupled to sensors, thin-film MIPs can be used for on-site on-line environmental monitoring, food and water analysis or simply biological applications [39]. A series of reports describe sensors coupled to a quartz microbalance, fiber optics and electrochemical detectors for analysis of small molecules, mainly persistent pollutants.

The persistent pollutants this research focused on are polycyclic aromatic hydrocarbons (PAHs). The next section will describe these compounds in terms of their occurrence, chemistry, health effects and current detection techniques to give a better understanding of the reasoning and urgency to develop imprinted materials for monitoring of these compounds in water.

## 1.3. PAHs

PAHs are ubiquitous toxic environmental contaminants with structures containing conjugated ring systems. According to the ring number, they can be classified into light PAHs with 2-4 rings and heavy PAHs with 4 to 8 rings. PAHs account for over 100 compounds that have been detected in air, water, soil and sediments [24, 42, 46, 56]. Many of these compounds have alkyl, nitro and amino functionalities, and heteroatoms such as nitrogen, sulfur and oxygen can be incorporated in the ring structures [3, 5, 46].

### 1.3.1. Definition and sources of PAHs

In 1775, Percival Pott found an association between the incidence of scrotal cancer in chimney sweeps and the exposure to soot [32, 42, 57]. Later in 1933 the main component of coal tar pitch was identified as benzo[*a*]pyrene (BaP), a compound in the class of PAHs [32]. These findings have catalyzed research in many fields to find out more about this class of compounds.

PAHs are released in the environment from anthropogenic and natural sources [28]. PAHs resulting from anthropogenic sources are either products of petrogenic activities, such as crude oil and derived products' leakages or results of incomplete combustion of coal, oil, wood and gas and pyrolysis of organic matter [17- 19, 24, 46, 56]. Natural sources are forest fires, volcanic eruptions, hydrothermal processes or natural leakage. These account for a smaller fraction of the total PAHs produced [17- 19, 24]. The precursors to PAHs are natural products, such as sterols in the case of PAHs found in crude oil [46].

Depending on the processes responsible for their formation and the temperature at which they occur, PAHs formed from petrogenic processes are most often light alkylated

PAHs, while those formed by combustion and pyrolysis are larger unsubstituted PAHs. Alkylated PAHs are those where the hydrogen atom on a ring has been replaced with an alkyl substituent. Petrogenic reactions occur at relatively low temperatures of 100 to 300 °C, over a long geological time scale when hydrocarbons re-arrange into small PAHs. These PAHs are more soluble in water and easier to detect, although mixtures of alkylated PAHs are difficult to separate by chromatography [58]. Most of these PAHs are released in the atmosphere and are transported to soils, water and gradually to biota by precipitation, snow, fog or currents [59]. The smaller ring number PAHs tend to be detected in seawater, possibly because of their higher solubility [14, 60].

During combustion at temperatures of 500 to over 700 °C, hydrocarbons in oil or coal crack, form unstable fragments and regroup into large PAHs [1, 61, 62]. The PAH structures and their complexity vary with the distinct temperatures of formation [1]. Similar PAHs form during pyrolysis. The heavier PAHs are more hydrophobic, less water soluble, thus more likely to adhere to particulates and sediments in water, and not as easily available for analysis. The concentration of the various petrogenic PAHs formed varies with the type and origin of the crude oil [63].

Exposure to PAHs has been shown to cause mutagenic, carcinogenic and genotoxic effects. This has caused national and international environmental health organizations to provide safety guidelines for allowed safe concentrations of PAHs in various media [60, 61]. The Environmental Protection Agency, US-EPA has identified 16 priority PAH pollutants and provided guidelines for their detection and quantification [64]. In Table 1.2, the structures of these PAHs, their molecular weight, water solubility and carcinogenic

potency are shown to assist in understanding their chemistry and behavior in the environment. Since the profile of BaP is similar to that of other PAHs of concern in foods, BaP is considered a marker such that the maximum safe contaminant level recommended by US-EPA is expressed as 0.2 µg $L^{-1}$ BaP in drinking water [61, 65].

Table 1.2. Name, structure, molecular weight, solubility in water and carcinogenic potency of the 16 priority PAHs as reported by US-EPA, [64, 66]

| Compounds | Structure | Molecular weight | Solubility in water (mg $L^{-1}$) at 25 °C | Carcinogenic potency IARC/ US EPA classification |
|---|---|---|---|---|
| Naphthalene |  | 128 | 32 | _ |
| Acenaphthylene |  | 152 | 3.93 | _ |
| Acenaphthene |  | 154 | 3.4 | _ |
| Fluorene | 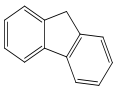 | 166 | 1.9 | _ |
| Phenanthrene | 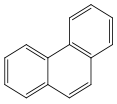 | 178 | 1.0-1.3 | 3 |
| Fluoranthene | 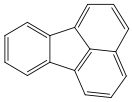 | 202 | 0.26 | 3 |
| Pyrene | 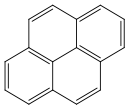 | 202 | 0.14 | 3 |
| Anthracene | 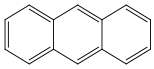 | 178 | 0.05-0.07 | 3 |

| | | | | |
|---|---|---|---|---|
| Benzo[*a*]anthracene | 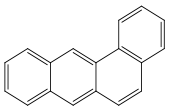 | 228 | 0.01 | 2A/B2 |
| Benzo[*a*]pyrene | 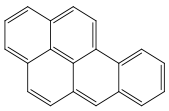 | 252 | 0.0038 | 2A/B2 |
| Chrysene | 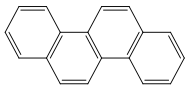 | 228 | 0.002 | 3/B2 |
| Dibenzo[*a,h*]anthracene | 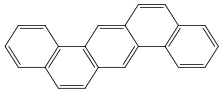 | 278 | 0.0005 | 2A/B2 |
| Benzo[*g,h,I*]perylene | 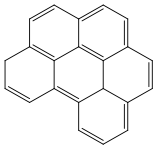 | 276 | 0.00026 | 3 |
| Benzo[*b*]fluoranthene | 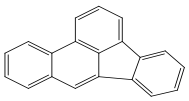 | 252 | _ | 2B/B2 |
| Benzo[*k*]fluoranthene | 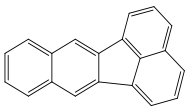 | 252 | _ | 2B |
| Indeno[1,2,3-*cd*]pyrene | 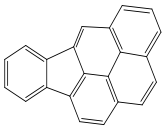 | 276 | _ | 2B/B2 |

2A/B2: Probably carcinogenic to humans;
2B: Possibly carcinogenic to humans;
3: Not classifiable as to human carcinogenicity;
Blank: Not tested for human carcinogenicity.
*IARC: International Agency for Research on Cancer; US EPA: US Environmental Protection Agency.

As suggested by their structures of fused benzene and cyclopentane rings, PAHs are non-polar hydrophobic compounds with high vapour pressure. Thus PAHs are soluble in

organic solvents or acids, and their volatility decreases with increase in molecular weight. PAHs are often released in the atmosphere, but there is migration to soils, water and gradually to biota influenced by seasonal weather phenomena [55, 59]. For example, in winter, both light and heavy PAHs are transferred from the atmosphere to soils and water through precipitation, snow or fog, while in summer, lighter PAHs can volatilize back into the atmosphere [59, 60]. The lower molecular weight PAHs have a higher solubility in water, such that water analysis for these compounds can be used as an indicator of the presence of other PAHs, or can assist in identifying their source in case of accidental spills by working out the ratio of lighter to heavier species [1]. The heavy, more hydrophobic PAHs are found associated with particulates in air, sediments or solubilized in oil fractions and droplets. Their degradation is slow and longer residence times cause accumulation mainly in vegetation, soils and water in this particular order, as suggested by studies carried in various areas in Asia [1, 59].

The aromaticity is delocalized throughout the molecule such that UV and fluorescence phenomena are possible. PAHs can be excited by UV radiation in sunlight making them more reactive with molecular oxygen, solvents or cell constituents [57]. Partially as a function of other compounds, PAHs can be oxidized to yield PAH quinone species or lower molecular weight products; or react with $NO_2$ or $NO_3$ radicals to form nitro-PAHs, following the reaction paths illustrated in Figure 1.10 [57, 59, 60].

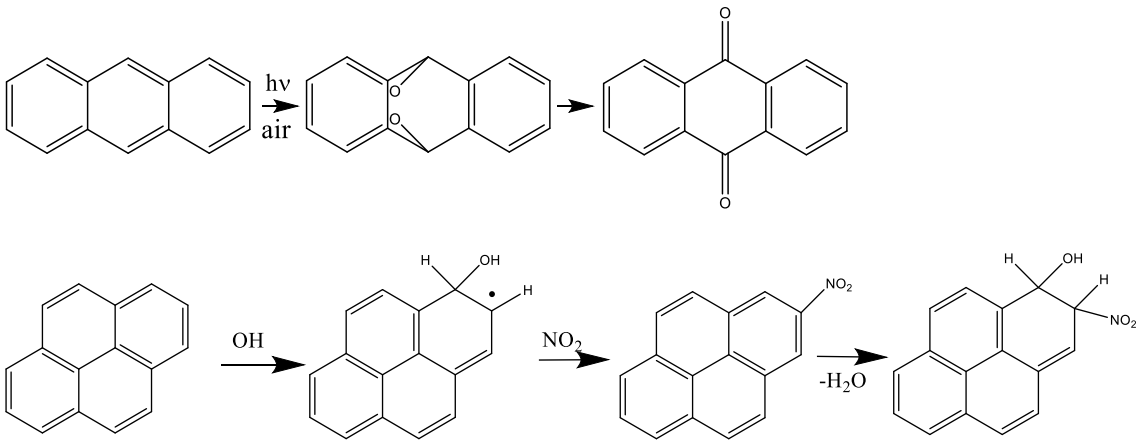


**Fig 1.10. Oxidation and nitration of PAHs, adapted with permission from [57]**

The products of these reactions are reactive species known to attack cell constituents by formation of DNA adducts [4, 57]. Sunlight is not the only catalyst in the chemical conversion of PAHs in the environment. Some species of fungi have been shown to halogenate PAHs [59]. The heavier PAHs have a more pronounced aromaticity due to the higher number of aromatic rings and hence they have a higher UV absorption capacity. This makes them more prone to these chemical changes [59].

PAHs and their by-products enter humans and other animals through inhalation, ingestion or dermal contact [57, 59, 65]. The following information on the metabolic fate of PAHs is based mainly on animal studies [65]. To facilitate their solubility and elimination, metabolism of PAHs occurs primarily in the liver and the kidneys into epoxides via CYP-450 enzymes [65]. The excretion half-life in feces and urine is between 22 and 28 hours, as reported by Becher and Bjorseth in 1983 [67]. The metabolites that form have been shown to induce growth of carcinogenic tumors or act synergistically with cancer cells with prolonged exposure [59, 61]. The lighter PAHs have a greater acute

toxicity, while the heavier PAHs are potentially more carcinogenic, more stable and less biodegradable [58, 61].

### 1.3.2. Sample treatment and detection methods – A brief overview

In general, two different approaches are used for assessing the concentration of PAHs in the environment. One route is by detection and quantification of all the 16 priority PAHs, which can involve some bulk quantification methods, such as fluorescence. The alternative is to selectively quantify a representative of the class, such as benzo[*a*]pyrene, the most potent identified carcinogenic PAH agent to act as a marker of the presence of other similar PAHs [24]. Regardless of the approach, all analyses of environmental samples containing PAHs entail sampling, pretreatment, detection and quantification. The interest in PAHs is evident from the number of sample treatment and analysis methods proposed in the specialized literature available on chemistry research databases such as SciFinder or ScienceDirect.

Depending on the nature of the sample, the pretreatment steps can be simple or complex but usually include at least a cleanup step or pre-concentration. This can prove difficult in a matrix containing a multitude of non-polar compounds since PAHs lack functionality and display high hydrophobicity. Nevertheless, a wide range of sample cleanup and pre-concentration methods have been used successfully [61, 66]. Of these, liquid extraction techniques are some of the oldest and most used extraction methods. In liquid phase extraction, liquid-liquid extraction or soxhlet extraction, organic compounds of low polarity partition in one of the two phases (normally an organic and an aqueous phase) based on the solubility in that phase. Problematic emulsions can form when

compounds with both lipophilic and hydrophilic properties are present. In addition, these techniques use large volumes of organic solvents, which render these methods expensive, polluting and time consuming.

More efficient alternatives have been solid-phase microextraction (SPME) or liquid-liquid microextraction (LLME), where small volumes of solvents are used. Solid phase extraction involves partitioning onto a solid adsorbent. These miniaturized techniques are efficient; however, the maintenance cost of the equipment used can be high and the issue of selectivity still remains. Cloud point extraction is an interesting pre-concentration method that uses surfactants to form micelles and selectively separate compounds based on their polarity [55].

Adsorbent materials investigated so far for removing PAHs from water samples include polymerin and lignimerin, activated carbon, porous carbon and imprinted polymers [47]. Other porous materials reported for adsorption of PAHs are waste avian egg shell or nanoporous polymorphic crystals of $CaCO_3$ [68]. Hydrophobic interactions govern adsorption of the PAHs into the egg shell pores but the material lacks the functionality of a MIP. The question of chemical selectivity has only been addressed through the use of molecular imprinting technologies that allow selective uptake of PAHs from complex samples. Storage following sampling is another issue, and protocols have been set in place regarding this aspect [4].

The most common detection techniques used in the methods proposed by the International Standardization Organization (ISO) and the US-EPA, are HPLC coupled with fluorescence or UV detection (EPA-610, EPA-8310 and ISO 17993:2002) and GC coupled

with MS (EPA-610 and EPA-8270D) [60, 61]. Other analytical techniques that have been used for the determination of PAHs in complex water samples are summarized in Table 1.3.

Most PAHs are actively fluorescent and can be detected in a mixture using specific excitation and emission wavelengths. High sensitivity down to 10 pg sensitivity is possible although the fluorescence signal intensity decreases for lighter PAHs such as naphthalene, acenaphthene, acenaphthylene and fluorene. UV spectroscopy is a reliable technique for detection of PAHs but it lacks the sensitivity of FLD, since the attainable detection limits by UV are in the low mg $kg^{-1}$ range [3].

Table 1.3. Summary of sample analysis and detection techniques for PAHs, [55, 61]

| Separation technique | Detection |
|---|---|
| LC | FLD |
| CE | UV |
| TLC | MS (ESI, APCI, APPI, DESI) |
| UHPLC | |
| GC | MS |
| | FID |

A valuable alternative to LC, especially for separation and analysis of weakly fluorescent low molecular weight and alkylated PAHs, is GC. It is argued that GC is

capable of better resolution of certain PAH peak pairs, such as anthracene/phenanthrene, when compared with LC [61].

GC coupled with MS is a powerful and versatile tool for volatile compounds. To enhance sensitivity, the selected ion monitoring (SIM) acquisition mode is frequently employed to enhance sensitivity.

The ionization techniques used mostly with modern MS are electrospray ionization (ESI) and atmospheric-pressure chemical ionization (APCI). Analysis in ESI results in little or no fragmentation and a strong protonated ion that enables easy identification, however this method of ionization may be ineffective for highly non polar compounds [68]. APCI is a soft ionization technique for polar and non polar low molecular weight compounds that occurs in atmospheric pressure conditions. This enhances the number of collisions between solvent ions and analytes, such that spectra are dominated by the molecular ion peak with little fragmentation [69]. A novel mass spectrometry ionization technique, desorption electrospray ionization (DESI) has been used successfully for the analysis of all 16 priority PAHs [70, 71]. DESI enables efficient ionization of low and non-volatile compounds such as explosives, herbicides, pesticides and pharmaceutical products in ambient conditions. The novelty of this technique is that no prior sample preparation steps are required [72].

Portability is another advantageous feature of a detector especially when it is cost effective. The reported techniques used for PAH sensing are fluorescence, field portable GC-MS and Raman spectroscopy [25]. Fluorescence and GC-MS are the techniques employed in the research described in this thesis.

### 1.3.3. MIPs for PAHs – A brief review

Preparations of MIPs for uptake of PAHs from various matrices and different applications of these systems have been reported by several research groups [16, 23, 31, 56, 73].

Krupadam *et al.* prepared MIPs for PAHs in bulk format from methacrylic acid, ethylene glycol dimethacrylate and 1,1′-azobis-isobutyronitrile in acetonitrile to measure existing or spiked PAHs in contaminated water, groundwater, coastal sediments and ambient air dust [16, 29, 30]. They used a multi-template imprinting of a group of six of the US- EPA priority PAHs with ring numbers ranging from 4 to 6 [16]. The sensors used were fluorescence and GC-MS. The MIPs sensitivity was 10 - 30 ng $L^{-1}$ in ground water, while in sediments and atmospheric particulates it was 0.1 - 2.9 µg $kg^{-1}$ [16, 30]. Given their large adsorption potential of 687 µg PAHs per g MIP, low manufacturing cost and possible regeneration, the use of these materials for environmental clean-up has been proposed [16].

The first report of a thin-film MIP for PAHs comes from Dickert's research group in 1999 [74]. They prepared polyurethane membranes in ambient conditions using bisphenol A and phloroglucinol monomers, *p,p′*-diisocyanatodiphenylmethane for crosslinking and tetrahydrofuran as the solvent. These membranes were used for the uptake of PAHs from aqueous solutions. The templates used varied from naphthalene on its own to a mixture of all the 16 priority PAHs. These membranes have been coupled to various sensors: FLD, quartz crystal microbalance (QCM), quartz microbalance (QMB), surface acoustic wave oscillator (SAW), UV and FTIR spectrometers [74-77]. UV and FTIR can

be used for rapid screening of PAHs while QCM and QMB sensors can monitor changes in the mass of the MIP as low as 1 pg in the case of QMB. Fluorescence spectroscopy proved to be highly sensitive and selective with detection limits as low as 30 ng $L^{-1}$ for pyrene although it had a low concentration threshold, due to formation of excimers [74]. The coupling of MIPs to a wide range of sensors demonstrates substantial potential for MIPs in analytical applications. However it is not clear how this system will behave in complex and harsh environmental conditions, although some of the potential issues such as the presence of possible interferences like humic acids, a common component of surface waters have been examined [75].

Polyurethane bonding was the basis of another film imprinted polymer targeting benzo(a)pyrene in water, reported by Gonzalez *et al.*, [73]. A phosphorescence detector coupled to the MIP was presented and sensitivities as low as 40 ng $L^{-1}$ were achieved [73]. The research into this subject was limited to one conference proceeding article, [73], which indicates just a proof of principle.

Similar interest in developing MIPs from 4-VP, DVB, AIBN in ACN-DCM, 80:20 v/v for detection of benzo(a)pyrene was expressed in the research of Lai *et al.*, [31]. MIPs were prepared by bulk and suspension polymerization, then were used for binding in SPE and HPLC columns. The results showed superior selectivity and recovery in tap water, lake water and coffee samples compared to a traditional $C_{18}$ SPE column [31].

The most recent account of MIPs for PAHs is the work of Chen *et al*. [23]. MIP membranes were developed by sol-gel imprinting on a solid substrate of silica particles for solid phase extraction coupled with GC-MS of PAHs in artificial seawater. A mixture of all 16 priority

pollutants was used for templating. Although seawater is a complex matrix, the large MIP surface area enabled detection limits ranging from 5.2 to 12.6 ng $L^{-1}$ for various individual PAHs [23].

The one aspect that all the previous reports of MIPs for PAHs have in common is that all use the same template as the target analyte. Removal of the template is often not appropriately dealt with. Excessive volumes of organic solvents are used for lengthy washes, which can damage the morphology of the polymer and are not sustainable. If the template is not completely removed then it can be difficult to claim low detection limits. A summary of previous work done on MIPs targeting PAHs is presented in Table 1.4.

Table 1.4. Summary of the research into MIPs for PAHs

| Investigator | Dickert [56, 74- 77] | Krupadam [16, 29, 30] | Chen [23] | Gonzalez [73] | Lai [31] |
|---|---|---|---|---|---|
| Template | acenaphthene<br>anthracene<br>benzo[a]anthracene<br>crysene<br>naphthalene<br>perylene<br>phenanthrene<br>pyrene | benzo[a]anthracene<br>benzo[a]pyrene<br>benzo[b]fluoranthene<br>crysene<br>dibenzo[a,h]pyrene<br>indeno[1,2,3]pyrene | all 16 priority pollutants | benzo(a)pyrene | benzo(a)pyrene |
| Type | film | bulk | film | film | bulk, microspheres |
| Composition | bisphenol A,<br>phloroglucinol<br>p,p′-diisocyanato<br>diphenylmethane<br>THF | MAA<br>EGDMA<br>ACN<br>AIBN | Phenyltrimethoxy-<br>silane<br>tetraethoxysilane<br>ACN<br>$CH_3COOH$ | bisphenol A, MDI<br>phloroglucinol<br>THF | 4-VP<br>DVB<br>ACN: DCM<br>AIBN |
| Matrix | water | air, sediments, water | water | water | water, coffee |
| Sensor | QCM<br>UV<br>FTIR<br>SAW<br>FLD | FLD<br>GC-MS | GC-MS | phosphorescence | SPE<br>HPLC |
| Imprinting factor | not determined | 2.37- 3.66 | 1.5- 3.12 | na | 8.4 |
| Lowest sensitivity | QCM - low mg $L^{-1}$<br>fluorescence- 30 ng $L^{-1}$ | 10 µg $L^{-1}$ | 5.2-12.6 ng$L^{-1}$ | 40 ng $L^{-1}$ | |

MDI - methylene diphenylene diisocyanate

### 1.4. Detection methods used with MIPs

MIPs have been coupled to a wide variety of sensors both online and offline [27]. It is beyond the scope of this chapter to offer a detailed insight into these techniques. Hence, the discussion has been limited to the techniques used in the research carried out in the following chapters.

#### 1.4.1. Gas chromatography

GC is a very popular separation technique and has been used in official US-EPA methods for analysis of PAHs coupled with FID in EPA-610 and with MS in EPA-8270D [60]. In GC, as the oven temperature is gradually increased, the compounds primarily separate according to their boiling points [61]. When coupled to MS, GC-MS becomes a powerful method for structural and quantitative analysis of volatile compounds; such that is has been used in official EPA detection methods EPA-625 and EPA-8270D. However, GC-MS does not adequately resolve heavier, priority PAHs: anthracene/phenanthrene, chrysene-benzo[α]/anthracene, benzo[b]fluoranthene/benzo[k]fluoranthene, and dibenzo[α,h]anthracene/ indeno[1,2,3-cd]pyrene.

#### 1.4.2. Mass spectrometry

MS is one of the most versatile analytical tools. Using fragmentation patterns and specific mass to charge ratios (m/z), MS can provide information on the composition of a sample in both organic and inorganic compounds, elemental analysis and the isotope ratio of the atoms [72]. Depending on the polarity of a compound, various ionization techniques exist. For relatively small non-polar molecules, such as PAHs with two to four rings, the

ionization techniques reportedly used are electron ionization (EI), electrospray ionization (ESI), atmospheric pressure chemical ionization (APCI) and atmospheric pressure photoionization (APPI). APCI and APPI are coupled to LC when working at low flow rates, however they have been successfully coupled to gas chromatography (GC) as well.

EI is a commonly used energetic ionization technique in GC-MS as it is suitable for stable volatile compounds. As shown in Figure 1.11, the sample is introduced in the source in gas phase where it is bombarded by a beam of fast moving electrons generated by a heated filament.

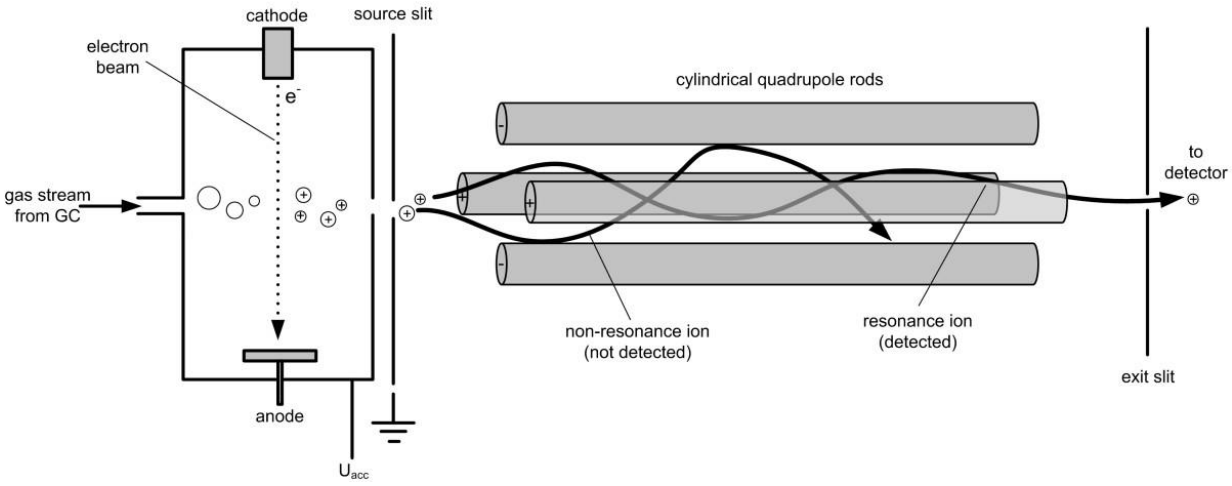


**Fig. 1.11. Electron ionization source coupled to a quadrupole mass analyzer adapted with permission from [78]**

The quadrupole mass filter is one of the most popular mass analyzers because it is compact, relatively inexpensive, highly sensitive and easy to operate. The quadrupole consists of four parallel metallic rods, as described in Figure 1.11. A fixed direct current,

(DC) voltage, and an alternating radio frequency, (rf) voltage, are applied to a pair of diagonally opposite rods. To the opposite pair of rods a DC voltage of opposite sign and an rf voltage with a 180° phase shift are applied. As the current alternates from positive to negative, the ions resonate between the negative and the positive rods. Ions with varying masses can be scanned by varying DC and rf while maintaining their ratio. Hence, for specific DC and rf values, ions of specific m/z values have a stable trajectory into the detector. The quadrupole is a low resolution analyser.

### 1.4.3. Fluorescence

Fluorescence is a radiative emission of photons from a molecule as it returns from an excited singlet state to the ground state. This concept can be better explained by use of the Jablonsky diagram in Figure 1.12. When a molecule is excited, electrons from a singlet ground state electron pair are promoted to a higher energy level without a change of spin. For the molecule to return to the ground state, energy is lost as non-radiative emission by transferring it to the surrounding molecules in the form of vibration, rotation or translation or as radiative emission of photons via a phenomenon called luminescence [79]. The emission of a photon occurs at a speed of $10^{-8}$ nanoseconds. Fluorescence is part of the broad category of the phenomena of luminescence.

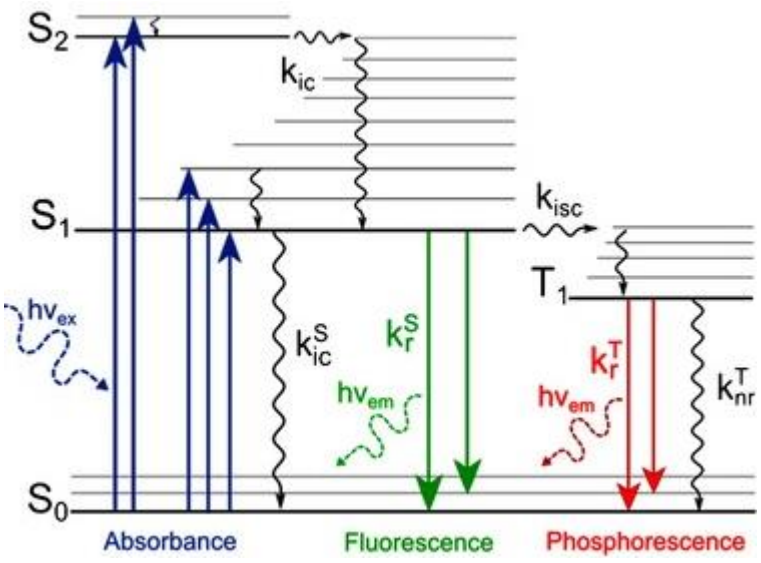


**Fig. 1.12. Jablonski diagram adapted with permission from [80]**

PAHs are known compounds capable of fluorescence referred to as fluorophores. The fused aromatic rings with conjugated double bonds and the rigidity of the molecule that does not allow for any translational, vibrational or rotational movements make the excited lifetime states of these molecules to be long enough, for the phenomenon of fluorescence to be observed and measured. However naphthalene, fluorene, acenaphthene, acenaphthylene PAHs give poor fluorescence signals [1]. These effects are most probably caused by the lower aromaticity associated with the presence of a cyclopentane ring in the case of the latter compounds. Despite the high sensitivity recorded in the measurement of PAHs, use of fluorescence is limited to low concentrations of PAHs. A higher amount of PAHs can result in formation of excimers that ultimately quench the fluorescence signal.

### 1.5. Microfluidic devices

Although coupling imprinting technology to a sensor for rapid and sensitive monitoring and detection of low concentration targets has been expressed in a number of articles, [46, 54, 81], very few reports of this coupling exist. Most of these reports have not crossed the barrier from a proof of principle, MIP based sensor to the consumer market. The interest in developing such systems lies in the capacity of a lab on a chip to integrate all the functions carried out in a normal laboratory setting out in the field in real time and using a limited amount of sample, which is an important factor especially in biomedical applications (e.g. blood). Microfluidics can be made using different approaches; however, the emphasis in this particular work was made on using low-tech methods such as soft lithography. The detection technique sought for the thin-film MIPs prepared in this work was MS. Despite its large instrumental footprint, mass spectrometry is highly suitable for coupling to microfluidic devices because it can achieve similar flow rates to those necessary in microfluidic devices and can provide high sensitivity [48]. For portability reasons, attempts to reduce interfaced microchips-MS for *in situ* analysis have started early in 1990 [67].

The applications for a microfluidic system containing a MIP are virtually unlimited and can range from high throughput analysis in laboratories and hospitals, to monitoring in environmental samples or for detection of narcotics and explosives in public settings [46, 81].

### 1.6. Thesis Objectives

Molecularly imprinted polymers continue to draw attention due to the extensive range of applications in many fields of chemistry and the great potential for large scale commercialization. Applications of current interest are the use of MIPs for environmental analysis for trace contaminants in the local and international context of oil extraction from the sea floor, discharge of produced water back into the ocean and monitoring of compounds indicating oil spills. In this thesis, the aim has been to advance environmental analysis and to develop commercially viable alternatives to traditional methods of analysis for contaminants in water. To reach this goal, a series of specific objectives had to be achieved, as follows:

1. First, it was necessary to review the literature to identify the PAHs relevant to monitoring of oil spills in water and provide the background to MIP preparation and analysis. From the review that is presented in the introductory chapter, four PAHs have been selected that are most representative of fresh inputs of crude oil contamination in water, namely naphthalene, fluorene, phenanthrene and pyrene.
2. The next objective was to develop a MIP selective for these light PAHs in water. Considering the previous reports of analysis of PAHs using MIPs [14, 21, 33, 68] and the current challenges to this type of analysis, thin-film MIPs using a toluene pseudo-template for the uptake of a group of four light PAHs were prepared. The pseudo-template enabled accurate determination of PAHs in aqueous samples at environmentally representative concentrations with no false positives. Chapters 2 and 3 describe two different thin-film MIP compositions targeting PAHs.

3. The next goal was to optimize the composition of the imprinted polymers to achieve a maximum response. Trial-and-error experiments are described in Chapters 2 and 3, while an experimental design approach is taken in Chapter 3.
4. Validation of the MIP method of analysis was achieved through evaluation of the sensitivity at low upload concentrations, selectivity in a complex matrix and in the presence of possible inhibiting compounds, and linearity over different upload amounts or over different upload time periods in various binding experiments. Both Chapters 2 and 3 describe these steps.
5. The applicability of the MIPs to environmental, complex aqueous samples was demonstrated through MIP binding tests in wastewater and seawater with no sample preparation or conditioning steps. The excellent sensitivity, recovery concentrations and linearity of response achieved indicate that both MIP compositions proposed can be readily used for real time analysis. These systems could be used successfully offline as demonstrated in Chapters 2 and 3 when coupled to a simple GC-MS equipped with a single quadrupole analyser. Alternatively, the MIPs could be integrated into a microfluidic device, and coupled online to a detection system for on-site real time analysis.
6. To achieve this goal, surface treatment experiments and different soft lithography, photolithography and etching techniques were tested and optimised. Chapter 4 describes all the efforts taken to manufacture efficiently, and with little use of technology, a microfluidic device from ITO coated glass slides with etched electrode pads and PDMS micro patterned surfaces.

### 1.7. Co-authorship statement

Chapter 2 was submitted for publication in peer reviewed journals with Stefana N. Egli as first author, Erika D. Butler as co-author and Dr. Christina S. Bottaro as the corresponding author. Chapter 3 was prepared for submission with Stefana N. Egli as first author, Kerri E. Burton as co-author and Dr. Christina S. Bottaro as corresponding author. Chapter 4 is a manuscript in preparation with Stefana N. Egli as first author and Dr. Christina S. Bottaro as the corresponding author. Chapter 5 includes ongoing and future work and conclusions.

The first author (Stefana N. Egli) contributed to all research chapters as the main investigator which included: literature review, performing and proposing new experiments, collecting and analyzing the data, writing the first drafts and preparing all necessary documents for the online paper submission. In addition, the first author acted as a mentor for two summer students, Kerri E. Burton and Erika D. Butler, by providing training with the experimental methods, the instruments and data collection and devising and supervising the experiments. Kerri E. Burton as a co-author followed the experimental method as devised by the first author and collected the data to produce some of the results in the experimental design section of Chapter 3. Erika D. Butler as a co-author followed the instructions of the first author to analyze seawater samples for PAHs using MIPs and to confirm certain linearity studies. Data from this work was used by the first author in calculations and figures presented in Chapters 2 and 3.

The idea of using PAHs as a class of targeted analytes arose from literature reviews and discussions between Stefana N. Egli and Dr. Christina S. Bottaro. The first author

proposed the idea of using toluene as a pseudo template and 1-octanol as a solvent. This would probably not have been possible without active discussions with the corresponding author, Dr. Christina S. Bottaro. In addition, the corresponding author has contributed to suggesting some of the method validation steps experiments, the use of experimental design in optimizing the MIP preparation and has revised the drafts of all the chapters with very helpful suggestions.

## 1.8. References


1. L. Wolska, A. Mechlińska, J. Rogowska, J. Namieśnik, Crit. Rev. Env. Sci. Technol. 42 (2012) 1172-1189
2. R. Greenwood, G.A. Mills, B. Roig, Trends Anal. Chem. 26 (2007) 263-267
3. R.N. Okparanma, A.M. Mouazen, Appl. Spectrosc. Rev. 48 (2013) 458-486
4. K. Hawboldt, B. Chen, W. Thanyamanta, S. Egli, A. Gryshchenko, Review of Produced Water – Management and Challenges in Harsh/Arctic Environments, submitted to the American Bureau of Shipping (ABS), 2010
5. A. Murray, B. Ormeci, Environ. Sci. Pollut. Res. Int. 19 (2012) 3820-3830
6. P. Manesiotis, G.A. Theodoridis, Encyclopedia of Chromatography, third ed., Taylor & Francis, 2010, pp 24-30
7. R. Arshady, K. Mosbach, Macromol. Chem. Phys. 182 (1981) 687-92
8. M.J. Whitcombe, M.E. Rodriguez, P. Villar, E.N. Vulfson, J. Am. Chem. Soc. 117 (1995) 7105-7111
9. J.L. Bowen, P. Manesiotis, C.J. Allender, Molecular imprinting 1 (2012) 35-40
10. L.X. Chen, S.F. Xu, J.H. Li, Chem. Soc. Rev. 40 (2011) 2922–2942
11. X. Shi, S. Song, A. Sun, J. Liu, D. Li, J. Chen, Analyst 137 (2012) 3381-3389
12. F. Chapuis, V. Pichon, M.C. Hennion, LC-GC Europe (2004) 408-417
13. R.C. Advincula, Korean J. Chem. Eng. 28 (2011) 1313-1321
14. X. Liu, H. Jia, L. Wang, H. Qi, W. Ma, W. Hong, J. Guo, M. Yang, Y. Sun,Y.F. Li, Ecotoxicol. Environ. Saf. 90 (2013) 151-156

15. A. Ellwanger, C. Berggren, S. Bayoudh, C. Crecenzi, L. Karlsson, P.K. Owens, K. Ensing, P. Cormack, D. Sherrington, B. Sellergren, Analyst 126 (2001) 784- 792
16. R.J. Krupadam, M.S. Khan, S.R. Wate, Water Res. 44 (2010) 681-688
17. www. mipdatabase.com-accessed on 18/07/2013
18. P.A. Lieberzeit, F.L. Dickert, Anal. Bioanal. Chem. 393 (2009) 467-472
19. B. Sellergren, M. Lepisto, K.J. Mosbach, J. Am. Chem. Soc. 110 (1988) 5853-5860
20. V.T. Remcho, J.Z. Tan, Anal. Chem. News Feat. (1999) 248A-255A
21. C. Baggiani, C. Giovanolli, L. Anfossi, C. Passini, P. Baravalle, G. Giraudi, J. Am. Chem. Soc. 134 ( 2012) 1513-1518
22. D.A. Spivak, R. Simon, J. Campbell, Anal. Chim. Acta 504 (2004) 23-30
23. X. Song, J. Li, S. Xu, R. Ying, J. Ma, C. Liao, D. Liu, J. Yu, L. Chen, Talanta 99 (2012) 75–82
24. L.I. Andersson, A. Paprica, T. Arvidsson, Bioinorg. Chem. 25 (1997) 203-211
25. H. Kim, D.A. Spivak, J. Am. Chem. Soc. 125 (2003) 11269-11275
26. D.A. Spivak, Adv. Drug Deliver. Rev. 57 (2005) 1779-1794
27. F. Meier, B. Mizaikoff B., Artificial receptors for chemical sensors, first edition, Wiley-VCH, 2011, pp 391-437
28. K. Haupt, Anal. Chem. (2003) 377A- 383A
29. R.J. Krupadam, B. Bhagat, M.S. Khan, Anal. Bioanal. Chem. 397 (2010) 3097-3106
30. R.J. Krupadam, B. Bhagat, G.L. Bodhe, B. Sellergren, Y. Anjaneyulu, Environ. Sci. Technol. 43 (2009) 2871-2877

31. J.P. Lai, R. Niessner, D. Knopp, Anal. Chim. Acta 522 (2004) 137- 144

32. I. Yungerman, S. Srebnik, Chem. Matter. 18 (2006) 657-663

33. E.V. Piletska, A.R. Guerreiro, M.J. Whitcombe, S.A. Piletsky, Macromol. 42 (2009) 4921-4928

34. B. Sellergren, K.J. Shea, J. Chromatogr. A 635 (1993) 31-49

35. S. Mallik, New. J. Chem. 18 (1994) 299-304

36. G.D Olsson, B.C.G. Karlsson, S. Shoravi, J.G. Wiklander, I.A. Nicholls, J. Mol. Recognit. 25 (2012) 69- 73

37. F. Wang, H. Yan, R. Wu, T. Cai, K. Han, Z. Li, Anal. Method. 5 (2013) 2398-2405

38. R.A. Lorenzo, A.M. Carro, C. Alvarez-Lorenzo, A. Concheiro, Int. J. Mol. Sci. 12 (2011) 4327- 4347

39. L. Levi, V. Raim, S.J. Srebbnik, J. Molec. Recognit. 24 (2011) 883- 891

40. B. Dirion, Z. Cobb, E. Schillinger, L.I. Andersson, B. Sellergren, J. Am. Chem. Soc. 125 (2003) 15101-15109

41. C. Iuga, E. Ortiz, L. Norena, NSTI-Nanotech. 3 (2011) 777- 780

42. G. Wulff, K. Knorr, Bioseparation 10 (2002) 257-276

43. N. Iqbal, P.A. Lieberzeit, Molecularly Imprinted sensors, first edition, Elsevier, 2012, pp 195-235

44. B.R. Hart, K.J. Shea, J. Am. Chem. Soc. 123 (2001) 2072- 2073

45. I.A. Nicholls, J.P. Rosengren, Bioseparation 10 (2002) 301-305

46. A. McCluskey, C.I. Holdsworth, M.C. Bowyer, Org. Biomolec. Chem. 5 (2007) 3233-3244

47. A.A. Costa, W.B. Wilson, H. Wang, A.D. Campiglia, J.A. Dias Micropor. Mesopor. Mat. 149 (2012) 186-192
48. W.J. Cheong, S.H. Yang, F. All, J. Sep. Sci. 36 (2013) 609-628
49. H. Kim, K. Kaczmarski, G. Guiochon, Chem. Eng. Sci. 60 (2005) 5425-5444
50. R.J. Umpleby, G.T. Rushton, R.N. Shah, A.M. Rampey, J.C. Bradshaw, J.K. Berch, K.D. Shimizu, Macromol. 34 (2001) 8446- 8452
51. C. Baggiani, G. Giraudi, C. Giovannoli, C. Tozzi, L. Anfossi, Anal. Chim. Acta, 504 (2004) 43-52
52. J. Svenson, J.G. Karlsson, I.A. Nicholls, J. Chromatogr. A 1024 (2004) 39-44
53. O. Péron, E. Rinnert, M. Lehaitre, P. Crassous, C. Compère, Talanta 79 (2009) 199-204
54. R.J. Umpleby II, S.C. Baxter, A.M. Rampey, G.T. Rushton, Y. Chen, K.D. Shimizu, J. Chromatogr. B 804 (2004) 141- 149
55. J. Guo, T. Ntakirutimana, X. Gao, D. Gong, Adv. Mat. Res. 524-527 (2012) 1739-1750
56. F.L. Dickert, O. Hayden, K.P. Halikias, Analyst 126 (2001) 766-771
57. P.P. Fu, Q. Xia, X. Sun, H. Yu, J. Environ. Sci. Health 30 (2012) 1-41
58. J.R. Law, J.L. Biscaya, Mar. Pollut. Bull. 235 (1994) 4-5
59. S. Manzetti, Polycyclic Aromatic Hydrocarbons in the Environment: Environmental Fate and Transformation, Taylor & Francis Group, 2013, pp 311-330

60. D.M. Pampanin, M.O. Sydnes, Polycyclic Aromatic Hydrocarbons a Constituent of Petroleum: Presence and Influence in the Aquatic Environment, Hydrocarbon, Dr. Vladimir Kutcherov, 2013, pp 83-118
61. G. Purcaro, S. Moret, L.S. Conte, Talanta 105 (2013) 292-305
62. US Department of Health and Human Services- Public Health Service, Toxicological profile for polycyclic aromatic hydrocarbons, august 1995
63. J. M. Kerr, H. R. Melton, S. J. Mc Millen, R. I. Magaw, G. Naughton, G. N. Little, Polyaromatic hydrocarbon content in crude oils around the world. Conference paper from the 1999 SPE/EPA Exploration and production environmental conference held in Austin, Texas, USA, 1999, 28 February-3 March
64. Environmental Protection Agency (EPA), Method 8310- Polynuclear aromatic hydrocarbons, <http://www.epa.gov/osw/hazard/testmethods/sw846/pdfs/8310.pdf >, (July 2013); Method 8100- Polynuclear aromatic hydrocarbons, http://www.epa.gov/osw/hazard/testmethods/sw846/pdfs/8100.pdf, (September 2013)
65. http://www.atsdr.cdc.gov/csem/pah/docs/pah.pdf -accessed 08/07/2013
66. E. Manoli, C. Samara, Trends Anal. Chem. 18 (1999) 417-428
67. G. Becher, A. Bjørseth, Cancer Lett. 17 (1983) 301–311
68. J. de Boer, R.J. Law, J. Chromatogr. A 1000 (2003) 223-251
69. P. Östman, S. Jäntti, K. Grigoras, V. Saarela, R.A. Ketola, S. Franssila, T. Kotiaho, R. Kostiainen, Lab Chip 6 (2006) 948-953
70. M. Li, H. Chen, B.F. Wang, X. Yang, J.J. Lian, J.M. Chen, Int. J. Mass Spectrom. 281 (2009) 31-36

71. H. Chen, M. Li, Y.P. Zhang, X. Yang, J.J. Lian, J.M. Chen, J. Am. Soc. Mass. Spectrom. 19 (2008) 450-454

72. J.M. Wiseman, D.R. Ifa, Q. Song, R.G. Cooks, Angew. Chem. Int. Ed. 43 (2006) 7188-7192

73. J. Gonzalez, J.C. Campo, M. Valledor, F.J. Ferrero, J.M. Traviesa, J.M. Costa, R. Pereiro, A. Sanz-Medel, I2MTC 2008 - IEEE International Instrumentation and Measurement Technology Conference, Victoria, Vancouver Island, Canada, May 12-15, 2008

74. F.L. Dickert, M. Tortschanoff, Anal. Chem. 71 (1999) 4559-4563

75. F.L. Dickerton, P. Achatz, K. Halikias, Fresen. J. Anal. Chem. 371 (2001) 11-15

76. P.A. Lieberzeit, K. Halikias, F.L. Dickert, Anal. Bioanal. Chem. 392 (2008) 1405-1410

77. F.L. Dickert, O. Hayden, Adv. Mater. 12 (2000) 311-314

78. C. Wittmann, Microb. Cell Fact. 6 (2007) 6-22

79. J.R. Lakowicz, Principles of Fluorescence Spectroscopy, second edition, Kluwer Academic/ Plenum Publishers, New York, 1999, pp 1-11, 53, 55, 187-188, 238-242, 638-639; P. Atkins, J. de Paula, Atkins' Physical Chemistry, seventh edition, Oxford University Press, 2002, pp 258-262, 550-551, 926- 927, 930-931, 962

80. M. Quaranta, S.M. Borisov, I. Klimant, Bioanal. Rev. 4 (2012) 115-157

81. R. Schirhagl, K.N. Ren, R.N. Zare, Sci. China Chem. 55 (2012) 469-483

# Chapter 2. Novel pseudo-template thin-film molecularly imprinted polymers for detection of polycyclic aromatic hydrocarbons in aqueous samples

## 2.1. Abstract

Thin-film molecularly imprinted polymers (MIPs) are sorption materials that allow for selective uptake and detection of low concentrations of pollutants, such as polycyclic aromatic hydrocarbons (PAHs), in complex aqueous matrices. To avoid quantitative inaccuracies caused by template bleeding, pseudo-templates can be used for imprinting. In this context, novel thin-film MIPs using toluene as a pseudo-template, 4-vinyl pyridine (4-VP) as functional monomer, ethylene glycol dimethacrylate (EGDMA) as cross-linker, 2,2-dimethoxy-2-phenylacetophenone (DMPA) as initiator and octanol as porogen were developed and optimized. The target compounds in this work are light PAHs: naphthalene, fluorene, phenanthrene and pyrene. Both the MIP preparation and sample uptake procedure are fast, low-tech, green and present no template bleeding issues. The MIPs were coupled to gas-chromatography-mass spectrometry (GC-MS) in selected ion monitoring (SIM) mode for offline analysis. Binding assays in standard aqueous solutions and wastewater samples using the MIPs showed superior selectivity over the non-imprinted materials and linearity for both types of materials over at least 2 orders of magnitude (10-100 μg $L^{-1}$). Calculated detection limits were as low as 18 ng $L^{-1}$ for naphthalene. Analysis of spiked PAHs in real influent wastewater and seawater samples was carried out successfully

considering no prior sample preparation steps were involved. Good recoveries of spiked PAHs from the wastewater were obtained and remarkable linearity with the lowest $R^2 \geq 0.978$ for naphthalene in seawater at spiked levels of 0.5 to 5.0 µg $L^{-1}$ was achieved.

## 2.2. Introduction

Polycyclic aromatic compounds (PAHs) represent a large class of non-polar organic compounds with a structure of two or more fused benzene rings. These compounds have been shown to possess carcinogenic and mutagenic effects such that monitoring guidelines for sixteen PAHs have been established by the United States Environmental Protection Agency (US-EPA). The PAHs with a smaller number of aromatic rings contained in the US-EPA list are mainly released into the environment in an unsubstituted or alkylated form from petrogenic sources (e.g. seeps), discharge of produced water, accidental spills or controlled release of petroleum products [1-4]. Depending on the solubility and hydrophobicity, which vary with the molecular weight, PAHs ultimately end up in ground water, vegetation, soils and oceans [1, 4, 5]. Light PAHs in seawater could thus indicate crude oil or petroleum contamination in water, which is relevant in an era of deep sea oil extraction. An extensive range of articles and reviews have been dedicated to describing and proposing analytical methodologies for the determination of PAH in various matrices as reflected by the 2008 Coelho *et al.* review [5]. Given the low concentrations of PAHs in the environment and the complexity of real samples, several requirements consistently appear, such as efficient sampling with no losses during storage (due to PAH hydrophobicity and volatility), effective pre-concentration and possibly clean-up steps, and methods that give efficient separations with selective detection and quantification [1]. Molecular imprinting technologies are useful in addressing most of these issues by selectively targeting PAHs in complex samples.

Molecularly imprinted polymers (MIPs) are smart materials with remarkable molecular recognition properties that rely on the memory of shape, size and position of functional groups of the template molecule. The MIPs have a similar uptake mechanism to biological antibodies. The advantages of using MIPs are the chemical and physical stability, easy preparation and the ability to recognize small organic molecules [6]. Typically, the material is made by polymerization from a solution containing a functional monomer, a cross linking agent, an initiator, a porogen and a template (usually the target analyte). Since the template must be bound to the monomer either through covalent or non-covalent interactions prior to polymerization, the approaches for MIP preparation are often categorized accordingly. Non-covalent bonding occurs through hydrogen bonding, Van der Waals forces, π-π interactions, etc., and can be particularly useful because the template can be easily released and the analyte uptake is favored by fast mass transfer [6].

For successful imprinting, the composition and all preparation steps – from identifying the most suitable components of the pre-polymerization complex to determination of the best template removal and analyte uptake conditions – must be optimized, most often through tedious experiments. For example, even a process as simple as template removal is key, where incomplete removal of the template can generate errors in accuracy (i.e. template bleeding) and may result in fewer cavities available for efficient re-binding. Template bleeding is an ongoing challenge and complete template extraction is hard to achieve [7]. Various template removal techniques have been reported, such as conventional solvent extraction, or Soxhlet extraction, sonication, and supercritical solvent extraction, but most often the stability of the imprinted cavities is at risk when aggressive

methods are used [7, 8]. Alternatives to avoid these tedious steps have been proposed such as isotope molecular imprinting, parallel extraction on blank samples and pseudo-template imprinting, though these still have drawbacks [9]. In this paper, pseudo-template imprinting was chosen based on toluene; its structure and functionality are similar to the target molecules and any residual template will not interfere with quantitation. In this case, the pseudo-template is smaller than the actual target analyte giving enhanced uptake of target analytes as reported by Dickert *et al.* [10, 11], but is also in contrast to other work in which larger pseudo-templates were used [12].

MIPs can be polymerized as bulk polymers, suspension particles or as thin-films on an inert support or membrane. Thin-film MIPs eliminate long sample preparation steps, can be interfaced with sensors for on-site monitoring or can be coupled with offline detection [13]. There has been a steady interest in developing effective imprinted polymers for uptake of PAHs and the first report of a thin-film MIP for PAHs was published by Dickert's research group in 1999, when polyurethane membranes were developed for use with a fluorescence detector, resulted in good sensitivity, and a prediction that a sensitivity of 30 ng $L^{-1}$ should be achievable [14]. The versatility of these MIP membranes for various applications is demonstrated in the range of sensors to which they have been successfully coupled, e.g., the quartz microbalance, fluorescence and surface acoustic wave oscillator [14]. Although described mostly as proof of principle, Gonzalez *et al.* proposed a phosphorescence detector for thin-film MIPs for bisphenol A with sensitivities as low as 40 ng $L^{-1}$ [15]. The most recent account of MIPs for PAHs is the work of Chen *et al.* [16]; MIP membranes were developed by sol-gel imprinting on a solid substrate of silica particles

for traditional solid phase extraction coupled with GC-MS of PAHs in seawater. Used as SPE packing, the large MIP surface area provided for detection limits ranging from 5.2 to 12.6 ng $L^{-1}$ for a mass of polymer of 150 mg in extensive prior conditioning [16]. Krupadam *et al.* developed MIPs in bulk format for uptake of PAHs from air and water [17].

In this work the preparation of a novel thin-film MIP with a toluene pseudo-template is described for uptake of PAHs with offline detection by GC-MS in SIM mode and fluorescence. Binding assays carried out in aqueous standards or real influent wastewater samples show superior selectivity of the MIPs over the corresponding non-imprinted polymers, NIPs, though there is a linear response for both materials. The direct applicability of these MIPs to environmental samples at relevant concentrations with no prior sample preparation is demonstrated by linear calibration curves with excellent coefficients of variation obtained for analysis in raw seawater and wastewater and good recovery concentrations in wastewater samples. The method gives sensitive detection limits for real water samples, for example as low as 18 ng $L^{-1}$ for naphthalene from spiked municipal wastewater.

## 2.3. Materials and Methods

### 2.3.1. Materials

Naphthalene, fluorene, phenanthrene and pyrene were used as models for PAH classes with different ring numbers as shown in Figure 2.1.

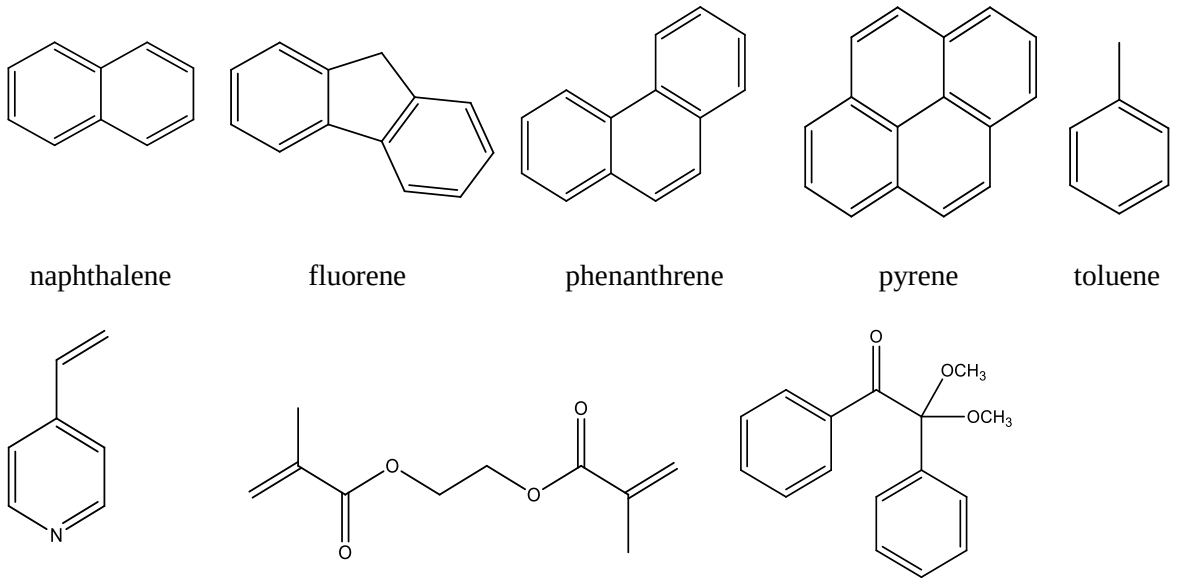


**Fig. 2.1. PAHs and MIP components structures**

Standards of naphthalene (99%), fluorene (99%), phenanthrene (99.5%) and pyrene (99%) were purchased from Sigma-Aldrich (St. Louis, Mo, USA) and were used without further purification. All organic solvents (toluene, ethyl ether, dichloromethane, acetonitrile and hexanes) were purchased with minimum 99.5% purity from ACP Chemicals. All compounds used in the preparation of the thin-film MIPs: 3-(trimethoxysylil) propyl methacrylate derivatizing agent, the 2,2-dimethoxy-2-phenylacetophenone (DMPA) initiator, ethylene glycol dimethacrylate (EGDMA) cross-linker, 4-vinyl pyridine (4-VP) monomer were purchased from Sigma-Aldrich in the best grade available and were used without further purification.

### 2.3.2. Derivatization of glass slides

Glass microscope slides were prepared for derivatization by cleaning in a solution of MeOH and HCl. The slides were then immersed overnight in a solution of 2.0% 3-(trimethoxysylil) propyl methacrylate in toluene. The resulting functionalized surface was rinsed with ethanol, dried under nitrogen and stored in the dark.

### 2.3.3. Preparation of the MIPs

The pre-polymerization mixture was prepared by pipetting or by weighing into a 2 mL vial the pseudo-template toluene, initiator DMPA, crosslinking agent EGDMA, monomer 4-VP and porogen 1-octanol (Table 2.1).

Table 2.1. MIP and NIP composition

| Pre-polymer component | MIP | NIP |
|---|---|---|
| toluene | 4.25 µL (0.0405 mmol) | _ |
| 4-VP | 17.0 µL (0.158 mmol) | 17.0 µL (0.158 mmol) |
| EGDMA | 151 µL (0.801 mmol) | 151 µL (0.801 mmol) |
| DMPA | 3.20 mg (0.0125 mmol) | 3.20 mg (0.0125 mmol) |
| 1-octanol | 200 µL (1.26 mmol) | 204 µL (1.28 mmol) |

An 8.0 µL aliquot of the pre-polymerization complex was dispensed on the derivatized glass surface and covered with a glass microscope cover-slide to minimize oxygen interference in the polymerization reaction. This "sandwich" was placed directly under a UVP handheld UV lamp ($\lambda$ = 254 nm, 6 watt) at ambient temperature (~20 °C) for 30 min.

Following removal of the cover slides, the imprinted polymers were soaked in ethyl ether for two hours to remove the pseudo-template and unbound polymer components.

### 2.3.4. Upload and analyte extraction

Stock multi-component solutions with each PAH at a concentration of 100 mg $L^{-1}$ were prepared in acetonitrile daily. Working solutions were prepared by appropriate dilution of the stock solutions with distilled water. For binding tests, a thin-film MIP was immersed in 80.0 mL of aqueous PAH solution under continuous stirring at room temperature (approximately 20 °C) for specified time intervals.

The MIPs were removed from the upload solution, rinsed with a small volume of water and dried briefly with a stream of nitrogen to remove visible water. The analytes were extracted in 10.0 mL of ethyl ether under stirring for two hours. The solvent was removed from the extract under reduced pressure with a rotary evaporator and made to volume with DCM in a 1.00 mL volumetric flask. Concentrations of PAHs measured in these solutions are referred to as recovery concentrations in this paper. Depending on the type of test, other factors were considered, such as concentrations of PAHs or upload times were varied.

### 2.3.5. Characterization of MIPs

The physical characteristics of the MIPs and NIPs were established by studies of morphology by SEM and film thickness using a KLA-Tencor Alpha Step Development Series Stylus Profiler D-120 profilometer. SEM images were recorded using a FEI MLA 650F SEM, operating at an accelerating voltage of 10 kV and a magnification of 50,000 times. All samples were sputtered with gold prior to analysis.

Analytical performance criteria were characterized with GC-MS and fluorescence. GC-MS was performed with an Agilent Technologies 6890 gas chromatograph coupled to an Agilent 7683 Series Injector and Agilent 5973 inert Mass Selective Detector (MSD). Compounds were ionized by electron ionization at 70 eV and mass spectra were acquired in selected ion monitoring (SIM) mode (Table 2.2).

Table 2.2. GC-MS settings: Quantifier and qualifier ions used to identify the PAHs

| Analyte | Quantifier (m/z) | Qualifier (m/z) |
|---|---|---|
| naphthalene | 128 | 127 |
| fluorene | 165 | 166 |
| phenanthrene | 178 | 176 |
| pyrene | 202 | 200 |
| octane | 114 | 85 |
| octanol | 97 | 84 |
| p-cresol | 108 | 107 |
| acenaphthene-$d_{10}$ | 162 | 158 |

Separation was carried out on a DB-5MS column capillary column (0.25 mm x 30 m) with a 0.25 µm stationary film thickness. The oven temperature was programmed as follows: initially at 45 °C (held for 0.8 min), increased to 200 °C at a rate of 45 °C $min^{-1}$, then to 216 °C at a rate of 5 °C $min^{-1}$, and finally to 260 °C at a rate of 10 °C $min^{-1}$. The total time for all analytes to be detected was ~12 min. The injector temperature was set at 290 °C, and the injection was performed in splitless mode. The carrier gas, helium with a purity of

99.999% had a flow rate of 1.3 mL $min^{-1}$. The calibration curves for PAH determinations were obtained by linear regression of data from analysis of multi-component solutions made in three concentrations ranges for each PAH: 0.500–10.00 µg $L^{-1}$; 10.00–100.0 µg $L^{-1}$ and 100.0–3000 µg $L^{-1}$. Fluorescence measurements were performed with a PTI (Photon Technology International) QuantaMaster 6000 Fluorometer. The excitation wavelength was 276 nm and data were collected at an emission wavelength of 303 nm.

## 2.4. Results and discussion

### 2.4.1. MIP preparation

Novel white opaque thin-film MIPs using toluene as a pseudo-template were prepared rapidly, using little organic solvent and low tech equipment: such as a vortex mixer, a sonicator and a hand held UV-lamp. SEM imaging of the imprinted polymer available in Figure 2.2 suggested a high degree of porosity.

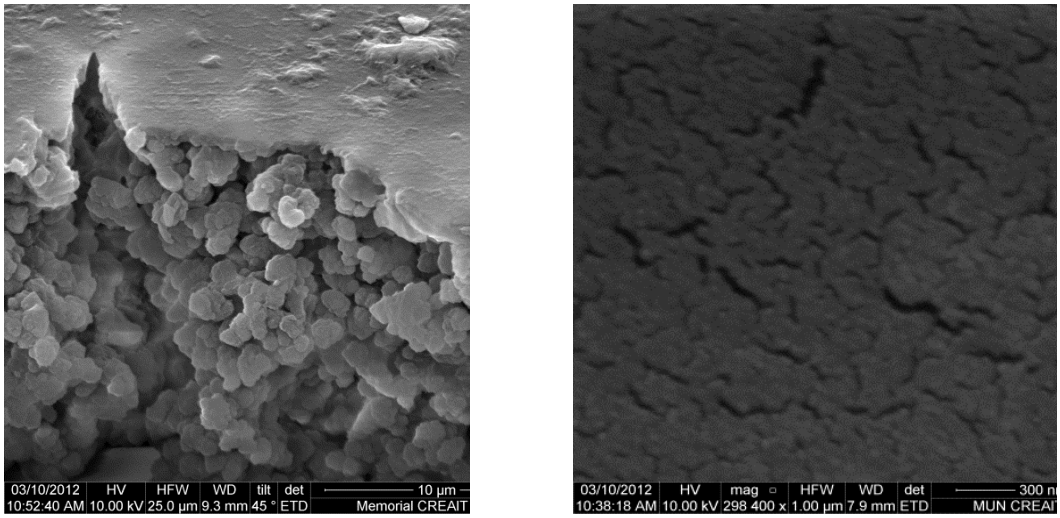


**Fig. 2.2. SEM micrograph of the MIP at 10 µm and 300 nm scales**

Thickness measurements of the MIP and NIP films showed a similar thickness for MIPs of 66.1 ± 0.90 µm as for NIPs of 65.6 ± 0.46 µm. A direct correlation was not found between the mass of the polymer, which varied from 2.10 - 3.71 mg for a constant surface area of 2.25 $cm^2$, and uptake of analyte. This is consistent with the idea that binding in these materials occurs near the surface, thus it was unnecessary to normalize the detector response to the mass of polymer in every instance. Because of the low mass of the polymer thin-film and the large relative mass of the glass slide limiting weighing to a four decimal place balance, data would have been limited to three significant figures when normalizing.

The main novelty of these MIPs lies in the use of a pseudo-template that is smaller than the target analytes. The pseudo-template approach has obvious advantages when it comes to template bleeding and for use with PAHs in particular, where even large PAH molecules will have substructures that are very similar to the structure and chemistry of toluene. Initially, we investigated the effect of the size of the various PAH templates on the uptake of key PAH targets. We noticed that use of phenanthrene as the template increased selectivity towards uptake of pyrene from a solution containing equal concentrations of pyrene and naphthalene. This was contrary to the expected "steric exclusion effect" anticipated for compounds larger than the template as discussed by Spivak *et al.* [12]. They observed that for some systems fast mass transfer kinetics favor small molecules with the optimum steric fit for accessible sites. However, findings published in Dickert *et al.* [10, 11] support our observations; they reported that addition of 20% naphthalene to the pyrene template in the pre-polymerization solutions gave a significant improvement in the uptake of pyrene compared to pyrene or naphthalene

templates alone [11]. To test the hypothesis that a smaller template can give MIPs with improved selectivity towards larger targets, PAH uptake from a 0.100 μg $L^{-1}$ PAH in the multi-component standard solution was measured for a series of MIPs made with different templates (toluene, naphthalene, fluorene, phenanthrene and pyrene) in an octanol porogen (Figure 2.3). The small template was selected from a range of compounds with one aromatic ring, with consideration given to lack of substitution by heterofunctionality and the toxicological profile [18]. Generally, all MIPs showed a good sensitivity and selectivity towards PAHs, with a higher uptake of the analyte by the MIP made with matching the template. However, since the analytes are analyzed as amount taken up by the polymer (as opposed to amount remaining in uptake solution), the possibility of template bleed cannot be fully excluded and the final assessment of the performance of a given MIP was based on the extraction efficiency for non-template targets, for example, a fluorene MIP toward phenanthrene or naphthalene. As can be seen in Figure 2.3., the highest uptake for all PAHs was observed for the toluene MIP, thus, the results of the performance of this new thin-film pseudo-template PAH MIPs are reported and discussed here.

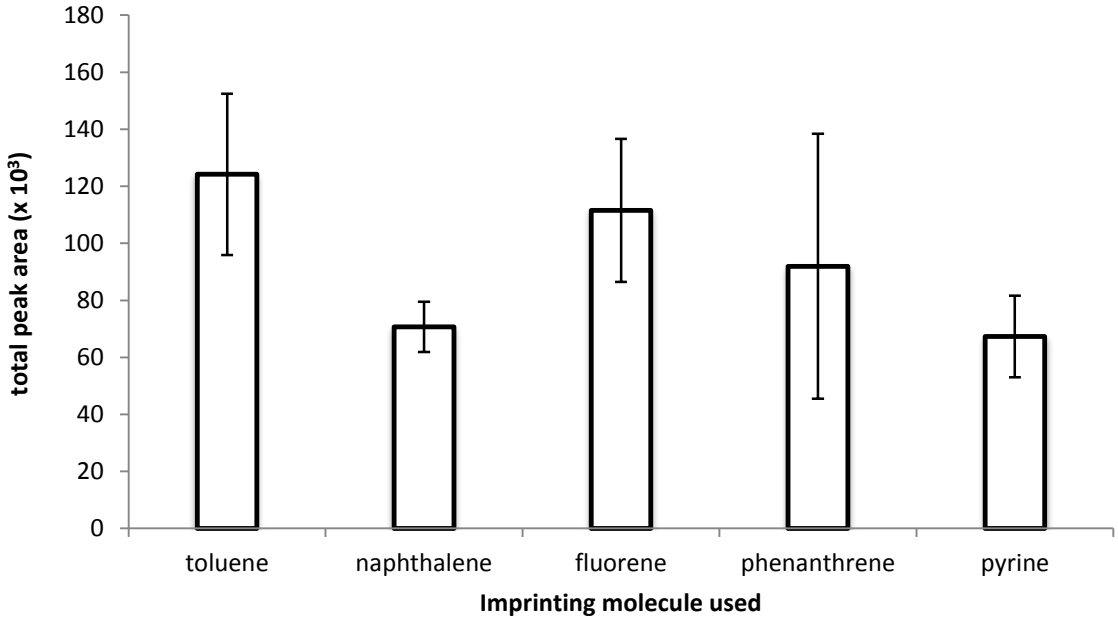


**Fig. 2.3. Total peak area corresponding to total PAH upload from 0.1 µg $L^{-1}$ for two hours PAHs, for MIPs with different templates; GC-MS in SIM mode**

The selection of the other components of the pre-polymerization complex was guided by extensive trial and error experiments, but the options with respect to composition tested were based on those proposed by others for non-polar targets [3, 17, 19, 20]. The final MIP composition used in the performance testing reported here was made from 4-VP as functional monomer, EGDMA as cross-linking agent and 1-octanol as porogen (Table 2.1). Some special attention was given to the selection of the appropriate porogen, as it influences the physical and chemical characteristics of the MIP, and it must also solubilize all the components of the pre-polymerization mixture while ensuring a stable chemical environment during polymerization. Sellergren and Shea [21] reported that the polarity and hydrogen bonding capacity of a porogen influence the growing polymer chain during the

phase separation process, and thus affect the morphology of the imprinted polymer. Therefore, for a non-covalent imprinted polymer, a non-polar porogen with a low dielectric constant can substantially increase the selectivity of a MIP [21]. A number of solvents were tested as porogens, DCM: MeOH: $H_2O$ (1:3:1), toluene itself ($\varepsilon = 2.38$), ethyl ether ($\varepsilon = 4.3$), and octanol ($\varepsilon = 10.3$), with octanol giving the best analytical performance. We believe that octanol performed well because, although it is generally considered hydrophobic, it has some polar character. The result is a material with good wetting properties when in contact with water, but also appropriate non-polar characteristics for binding hydrophobic compounds like PAHs as reflected by their high log $K_{ow}$ range values: naphthalene, log $K_{ow\ (naphthalene)} = 3.5$ to log $K_{ow\ (pyrene)} = 4.9$ (Table 2.3).

Table 2.3. Physicochemical properties and carcinogenic potency of the PAHs studied

| Compound | MW | Log $K_{ow}$ | Water solubility at 25°C (mg $L^{-1}$) | Melting point (°C) | Vapour pressure at 25 °C (mPa) | Carcinogenic potency (IARC/US EPA classification) | Concentration in produced water (µg $L^{-1}$), [29] |
|---|---|---|---|---|---|---|---|
| naphthalene | 128.16 | 3.5 | 31.7 | 80.5 | 11960 | | 5.3-394 |
| fluorene | 166.23 | 4.18 | 1.98 | 116.5 | 94.7 | | 0.06- 21.7 |
| phenanthrene | 178.24 | 4.5 | 1.29 | 101 | 90.7 | 3* | 0.11- 32.0 |
| pyrene | 202.26 | 4.9 | 0.135 | 156 | $91.3x10^{-6}$ | 3 | 0.01- 1.9 |
| toluene | 92.14 | 2.69 | | | | | _ |
| 1-octanol | 130.23 | 2.8-3.15 | | | | | _ |

To determine the optimum template and analyte extraction solvent, we looked for a compound with a similar polarity index to toluene ($P'_{toluene} = 2.4$) to effectively match the template but lacking aromaticity to avoid any binding to the polymer network through π-π interactions, that could possibly inhibit uptake of PAHs. We found that ethyl ether with $P'_{ethyl\ ether} = 2.8$ was effective, it is also volatile, which makes the analyte extracts easy to concentrate.

The polymerization and uptake conditions were optimized through a series of experiments that will not be presented in detail here. For example, we found that stirring is a factor that influences considerably the uptake which indicates a diffusion limited process. Stirring ensures continuous replenishment of the analyte near the surface of the polymer. MIPs were left for upload in 80.0 mL of 10.0 μg $L^{-1}$ multi-component PAH solutions for 18 hours in stirring and standing modes (Figure 2.4).

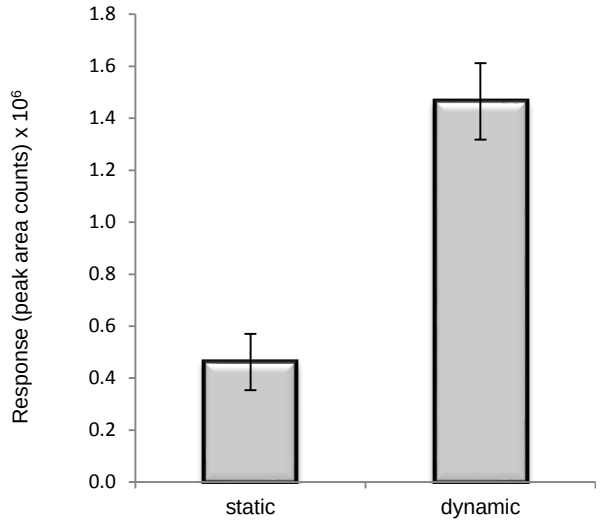


**Fig. 2.4. Effect of stirring over the binding for MIPs, over 18 h (n=3). The response is the mean value of three measurements. Bars represent standard deviation.**

Analyte uptake was three times higher in dynamic mode than in standing mode. Stirring favored replenishment at the surface of the diffusion layer with new analytes, which in turn favored frequent interactions of PAHs with the cavities and a higher uptake.

### 2.4.2. Binding capacity of MIP

In non-covalent imprinted polymers the template-monomer interactions are weak such that equilibrium has to be shifted towards using all the template molecules by addition of monomer in excess. Despite this, only 10-15% of the template molecules are used to form high affinity binding sites in non-covalent imprinting, and cavities with varying structure and affinity are formed [21-23]. This results in heterogeneous MIP surfaces and non-linear response curves in sensors [23]. Optimization of the imprinting process could afford systems that yield linear response curves with varying slopes for distinct concentration ranges. Furthermore, the amount of excess non-complexed monomer is distributed randomly into the polymer network, adding functionality to the polymer surface outside of the binding cavities. This may be one of the factors responsible for non-specific binding in both MIPs and NIPs [24].

To evaluate the selectivity of the MIPs and NIPs, a series of two hour binding experiments in aqueous PAHs solutions with concentrations in the 10.0-120 μg $L^{-1}$ were run. Figures 2.5 (a) and (b) show the uptake of PAHs by MIPs and NIPs in terms of the peak area with respect to the initial upload concentration. The slopes show that sensitivity is higher for the MIPs than for the NIPs.

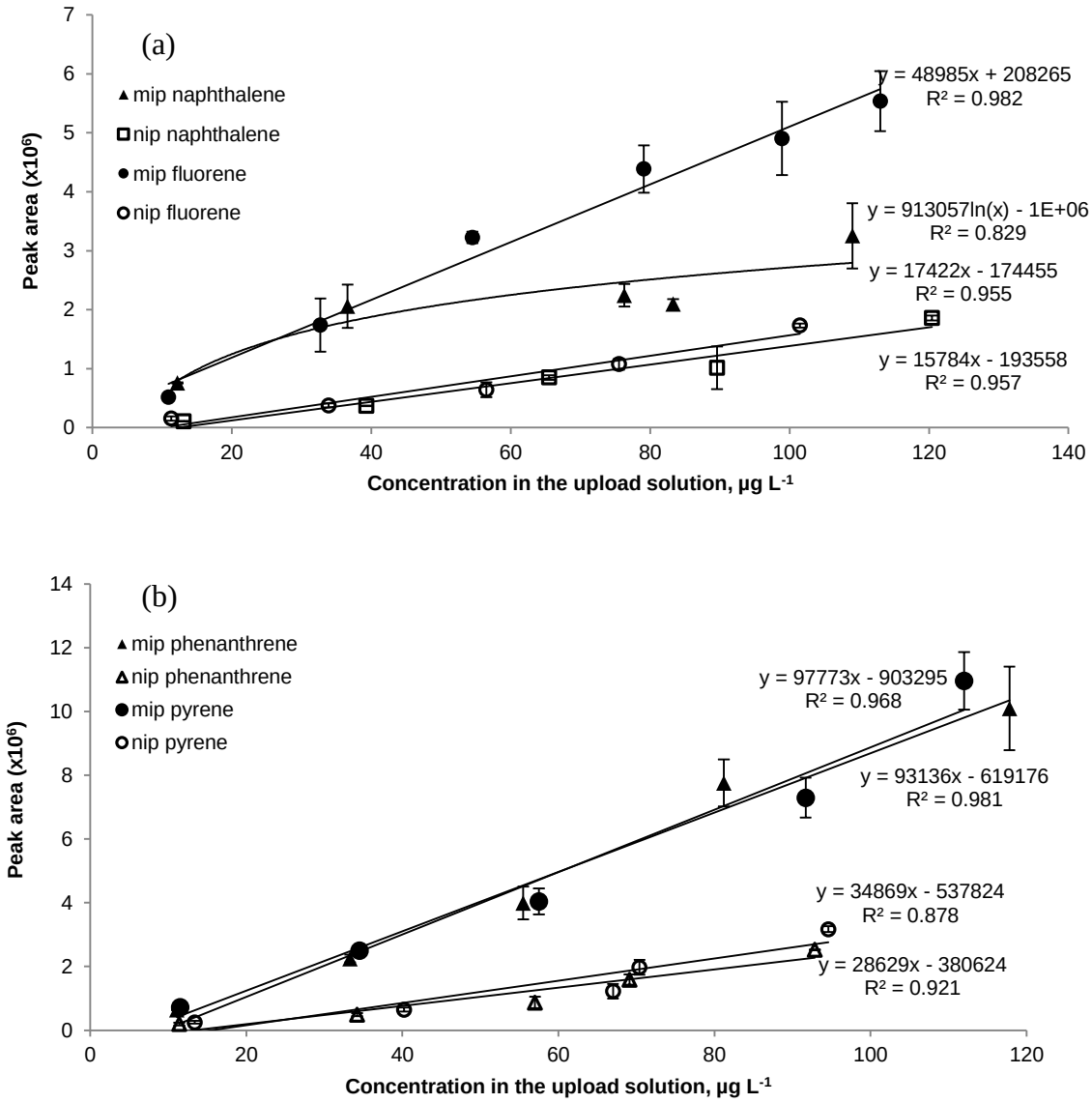


**Fig. 2.5. Increase in peak area of MIPs and NIPs defined as the amount extracted of (a) naphthalene and fluorene, and (b) phenanthrene and pyrene determined by comparison to a calibration curve for MIPs and NIPs with increase in the upload concentration; experimental conditions of 80.0 mL sample for two hours, GC-MS in SIM mode. The response is the mean value of three measurements. Bars represent standard deviation.**

The higher overall linear sensitivity of MIPs is indicative of a higher affinity of the MIPs for PAHs, which can be attributed to selective binding through π-π type interactions between the PAHs and the functionalized polymer network as well as conformational aspects of molecular recognition [14]. The MIPs showed the highest sensitivity toward pyrene and phenanthrene, followed by fluorene. All the curves show a clear linear relationship between uptake and concentration, except in the case of naphthalene (curved line in Figure 2.5 (a)), which starts to level off around 60.0 μg $L^{-1}$. It is likely that naphthalene uptake is inhibited by the increase in concentration of other larger, more hydrophobic PAHs; further data demonstrating this competitive effect will be presented in this thesis.

Some PAHs, such as fluorene and phenanthrene have angled geometries (thus lower electron densities), while naphthalene and pyrene have planar structures and higher electron density [16]. A bent geometry can enhance binding into the cavities with appropriate shape and functionality, but changes in their conformations can also be distorted to fit in smaller cavities. These aspects of geometry combined with the fact that hydrophobicity of PAHs increases with molecular mass, provide a MIP material with a higher selectivity towards phenanthrene, pyrene and fluorene. Similar conclusions were reported by Song *et al.* [16].

The NIPs showed uptake even in absence of the selective cavities associated with the presence of template. To some extent this was anticipated; the PAHs can interact with the aromatic monomer through π-π interactions, as well as the bulk polymer through hydrophobic effects. This is supported by the consistent level of sensitivity for all PAHs

(see regression data in Figure 2.5. (a) and (b)), which also highlights the non-selective uptake by the NIPs.

### 2.4.3. Characterization of heterogeneity

To assess the heterogeneity of the MIP surface several types of binding assay experiments can be used, for example, concentration in the uptake solution can be kept constant and the exposure intervals are varied, or concentration can be varied for a specific time period. In this work, an experimental binding isotherm was obtained by equilibrium binding experiments at a constant upload concentration of 10.0 μg $L^{-1}$ PAH over a range of time intervals that varied from 30 min to 23 h. The amount of analyte extracted was measured directly by GC-MS in SIM mode. We also measured the residual concentration by fluorescence, as has been done by other researchers [17], thereby indirectly determining the amount extracted by calculating the decrease from the initial concentration. We found that it was challenging to accurately determine by fluorescence low concentrations of individual PAHs in multi-component mixtures. Nevertheless, characterization of the MIP performance using fluorescence measurements for total PAHs were still quite useful and the uptake calculated displayed a similar trend to the results obtained by GC-MS.

In a first binding assay, where the upload time was varied for a constant concentration, a steady linear PAH upload was observed for the first three hours. With increase in the upload time, the amount of PAHs leveled out giving a typical adsorption isotherm (Figure 2.6). This could be useful for a rapid analysis of PAHs when a high uptake could be reached within the first three hours. For this reason, most uploads in the binding assays presented here were carried out within two hours. If time was not an easy factor to

control, which is the case in environmental remote sensing, then uptake carried out in the 4 to 23 h range could ensure a constant maximum response. The shape of the response curve over time may be rationalized by understanding the chemistry of the MIP, where the material is thought to be made of both highly selective sites with appropriate geometry and chemistry, which should show more rapid binding behavior. All the PAHs fit an adsorption isotherm profile, except for naphthalene (Figure 2.6.), which decreases over time.

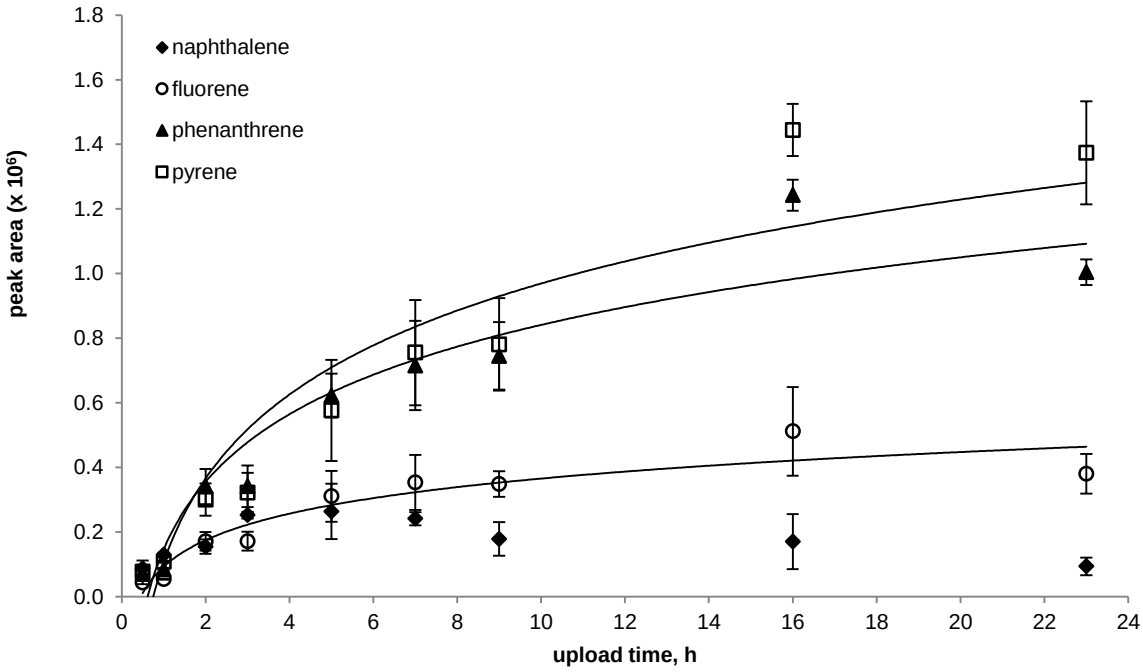


**Fig. 2.6. Effect of upload time on the peak area of the signal of four PAHs at experimental conditions of 80.0 mL sample (10 µg $L^{-1}$), GC-MS in SIM mode. The response is the mean value of three measurements. Bars represent standard deviation.**

A possible explanation for this effect may be the semi-volatile nature of naphthalene. This has been observed and reported previously, where it was shown that

storing a solution containing naphthalene in an opened container leads to loss of the analyte within very short time intervals [25]. Also, to a certain extent, adsorption onto the glass surface could be considered.

Fluorescence was used to determine the residual concentration of PAHs in the above experiment. A low intensity signal was observed for naphthalene and fluorine individually, such that the estimate of the uptake was expressed as the overall signal of PAHs, thus the overall amount. The fluorescence data shown in Figure 2.7 (b) gives a similar adsorption curve to the overall amount of PAHs detected by GC-MS in Figure 2.7 (a).

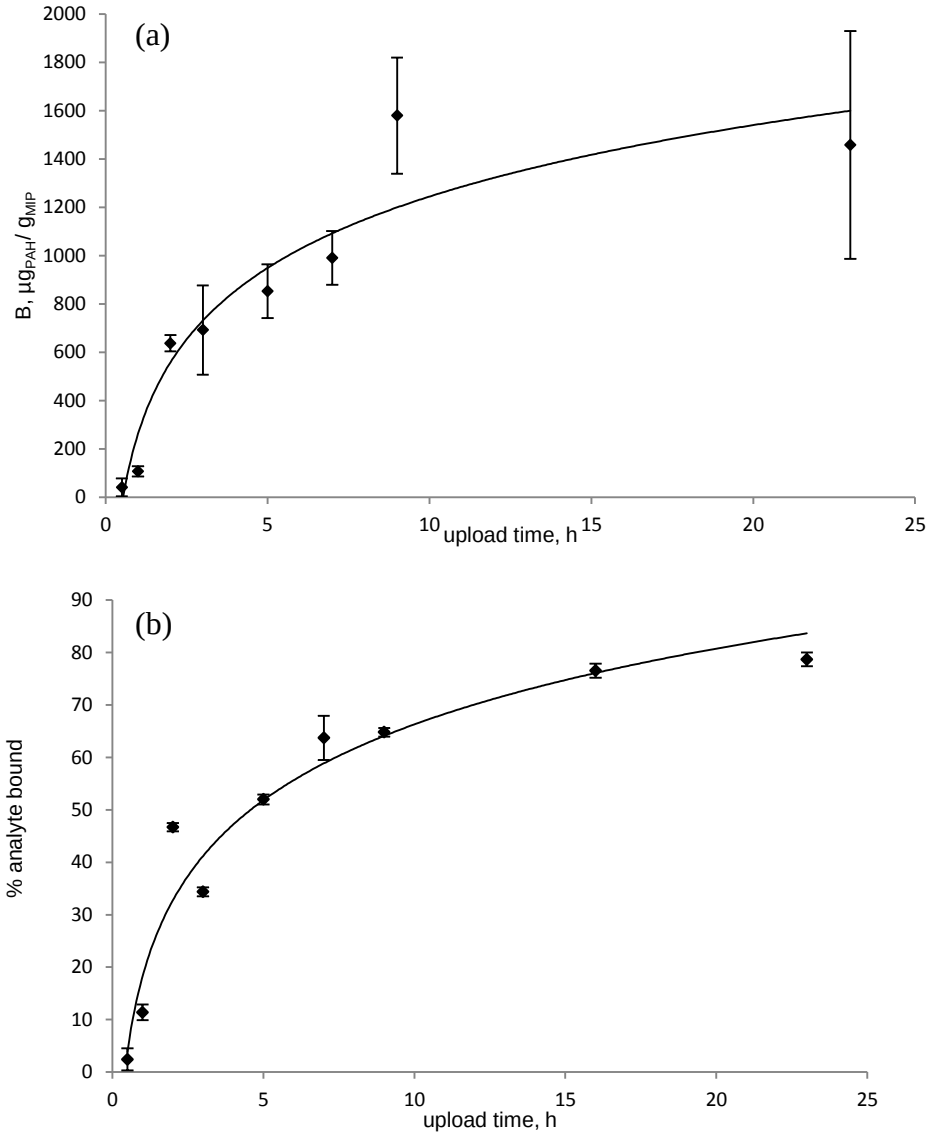


**Fig. 2.7. Effect of upload time on the concentration recovery of the total amount of PAHs for a 80.0 mL sample (10 µg L$^{-1}$) (a) overall binding capacity expressed as** $B = \frac{\mu g\ PAH}{g\ MIP}$ **, measured by GC-MS in SIM mode (b) percent recovery in aqueous PAH multicomponent solution expressed as** $\% = \frac{m_{PAHs\ bound\ to\ MIP}}{m_{PAHs\ in\ aqueous\ solution}} x100$ **, fluorescence measurements. The response is the mean value of three measurements. Bars represent standard deviation.**

This confirms that both the more selective and direct measurements by GC-MS are suitable to the purpose, and that in this instance the mass of the polymer is not relevant in assessing the binding properties of the thin-film MIPs, which may also indicate that uptake is mainly a surface or near-surface phenomenon.

Longer exposure times may be needed for *in situ* monitoring applications, and longer experiments could also yield improved detection limits, thus binding assays for linearity and capacity were carried out over a longer period of time. MIPs were equilibrated for 19 h in multi-component PAH aqueous standards at varying concentrations: 1.00; 4.00; 6.00; 10.0; 30.0; 50.0 and 80.0 μg $L^{-1}$ with four replicates for each system. Direct analysis of the extracts by GC-MS showed a linear trend with high correlation coefficients for all the PAHs (Figure 2.8) even after exposure of the MIPs to concentrations higher than 80.0 μg $L^{-1}$. Pyrene and phenanthrene showed highest upload, as with the previous study (Figure 2.5.(b)).

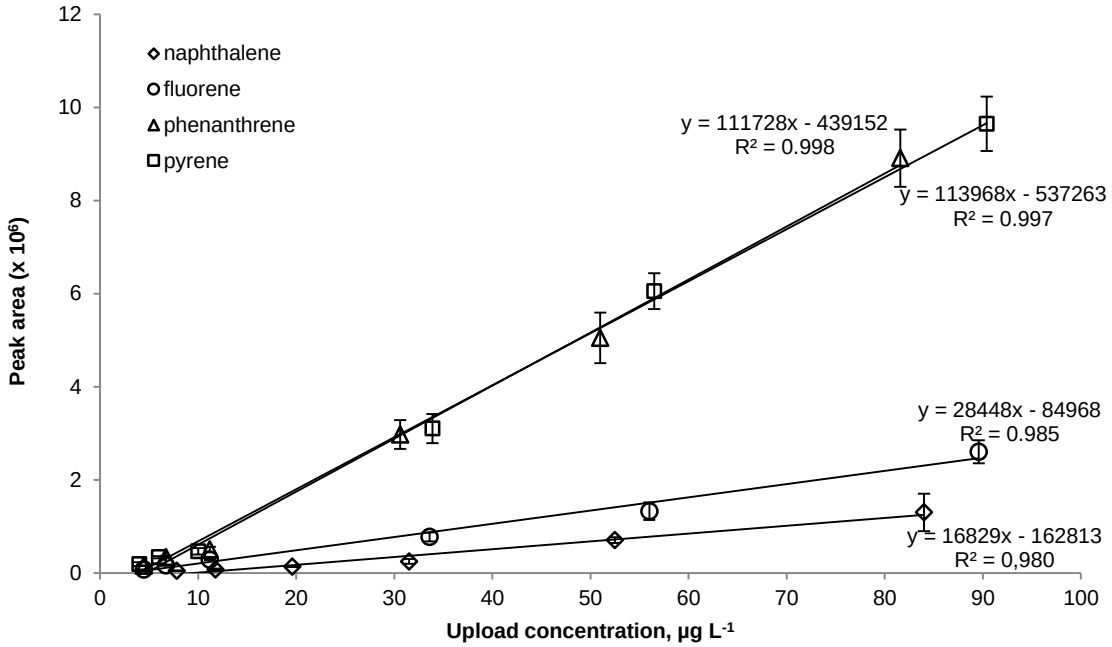


**Fig. 2.8. Calibration curve constructed as peak area of each PAH against upload concentration; experimental conditions: upload over 19 h; GC-MS measurements. The response is the mean value of three measurements. Bars represent standard deviation.**

### 2.4.4. Inhibition studies

Since applications to real-world samples will involve highly complex mixtures of PAHs and other components of oil it was interesting to assess the degree of competition for binding sites between the different PAHs in the uptake process. These interactions were evaluated by comparing the percent recovery when the MIP was exposed to pure solutions of 10 µg $L^{-1}$ of naphthalene or 10 µg $L^{-1}$ pyrene single PAH solutions versus a 10 µg $L^{-1}$ naphthalene and pyrene multi-component solutions, [10, 12]. The MIP showed the most consistent uptake for pyrene, with similar results for both experiments involving pyrene:

11.9 % ± 1.52 recovery when in presence of naphthalene, versus 13.5 % ± 3.19 recovery from a single-component solution. This indicates a high selectivity of the MIP towards pyrene. The uptake of naphthalene was lower in presence of pyrene by a factor of two (from 12.5 % ± 1.2 recovery when singly in solution to 6.3 % ± 0.24 when in presence of pyrene), which indicates a high degree of competition for binding sites. This may be related to the higher hydrophobicity of pyrene that enhances its interactions with the polymer network.

The interference in the selective uptake of PAHs caused by a non-PAH compound, octanol, a mostly nonpolar alcohol with a chain like structure, was determined through binding experiments in 80.0 mL of 0.5 μg $L^{-1}$ multi-component PAH solutions over 2 hours. As can be seen from percent recovery as reported in Table 2.4, the presence of octanol does have an inhibitory effect, with the uptake of the analytes about half of what is seen with the interfering species. Given its relatively long alkyl chain, it is unlikely that octanol would compete for selective sites within the polymer network. Thus non-selective interactions are likely to be responsible for the difference in overall percent recovery. In addition to occupying potential non-selective binding sites, the hydrophobicity of octanol may also reduce the interactions of other PAHs with the polymer surface by inhibiting their approach to the polymer surface. This conclusion is supported by the result for phenanthrene, where the impact on recovery due to octanol is lower and the hydrophobicity of phenanthrene is the highest among the group studied.

Table 2.4. Interference of 1-octanol in the adsorption of PAHs into MIPs; experimental conditions: concentration 0.50 µg $L^{-1}$ for each compound in 80.0 mL; GC-MS measurements, SIM mode

| | In presence of 0.50 µg $L^{-1}$ 1-octanol | | In absence of 1-octanol | |
|---|---|---|---|---|
| PAH | Initial PAH concentration, µg $L^{-1}$ | Percent recovery | Initial PAH concentration, µg $L^{-1}$ | Percent recovery |
| naphthalene | 0.555 | 27.6 % | 0.555 | 47.0 % |
| fluorene | 0.505 | 19.0 % | 0.545 | 35.3 % |
| phenanthrene | 0.520 | 21.8 % | 0.560 | 34.2 % |
| pyrene | 0.520 | 11.9 % | 0.540 | 28.3 % |

### 2.4.5. Real samples

The applicability of these novel systems for the detection of PAHs in aqueous samples was determined by MIP analysis in influent water samples from Riverhead Waste Water Treatment Facility and seawater samples collected from the St. John's harbor.

Assuming there is no response when no analyte PAH is present, MIPs and NIPs were exposed to wastewater samples with added 50.00 µg $L^{-1}$ multi-component PAH standard for two hours (Table 2.5.). Four replicates were used in each case. After recovery, the extracts were analyzed by GC-MS, in SIM mode. The concentration of PAHs in the wastewater was determined by the standard addition method. A total concentration of 103.3 µg $L^{-1}$ PAHs was detected with the MIPs in the wastewater samples. This is remarkable for

a polymer with a mass close to 3 mg. Uptake by the NIPs was approximately five times lower at 19.07 µg $L^{-1}$ total PAHs.

Table 2.5. Concentration detected (µg $L^{-1}$) in waste water samples for PAHs using MIP and NIP extraction coupled to off -line GC-MS

| PAHs | NIP | MIP |
|---|---|---|
| | Concentration detected | Concentration detected |
| naphthalene | 4.17 ± 2.17 | 18.83 ± 0.46 |
| fluorene | 5.06 ± 2.51 | 28.70 ± 3.16 |
| phenanthrene | 6.84 ± 0.66 | 32.34 ± 1.61 |
| pyrene | 2.99 ± 0.0096 | 23.45 ± 1.57 |
| total PAHs | 19.07 ± 3.38 | 103.33 ± 3.90 |

Similar MIP and NIP studies to evaluate linearity to those illustrated in Figure 2.5. (a) and (b) were carried out in wastewater samples in similar conditions and without any prior sample pretreatment. These studies are shown in Figure 2.9. The response of the MIPs was lower in the wastewater samples; however the MIPs versus NIPs uptake and the different individual PAHs uptake trends were similar in both studies.

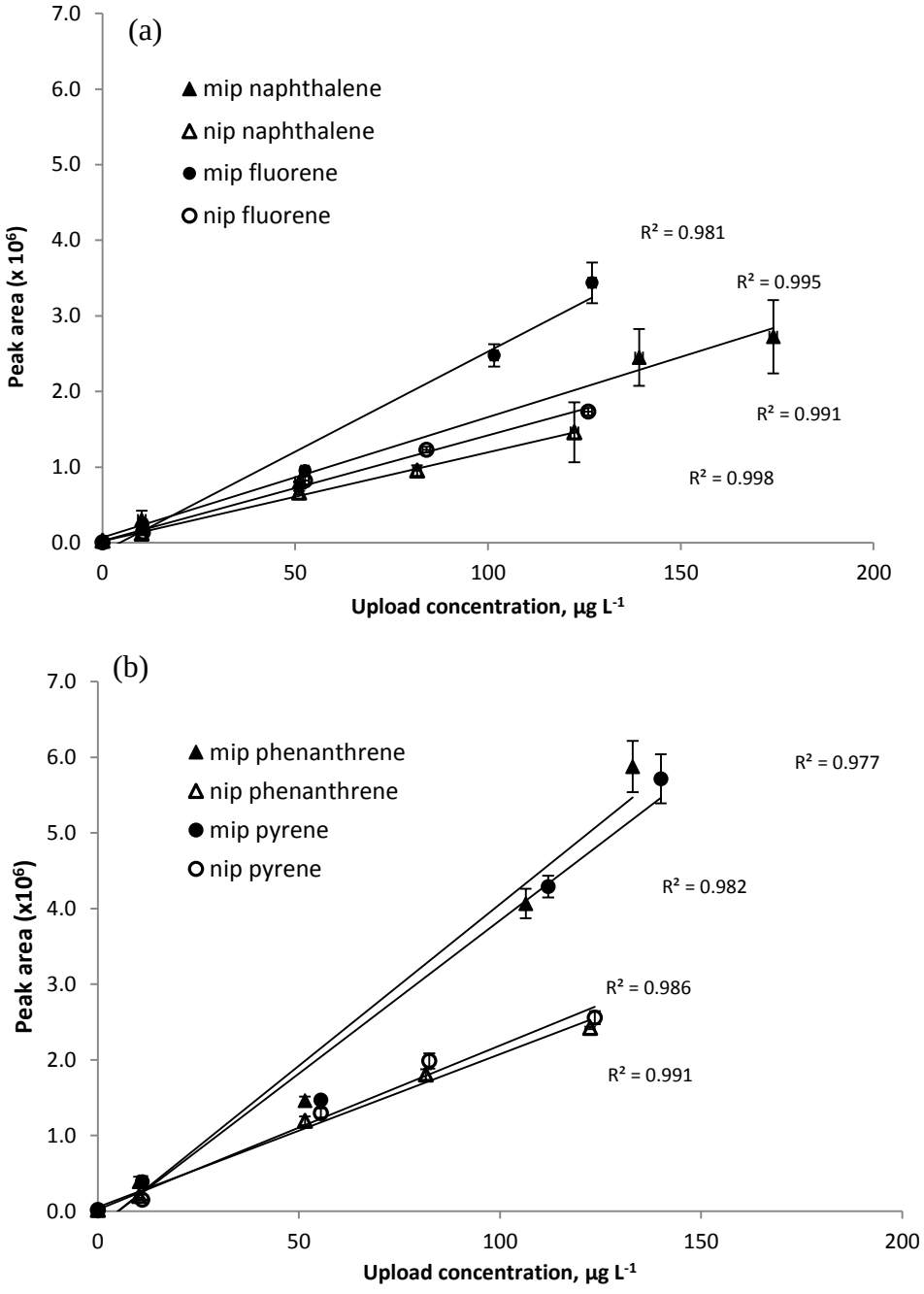


**Fig. 2.9. Calibration curve constructed as peak area against upload concentration: (a) for naphthalene and fluorene (b) for phenanthrene and pyrene; experimental conditions: upload 2 h; GC-MS measurements. The response is the mean value of three measurements. Bars represent standard deviation.**

The applicability of this MIP system to seawater was evaluated by carrying out binding assays in samples spiked with low concentrations of PAHs in the 0 to 5.0 μg $L^{-1}$. The results shown in Figure 2.10. were remarkable considering the high linearity coefficient obtained for all the PAHs, the low concentration of PAHs present in solution and the lack of any preparative steps. The high sensitivity is justified by the salting out effect, where the high salt content in seawater increases the amount of interactions of hydrophobic particles with the polymer surface.

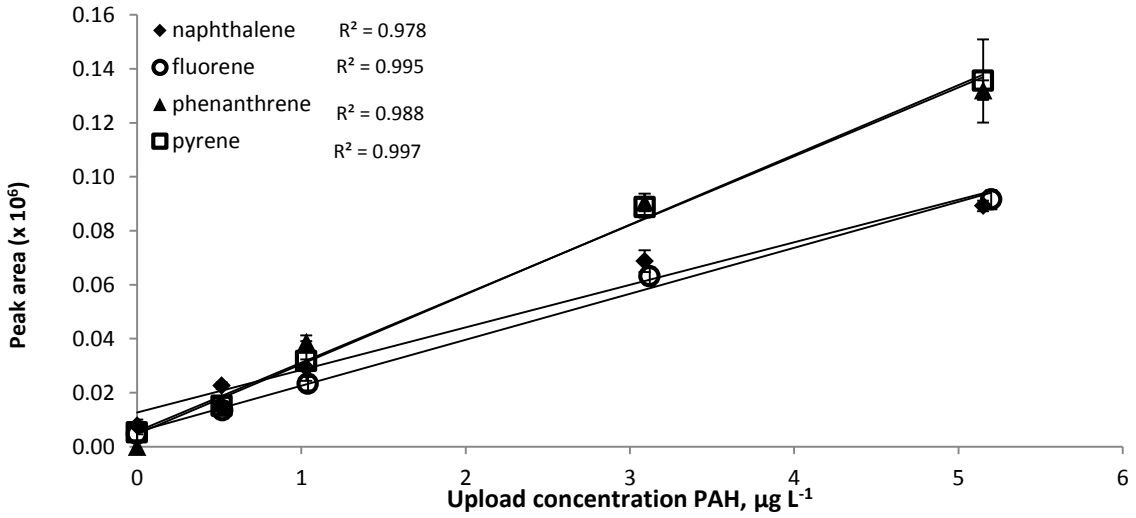


**Fig. 2.10. Calibration curve constructed as the relative response against the upload concentration in raw sea water; experimental conditions: upload 2 h; GC-MS measurements. The response is the mean value of three measurements. Bars represent standard deviation.**

The limit of detection was calculated for the MIP from the standard deviation near the lowest detectable concentration. For naphthalene a detection limit of 18 ng $L^{-1}$ was determined. The detection limit was lower for almost all PAHs than the maximum allowable contaminant level in drinking water of 0.2 µg $L^{-1}$ for PAHs as stipulated by the United States EPA [16]. Considering the recorded concentrations of light PAHs in produced water from various oil platform areas (Gulf of Mexico, North Sea and Grand Bank), as compiled by Pampanin and Sydnes (Table 2.3), the polymers could be used for detection in complex matrices and to meet regulatory monitoring requirements [26].

## 2.5. Conclusions

A novel thin-film MIP with a toluene pseudo-template was developed for detection of PAHs. The suitability of this MIP for aqueous environmental monitoring has been demonstrated with selective uptake from various complex matrices. Surface and binding studies suggested that the MIPs are porous, but that selective adsorption occurs mainly at and near the surface. To a certain degree, NIPs were found to be sensitive toward PAHs which they owe to the optimized pre-polymerization composition. Binding assays for the MIPs showed a saturation of the selective cavities with increase in the upload time but a linear response with increase in concentration. Analysis of MIPs in real environmental samples showed very good recovery capacity and detection limits in wastewater, and excellent sensitive and linear response in seawater for individual PAHs. These findings indicate a great potential for use of the MIPs for in-situ real time environmental monitoring of light PAHs given the simple low tech method we proposed that includes the preparation

of the polymer as well as the use of a simple detection system, a GC-MS with a simple quadrupole analyzer. The thin-film format is advantageous for direct analysis by DESI as shown by previous research in our group, [27] or for integration into a microfluidic device for real time analysis.

## 2.6. Acknowledgements

This research project was undertaken and completed with the financial assistance of Petroleum Research Newfoundland & Labrador, Research and Development Corporation (RDC), Natural Science and Engineering Research Council of Canada (NSERC) and School of Graduate studies at Memorial University of Newfoundland. This project is supported by Atlantic Canada Opportunities Agency (ACOA) under the Atlantic Innovation Fund (AIF) program.

## 2.7. References


1. E. Manoli, C. Samara, Trends Anal. Chem. 18 (1999) 417-428
2. J.R. Law, J.L. Biscaya, Mar. Pollut. Bull. 235 (1994) 4-5
3. R.J. Krupadam, M.S. Khan, S.R. Wate, Water Res. 44 (2010) 681-688
4. P. Plaza-Bolanos, A.G. Frenich, J.L.M. Vidal, J. Chromatogr. A. 1217 (2010) 6303-6326
5. E. Coelho, C. Ferreira, C.M.M. Almeida, J. Braz. Chem. Soc. 19 (2008) 1084-1097
6. G. Wulff, K. Knorr, Bioseparation 10 (2002) 257-276
7. R.A. Lorenzo, A.M. Carro, C. Alvarez-Lorenzo, A. Concheiro, Int. J. Mol. Sci. 12 (2011) 4327-4347
8. A. Ellwanger, C. Berggren, S. Bayoudh, C. Crecenzi, L. Karlsson, P.K. Owens, K. Ensing, P. Cormack, D. Sherrington, B. Sellergren, Analyst 126 (2001) 784-792
9. L. Chen, S. Xu, J. Li, Chem. Soc. Rev. 40 (2011) 2922-2942
10. F.L. Dickert, P. Achatz, K. Halikias, Fresenius J. Anal. Chem. 371 (2001) 11-15
11. P.A. Lieberzeit, K. Halikias, F.L. Dickert, Anal. Bioanal. Chem. 392 (2008) 1405-1410
12. D.A. Spivak, R. Simon, J. Campbell, Anal. Chim. Acta 504 (2004) 23-30
13. E. Turiel, A. Martín-Esteban, Anal. Chim. Acta 668 (2010) 87-99
14. F.L. Dickert, M. Tortschanoff, Anal. Chem. 71(1999) 4559-4563

15. J. Gonzalez, J.C. Campo, M. Valledor, F.J. Ferrero, J.M. Traviesa, J.M. Costa, R. Pereiro, A. Sanz-Mede I2MTC 2008 - IEEE International Instrumentation and Measurement Technology Conference, Victoria (2008)784-792
16. X. Song, J. Li, S. Xu, R. Ying, J. Ma, C. Liao, D. Liu, J. Yu, L. Chen, Talanta 99 (2012) 75-82
17. R.J. Krupadam, B. Bhagat, M.S. Khan, Anal. Bioanal. Chem. 397 (2010) 3097-3106
18. Agency for Toxic Substances and Disease Registry- www.atsdr.cdc.gov/interactionprofiles/ip05.html -accessed December 9, 2013
19. M.J. Hwang, W.G. Shim, C.Y. Yang, H. Moon, J. Nanosci. Nanotehnol. 11 (2011) 7206-7209
20. R.J. Krupadam, B. Bhagat, S.R. Wate, G.L. Bodhe, B. Sellergren, Y. Anjaneyulu Environ. Sci. Technol. 43 (2009) 2871-2877
21. B. Sellergren, K.J. Shea, J. Chromatogr. 635 (1993) 31-49
22. I. Yungerman, S. Srebnik, Chem. Matter 18 (2006) 657-663
23. R.J. Umpleby, G.T. Rushton, R.N. Shah, A.M. Rampey, J.C. Bradshaw, J.K. Berch, K.D. Shimizu, Macromolecules 34 (2001) 8446-8452
24. A.J. Hall, M. Quaglia, P. Manesiotis, E. De Lorenzi, B. Sellergren, Anal. Chem. 78 (2006) 8362-8367
25. P. H. Howard, Handbook of Environmental Fate and Exposure Data for Organic Chemicals. Lewis Publishers: Chelsea, 1 (1989) 408-422

26. D.M. Pampanin, M.O. Sydnes, Polycyclic Aromatic Hydrocarbons a Constituent of Petroleum: Presence and Influence in the Aquatic Environment, Dr. Vladimir Kutcherov Ed., 2013, 83-118
27. G. Van Biesen G., J.M. Wiseman, J. Li, C.S. Bottaro, Analyst 135 (2010) 2237-2240

# Chapter 3. Developments in the synthesis of a water compatible thin-film molecularly imprinted polymer as artificial receptor for detection of trace concentrations of polycyclic aromatic hydrocarbons

## 3.1. Abstract

Novel thin-film toluene MIPs with toluene as both pseudo-template and porogen were developed for uptake of a group of light polycyclic aromatic hydrocarbons (PAHs) from aqueous media. Optimization included trial-and-error experiments to identify the most suitable polymerization components, followed by factorial design to optimize the ratios. GC-MS in selected ion monitoring (SIM) mode was used as an offline sensor to characterize the imprinting characteristics of these materials. MIPs showed linearity over an upload concentration of 0.1 to 120.0 µg $L^{-1}$ and selectivity towards PAHs in a solution containing compounds similar in structure or hydrophobic character, octane, octanol and p-cresol. Similar behavior was detected in wastewater samples spiked with a PAH multicomponent solution and detection limits were calculated in a range from 0.235 to 258 ng $L^{-1}$ for naphthalene and phenanthrene respectively. Large recoveries of the PAHs were possible in these matrices of 6.22 to 66.9% for naphthalene and phenanthrene respectively. The imprinted polymer proves robustness and sensitivity to be used in environmental monitoring of PAHs in water.

## 3.2. Introduction

Inspired by nature's antibody recognition processes, MIPs are superior to their biological counterparts due to their compatibility with a range of temperatures and chemical environments, as well as mechanical stability [1-3]. Molecular imprinting has been applied successfully over the years to extraction and pre-concentration of specific analytes from complex matrices in analytical and environmental applications, such as enantiomeric chromatographic stationary phases, solid phase extraction and microextraction or in the development of sensors [2, 3, 4, 5].

The MIP preparation first requires combination of the template with a monomer to form a pre-polymerization complex (PPC), then copolymerization of a crosslinking agent with the PPC. Upon template removal, a network of cavities complementary in morphology and functionality to the template molecule is created. Depending on the interaction established between the template and the monomer, a few approaches for making MIPs have been identified: covalent, semi-covalent, non-covalent or metal-coordination [4]. In this work, the non-covalent route was used, which also afforded high upload efficiency, simplicity and versatility with respect to analyte choice and preparation [2].

Although MIPs allow flexibility in choosing the materials and selecting the target compound their amorphous structure does not allow for use of X-ray or other microscopy techniques to understand, and thus predict or fully control, the mechanisms involved in binding [6]. However, several studies were carried out by NMR and FTIR to determine the nature of template-monomer interactions as well as the potential for template-template adduct formation by NMR titration and FTIR [7]. With a limited understanding of the

influence of each component of the MIP on its imprinting capacities, the routes taken to optimize the composition of a MIP often involve trial-and-error experiments. In developing a method to produce MIPs, a wide range of factors is considered, ranging from the type and ratio of components in the PPC, polymerization conditions (temperature, stirring, pre-polymerization steps), template removal solvent and analyte extraction solvent [1, 8, 9]. In this context, trial and error experiments where an independent variable is changed while the others are kept constant can be tedious and expensive. Easier and more elegant approaches are computational modeling, use of a combinatorial polymer library or experimental design [2, 5, 10, 11]. These methods and suitable applications have been thoroughly reviewed elsewhere [10]. In experimental design, the optimum experimental conditions can be determined with a minimum number of experiments. A number of major independent variables named factors are selected. In this paper, the factors considered were the ratios of monomer and crosslinker to the template, with each factor studied at two more levels. When these levels are represented by discrete values, the contribution of each factor on the behavior of the MIP can be modeled into a curve with a minimum and a maximum response. This represents a common multilevel surface response, in this case a central composite design, CCD. A CCD is a two-level factorial design with $2^k$ points, where *k* is the number of factors. When using discrete values, the number of design points, N, necessary for this type of analysis is calculated as $N = 2^k + 2k + C_0$, where $C_0$ is the replication number of center points [12].

We used the CCD experimental design approach to determine the optimum composition of a novel thin-film MIP with toluene as pseudo-template and porogen. The

use of a pseudo-template compensates for an often incomplete removal of the template after polymerization that often gives false positives, which can limit the accuracy of quantitative analysis, especially when working at environmental trace level concentrations [8]. The MIP was used for uptake of PAH model compounds from aqueous solutions. PAHs are secondary combustion products and can assist in identifying timely any signs of oil spills.

In this chapter the optimization process to prepare novel thin-film MIPs with toluene as pseudo-template and porogen is described and discussed. The resulting polymers showed a linear uptake profile with increase in concentration of four light PAHs: naphthalene, fluorene, phenanthrene and pyrene. Tests in wastewater samples indicate that applications for direct environmental analysis are viable.

## 3.3. Materials and Methods

### 3.3.1. Preparation of the MIPs

Naphthalene, fluorene, phenanthrene, pyrene and acenaphthene-$d_{10}$ PAHs in a 99% purity or higher were used as received (Table 3.1). Pre-polymerization components 3-(trimethoxysylil) propyl methacrylate, MPS 2.2-dimethoxy-2-phenylacetophenone (DMPA), ethylene glycol dimethacrylate (EGDMA) and 4-vinyl pyridine (4-VP) were purchased from Sigma-Aldrich (Oakville, Canada) in the best quality available and used without further purification (Figure 3.1).

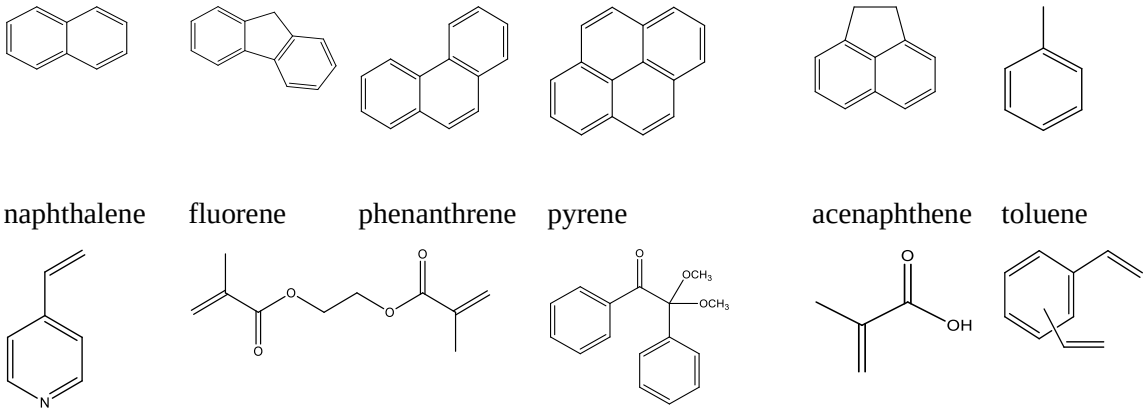

naphthalene fluorene phenanthrene pyrene acenaphthene toluene

4-vinyl pyridine (4-VP) ethylene glycol dimethacrylate (EGDMA) 2,2-dimethoxy-2-phenylacetophenone (DMPA) methacrylic acid (MAA) divinyl benzene (DVB)

**Fig. 3.1. PAHs and MIP components structures**

The organic solvents toluene, ethyl ether, dichloromethane and acetonitrile were purchased in purity of 99.5% or higher from ACP Chemicals (Montreal, Canada). Each sample (~2 $cm^2$) of thin-film MIP was prepared by photo-initiated polymerization of the pre-polymerization solution sandwiched between a slide functionalized with MPS and a glass cover slide (Table 3.1), which resulted in a white opaque coating. Since toluene was both the template and the porogen and preparation of an analogous non-imprinted polymer could not be made, a control polymer (CP) was prepared similarly using ethyl ether as a porogen.

Table 3.1. MIP and CP composition

| Compound | MIP | CP |
|---|---|---|
| toluene | 200 µL | _ |
| ethyl ether | _ | 200 µL |
| 4-VP | 17.0 µL (0.158 mmol) | 17.0 µL (0.158 mmol) |
| EGDMA | 151 µL (0.801 mmol) | 151 µL (0.801 mmol) |
| DMPA | 3.20 mg (0.0125 mmol) | 3.20 mg (0.0125 mmol) |

The pre-polymerization complex was prepared by pipetting or by weighing into a 2 mL vial all the components above. The solution was vortexed until all components dissolved. To remove any excess oxygen that may interfere during polymerization, the mixture was degassed for five min. A volume of 8.00 µL of the pre-polymerization complex was dispensed on the derivatized glass surface and covered with a microscope cover slide. The set-up was placed under a UVP 6 W handheld UV lamp at a $\lambda = 254$ nm at 20 °C room temperature for 30 min. The cover slides were removed and the imprint molecules were extracted by washing in ethyl ether for two hours.

### 3.3.2. Experimental design

Experimental design and analysis was carried out using the Minitab$^{TM}$ 16 software package. The objective was to optimize the ratios of monomer and crosslinking agent to the template to obtain the optimum response, which in this case is the detector's response in peak area units, thus produce a highly selective and sensitive MIP. The ratios of the monomer (4-VP), crosslinking agent (EGDMA) and template/porogen (toluene) were all

found to be essential for this purpose. Appropriate ranges for each factor were determined using preliminary results, and guided by consensus from the literature [11, 16]. MIPs with different compositions (combinations determined by Minitab to be necessary for the data analysis phase) were prepared and used for upload. The response was peak area of the PAH normalized to the mass of the MIP.

### 3.3.3. Binding tests

MIPs were immersed in a fixed volume of aqueous multi-component PAH standards, at room temperature (approximately 20 °C) for specific time intervals. The bound analytes were then extracted into ethyl ether, and then the extract was reduced under pressure and made to 1.00 mL in DCM for analysis by GC-MS.

### 3.3.4. Characterization of MIPs

The MIPs and CPs were characterized by atomic force microscopy (AFM) and GC-MS. AFM images were recorded using the Ambios AFL. GC-MS was carried out using an Agilent GC 6890 coupled to an Agilent 5973 MS detector. Compounds were ionized by electron ionization at 70 eV and mass spectra were acquired in selected ion monitoring (SIM) mode (Table 3.2).

Table 3.2. GC-MS settings: Quantifier and qualifier ions used to identify the PAHs

| | Quantifier (m/z) | Qualifier (m/z) |
|---|---|---|
| naphthalene | 128 | 127 |
| fluorene | 165 | 166 |
| phenanthrene | 178 | 176 |
| pyrene | 202 | 200 |
| octane | 114 | 85 |
| p- cresol | 108 | 107 |
| acenaphthene $d_{10}$ | 162 | 158 |

Separation was carried out on a DB-5MS column capillary column (0.25 mm x 30 m, 0.25 µm film thickness). The oven temperature was optimized as follows: initial temperature of 45 °C was held for 0.8 min, ramped at 45 °C $min^{-1}$ to 200 °C, then at 5 °C $min^{-1}$ to 216 °C and finally at 10 °C $min^{-1}$ to 260 °C. The injection was performed in splitless mode from an injector port temperature of 290 °C. Helium, with a purity of 99.999% was used as a carrier gas at a flow rate of 1.3 mL $min^{-1}$. Acenaphthene-$d_{10}$ was used as an internal standard and calibration curves for PAHs determination were obtained by linear regression analysis of data from analysis of multi-component solutions in appropriate concentration ranges.

### 3.4. Results and discussion

White, opaque MIP films using toluene as pseudo-template and porogen, EGDMA as crosslinker, 4-VP as monomer and DMPA as photoinitiator were prepared using a method previously reported in the Bottaro group [13]. The corresponding CP had a slightly-cloudy white appearance. The difference between the two materials was evident when initial surface characterization of both materials using AFM was carried out: the MIPs have a porous surface with different size cavities and the CPs have a non-porous surface, Figure 3.2. (a) and (b).

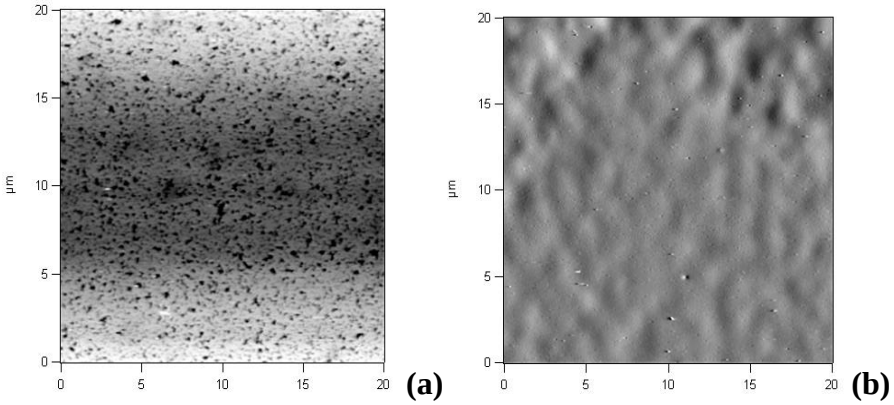


**Fig. 3.2. AFM micrograph of (a) MIP and (b) CP**

Porosity is a result of the solvent, or porogen used [14]. A porogen provides a chemically stable environment where the monomer and crosslinker units can organize around the template. Good mobility of all components with no interference enables polymerization in the most stable configurations, thus even, robust pores are created [2, 5, 14]. In addition, a higher amount of imprint molecules would increase the number of

selective cavities, thus potentially enhancing selectivity and sensitivity [14]. In this case, the solvent was also the template, and excess of the toluene template seemed to have a positive effect on PAH uptake and if there was any residual toluene present following template removal there was no evidence that it interfered in the PAH analyte uptake process or analysis. To determine a suitable CP, we considered a solvent that would lack aromaticity but display a similar polarity as toluene, with a polarity index of 2.4 was considered. The polymerization environment and ultimately the polymer surface would still exhibit similar overall hydrophobic surface characteristics as the toluene MIP without the possibility for aromatic cavity formation. Ethyl ether, a readily available solvent with a polarity index of 2.8 was used. Although ethyl ether was used to prepare a suitable CP, the material was considered too different from the MIPs structure to fully account for the effects of toluene as a porogen and facilitate a comparison of their binding interactions.

The optimized composition of the toluene MIPs was determined from preliminary binding studies. Common monomers and crosslinkers previously reported for the preparation of non-covalent MIPs for uptake of similar compounds in aqueous matrices were investigated for this purpose [16, 20]. It was decided that MAA and 4-VP monomers and DVB and EGDMA crosslinkers would be most suitable [1, 9]. The functionality of the monomer and its interaction with the template during polymerization determine the accuracy and selectivity of the imprinted polymer. A strong interaction results in a stable complex and an increased binding capacity of the available cavities [12]. Two monomers with different types of structure were considered that would potentially provide this type of interaction with toluene: MAA, with a non-aromatic linear structure and 4-VP, with an

aromatic nucleus (Figure 3.1). MIPs prepared using the two different monomers were exposed to solutions containing 1.00 mg $L^{-1}$ of multi-component PAHs. When 4-VP monomer was used, the response was higher (Figure 3.3 (a)). Although MAA is a more versatile monomer, the π-π and other electrostatic interactions (hydrophobic) that occur between the aromatic PAHs and the 4-VP increase the uptake capacity [12, 15].

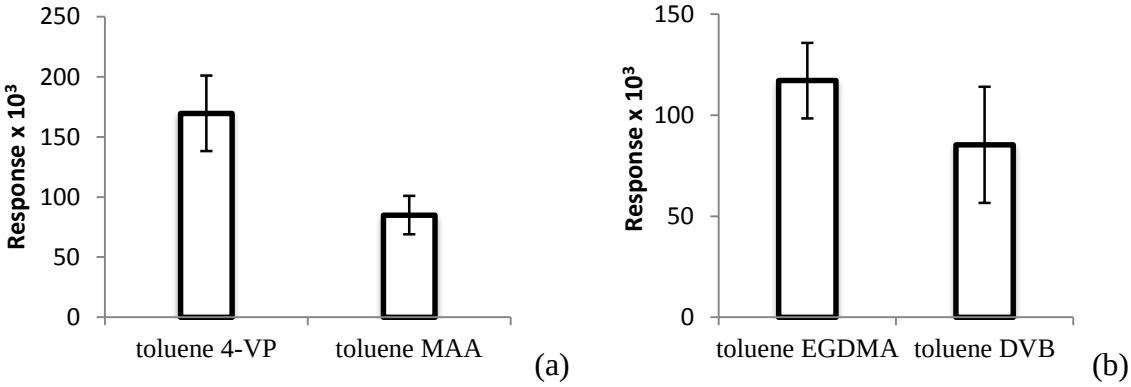


**Fig. 3.3. MIP behavior is different when the components of the PPC are varied: (a) monomers 4-VP and MAA (b) crosslinking agents EGDMA and DVB; experimental conditions: upload in 25.00 mL of 1.00 mg $L^{-1}$ multi-component PAH solution for two hours. The response is the mean value of three measurements. Bars represent standard deviation.**

The crosslinker is equally essential in the MIP structure; it preserves and stabilizes the whole template-monomer complex without interfering later in the uptake process such that during polymerization robust cavities with high fidelity to the template are formed. Two crosslinkers were selected with two polymerizable double bonds but different structures: EGDMA and DVB (Figure 3.1). Their effect on the binding capacity of the

MIP, when used with the optimum monomer, 4-VP was determined by binding tests in 1.00 mg $L^{-1}$ multi-component PAH solution. A better uptake was observed for the toluene/4-VP/EGDMA complex, most probably because of steric effects (Figure 3.3(b)). The linear structure of EGDMA allowed an easy co-polymerization around the template cavities without any interference. In addition, EGDMA is less compatible with water which might enhance the interactions with the PAHs. The lower response of the toluene/4-VP/DVB to PAH uptake is believed to be due to the bulkiness of the crosslinker as well as the aromaticity, which may affect the stability of the toluene/4-VP complex through competing electrostatic interactions. While it may have been possible that the DVB would have aided in the uptake of the PAHs due to the possibility of $\pi-\pi$ interactions, experimental results do not support this.

### 3.4.1. Optimization using the central composite design (CCD)

The importance of the choice of main components in the pre-polymerization complex for preparation of a selective and sensitive MIP has been discussed, however the proportion is also important and dictates whether the polymer will achieve the maximum uptake potential. CCD was used to determine the optimum composition. The factors selected in this mode were the amounts of monomer, 4-VP, and crosslinking agent, EGDMA; the levels studied were at high, center and low values of molar ratios (Table 3.3) based on the average reported ratio values of template: monomer: crosslinker of 1:4:20 [11, 16]. The initiator and template were kept at a constant level while the selected factors were varied, and their effects on the synthesis of the MIPs evaluated.

Table 3.3. Factors and levels (mmol) used in the response surface

| | Mole Ratios (Level Designation in CCD) | | |
|---|---|---|---|
| Factor | Low (-1) | Center (0) | High (+1) |
| Monomer, 4-VP | 2 | 4 | 8 |
| Crosslinking agent, EGDMA | 12 | 20 | 28 |

The amount of monomer affects the number of potential template-monomer interactions, thus the number of binding sites that form during polymerization and ultimately, the sensitivity. Low monomer content results in fewer template-monomer interactions, thus a lower number of binding sites. Excess monomer could create more binding sites but could also generate some non-specific binding [1]. The amount of crosslinker influences the rigidity and robustness of the imprinted cavities, thus a low crosslinking degree would affect the overall MIP selectivity. Too much crosslinker could decrease the number of recognition sites per unit mass of MIPs [1].

Peak area for each analyte measured by GC-MS was recorded for 18 binding experiments combining various levels of pre-polymerization components as dictated by the CCD approach. The upload concentration was kept constant at a 50 μg $L^{-1}$ level for each PAH. Since peak area should be proportional to analyte uptake by any given MIP under standard conditions, the results shown in Figure 3.4 were evaluated such that the most desirable composition would yield the highest response. The Minitab™ "desirability" function is a convenient way to express the combination of levels that led to a given response as a value from 0.0 (undesirable) to 1.0 (highly desirable) response. Optimal

conditions under the constraints set by the user will give the highest "desirability" value. As the intent of optimization of composition is to maximize response for all analytes, the desirability of response in itself is not as important as where the maxima occur. As such, the targets used were simply based on the average responses for each analyte in a range of MIP compositions. The optimum conditions for a total PAH uptake are the ratio of 4-VP:EGDMA= 4.81:19.77. This agrees in general with the literature on the subject [11, 16], but what is significant is the flat shape of the composite desirability graph for both monomer and crosslinker composition displaying a rather large interval where values close to an optimum response can be achieved by varying the amount of monomer or crosslinker.

For the monomer factor, the maxima varied from one PAH to another, however this does not interfere with attaining a similar desirability factor for all the analytes. Also, considering the higher hydrophobicity of the larger PAH targeted in this study, the percent of monomer could be tuned to increase the binding of naphthalene and fluorene, without significantly reducing the concentration of phenanthrene and pyrene being adsorbed to the surface. For the crosslinker, the maximum response was found to be constant for all PAHs. This suggests that the crosslinker plays a less important role in the binding mechanism that influences the uptake. Thus, depending on the requirements of a polymer application, the amount of crosslinker could be varied to achieve better mechanical properties. The success of this optimization method depends on the assumption that the random errors in measurement of the peak areas are significantly small.

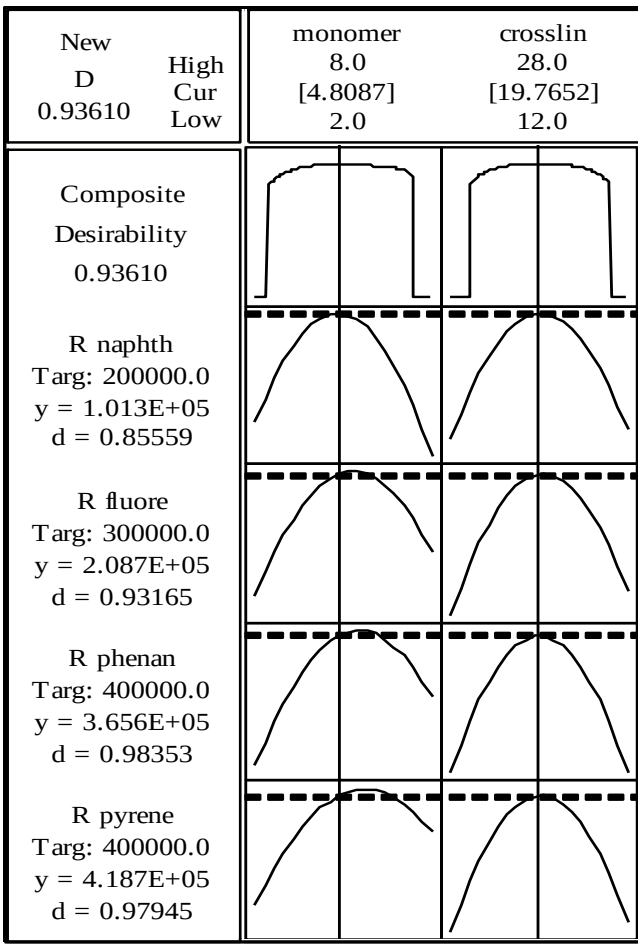


(a)

(b)

(c)

(d)

**Fig. 3.4. Minitab separation dashboard showing the influence of each of the factors on the responses (left column, with y: predicted responses and d: desirability) for (a) naphthalene (b) fluorene (c) phenanthrene (d) pyrene**

### 3.4.2. Characterization of the MIPs

The MIPs were characterized in terms of linearity, selectivity and sensitivity using binding tests in aqueous standard solutions. Robustness and sensitivity of uptake in a real sample were later evaluated by binding in spiked real waste water samples. Linearity of uptake and selectivity were evaluated using binding assays, where the upload PAH

concentration was varied from 0.1 µg $L^{-1}$ to 100 µg $L^{-1}$ over a constant exposure time of two hours. The experiments were carried out in four replicates. The PAHs were recovered from the MIP and analyzed directly by GC-MS in the presence of acenaphthene-$d_{10}$ internal standard in SIM mode, Figure 3.5.

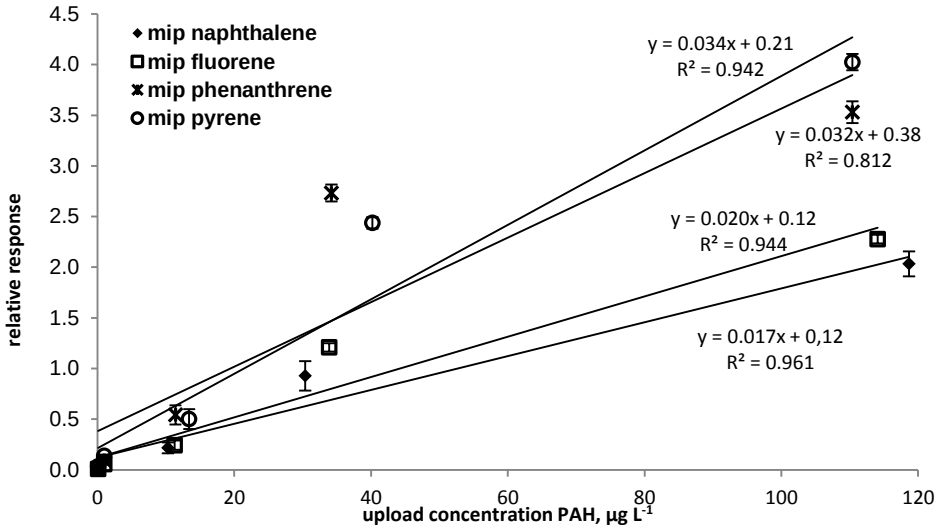


**Fig. 3.5. The relative response normalized against the internal standard response of the MIPs with increase in the upload PAH concentration; experimental conditions: acenaphthene-$d_{10}$ concentration was kept constant at 123 µg $L^{-1}$ 80.0 mL sample exposed for two hours, GC-MS in SIM mode. The response is the mean value of three measurements. Bars represent standard deviation.**

The results showed a linear uptake over the range of 0.1 – 100 µg $L^{-1}$ with high correlation coefficients for all the PAHs. The efficiency of uptake toward the various PAHs increased from naphthalene, fluorene, phenanthrene to pyrene. Hydrophobicity increase with molecular mass enhances the binding of larger PAHs by the MIPs. The experiments

were run in parallel for the CPs and imprinting factors were determined as the ratio of the ratio of average response from the PAHs taken up by the MIP compared to the CP, with values of 1.25, 1.14, 1.22 and 1.39 for naphthalene, fluorene, phenanthrene and pyrene respectively. The MIPs showed a better uptake than the CPs, although the values obtained for the imprinting factors suggest the difference in selectivity is small for this range of concentrations. The chemistry of the polymer surface for the MIPs and CPs is suitable for uptake of aromatic hydrocarbons through hydrophobic interactions and to some extent through π-π interactions. The higher selectivity in the MIPs can be attributed to the selective geometrically constrained cavities with the appropriate π-π bonding motif that result in stronger binding between the PAHs and the functionalized polymer network.

### 3.4.3. Inhibition studies in aqueous and real samples

Uptake of PAHs in presence of compounds with similar structure and hydrophobicity is important in predicting their selectivity in real samples. Initial tests under ideal upload conditions in distilled water were carried out in an upload aqueous solution containing PAHs, p-cresol, octane and octanol over a period of 2 hours. After recovery, the extracts were spiked with the internal standard and analyzed by GC-MS in SIM mode. p-Cresol is a compound similar in structure to PAHs (Figure 3.6), with a polar hydrophilic character due to the hydroxyl moiety.

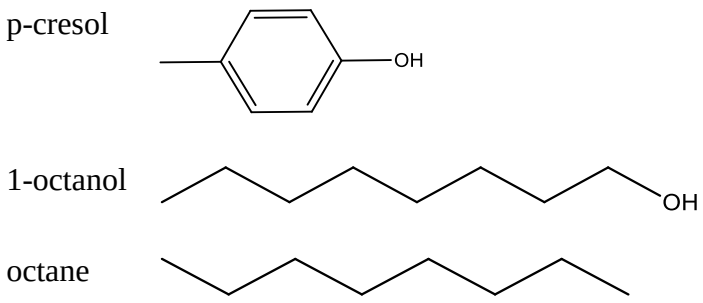


**Fig. 3.6. Structure of compounds used for inhibition studies**

p-Cresol could in theory have a similar π-π interaction with the monomer or the toluene embedded at the surface of the polymer. Octane and octanol are both long chain compounds with pronounced hydrophobic character; however, octanol is more polar due to the hydroxyl terminal group. Binding to the surface of the polymer would be possible through hydrophobic interactions. The results in Table 3.4. indicate that both MIPs and CPs did not show any selectivity towards the hydrocarbon chain like structures but did pick up a negligible amount of p-cresol.

The amount of p-cresol retained is similar for both polymers indicating a non-selective interaction. This suggests that uptake binding in the non-covalent imprinted polymers is mainly governed by structural complementarity and π- π stacking seconded by hydrophobic interactions. According to the response values for the MIPs, the efficiency of uptake of the various PAHs by the MIPs followed the same trend as seen in Figure 3.4, where a multi-component standard was used with no potential interference.

The imprinting factor, IF, is a measure of the selectivity of the MIP with respect to the CP. It can be calculated as the ratio of the relative response of each target analyte of

the MIP to that of the CP. For an average of 10 μg $L^{-1}$ upload concentration of each PAH (Table 3.4), the IF for naphthalene was 1.18, for fluorine was 1.32, for phenanthrene was 1.29 and for pyrene was 1.35. These values are comparable to other IF values reported in literature and are an indication of the role of the pore structure in the uptake. The IF values for the different PAHs are close in value to each other suggesting a large pore size distribution.

Table 3.4. MIP and CP selectivity in pure water towards PAHs in presence of 1-octanol, octane and p-cresol; experimental conditions: concentration 10 µg $L^{-1}$ for each compound in 80.0 mL; GC-MS in SIM mode measurements

| | | MIP | | | Control polymer | | |
|---|---|---|---|---|---|---|---|
| Target analytes | Initial concentration, µg $L^{-1}$ | Relative response* | % RSD | Percent recovery** | Relative response | % RSD | Percent recovery |
| octane | 11.7 | _ | _ | _ | _ | _ | _ |
| 1-octanol | 8.79 | _ | _ | _ | _ | _ | _ |
| p-cresol | 13.6 | 0.0080 | 4.24 | _ | 0.0068 | 7.78 | _ |
| naphthalene | 12.1 | 0.176 | 4.43 | 0.78 | 0.165 | 8.09 | 0.71 |
| fluorine | 10.7 | 0.283 | 3.86 | 3.03 | 0.215 | 7.43 | 2.28 |
| phenanthrene | 10.6 | 0.437 | 5.47 | 2.55 | 0.338 | 8.18 | 1.96 |
| pyrene | 10.1 | 0.413 | 3.50 | 2.55 | 0.306 | 2.80 | 1.81 |

*The relative response is calculated as the ratio of peak area corresponding to each PAH to the peak area of acenaphthene-$d_{10}$ internal standard.
**The percent recovery was calculated as the ratio of the recovered concentration to the initial upload concentration in 80.0 mL solution

Heterogeneity of the binding sites is characteristic of non-covalent type polymers and is mainly due to formation of various types of adducts at the surface and in the network of the polymer prior to polymerization [2]. The % RSD lower than 8.5% for all the compounds indicates a low variability of the extraction procedure.

The binding experiments were repeated in complex matrix: municipal influent wastewater from Riverhead Waste Water Treatment Facility, St. John's NL. The samples were spiked with PAHs, p-cresol and octane and were exposed to MIPs over an interval of two hours. The response to the various compounds (Table 3.5) was similar to that obtained in distilled water (Table 3.4) with one exception; larger recoveries were obtained in the waste water samples. This is remarkable considering a MIP surface area of only 2.25 $cm^2$ for a 65 µm thickness exposed to 80 mL of sample over two hours. An opposite effect would be expected since a higher upload would be possible in absence of any interference. We do not have a full understanding of these effects but we believe it could be due to electrostatic effects caused by other compounds in the matrix which should normally increase the uptake of hydrophobic compounds. Identification of all the components in the wastewater sample could provide a more in depth analysis of the more selective behavior of MIPs in wastewater. No response was recorded for octane or p-cresol, even for a tenfold higher p-cresol concentration, indicating that successful binding to the MIP surface occurs as a result of both structural match and complementary functionality. Considering the complex matrix and the lack of any sample preparative steps before uptake, the percent recovery values of each compound were relatively high.

The lowest limit of detection was calculated according to the guidelines provided by Harris [19] using the signal and the variability from a blank MIP and a low MIP upload concentration. The lowest detection limit for all the PAHs was in the range of the minimum values in produced water recorded at different oil platform sites worldwide, [17] and within the range recorded for PAHs in freshwater in several provinces in Canada [18].

The variability of analysis is under 5% as shown by the %RSD values, thus the imprinted polymers are a viable alternative for detection of PAHs at environmentally representative concentrations [17]. This suggests that these materials have the potential to be developed further into water cleaning materials.

Table 3.4. Interference of octane and p-cresol in the adsorption of PAHs into MIPs in wastewater samples; experimental conditions: 80.0 mL of waste water samples spiked with 50 µg $L^{-1}$ of each PAH, 50 µg $L^{-1}$ octane and 500 µg $L^{-1}$ p-cresol; GC-MS in SIM mode measurements

| PAH | Relative response | % RSD | Initial upload concentration, µg $L^{-1}$ | Percent recovery * | LOD, ng $L^{-1}$ | Concentrations of individual PAHs in produced water, µg $L^{-1}$ [17] | Concentrations of individual PAHs in fresh water, µg $L^{-1}$ [18] |
|---|---|---|---|---|---|---|---|
| octane | 0.012 | 12.73 | 50.0 | _ | _ | | |
| p-cresol | 2.96 | 14.48 | 523 | _ | _ | | |
| naphthalene | 5.18 | 4.74 | 60.5 | 6.22 | 0.235 | 5.3- 1512 | 0.0036- 8.5 |
| fluorene | 23.68 | 3.51 | 57.5 | 41.8 | 9.95 | 0.06-16.5 | 0.0007- 116 |
| phenanthrene | 53.74 | 5.06 | 60.0 | 66.9 | 258 | 0.11- 32.0 | 0.0021-1027 |
| pyrene | 60.89 | 1.88 | 52.5 | 65.7 | 3.60 | 0.01- 1.9 | 0.0003- 1233 |

* The percent recovery was calculated as the ratio of the recovered concentration to the initial upload concentration in 80.0 mL solution

Another binding study was carried out in PAH-spiked raw seawater samples collected from the St. John's harbor area. For PAH concentrations ranging from 10 to 130 µg $L^{-1}$, an excellent linearity of response was obtained for all the PAHs considering the small mass of adsorbent, the lack of conditioning steps of the MIPs or the simple detection configuration system (Figure 3.7). The imprinted materials are thus very selective and could be readily used for analysis in the environment.

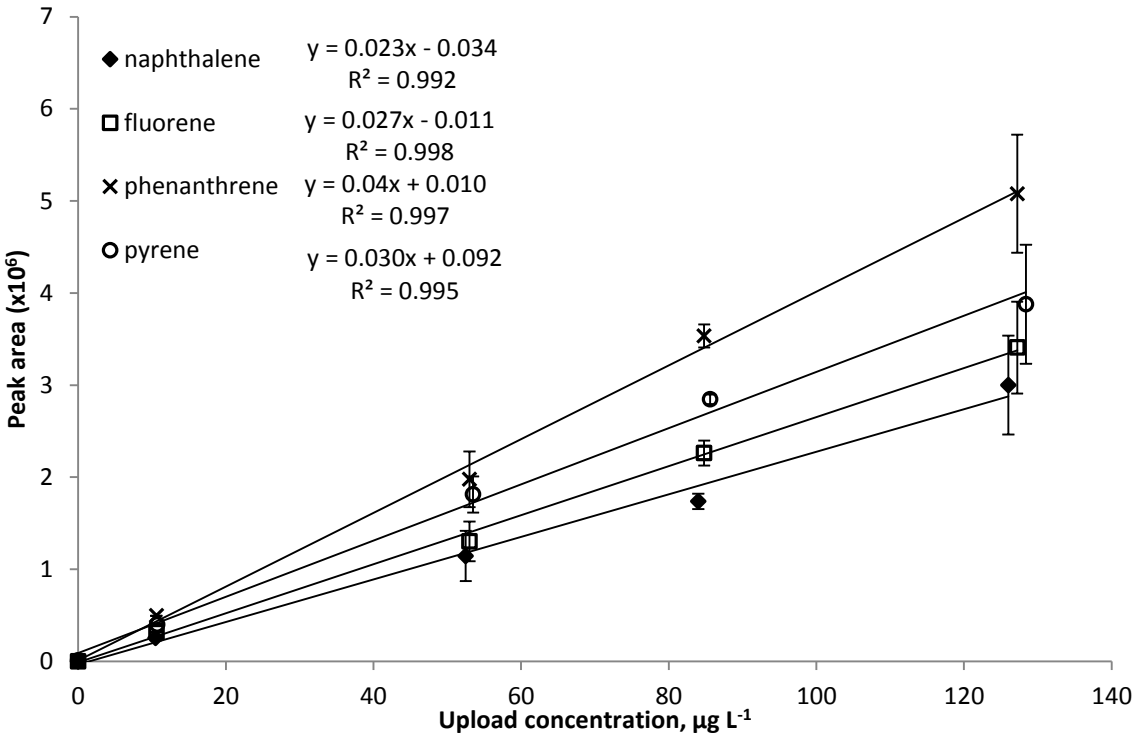


**Fig. 3.7. Calibration curve constructed as the relative response against the upload concentration in raw sea water; experimental conditions: upload 2 h; GC-MS measurements. The response is the mean value of three measurements. Bars represent standard deviation.**

A study to assign the limit of quantitation of the MIPs uptake of the different ring size PAHs for an upload concentration of 1.00 ng $L^{-1}$ was carried out in parallel with blank uploads. MIPs displayed a high sensitivity towards naphthalene and an imprinting factor of 3.13 but none of the other PAHs were detected (Figure 3.8). This may also be related to the limited capacities in terms of sensitivity of a GC-MS.

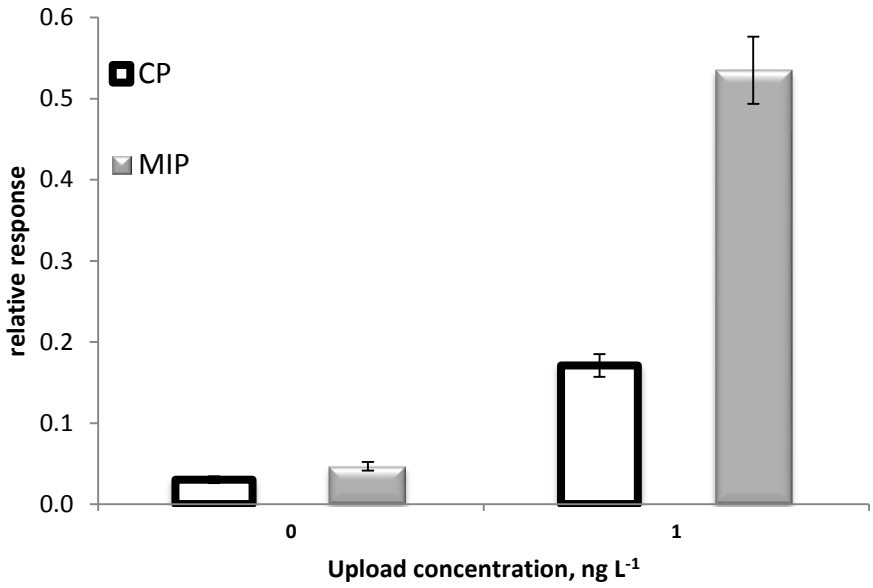


**Fig 3.8. Relative response of the MIPs and CPs to naphthalene for a blank and a 1.00 ng $L^{-1}$ PAH upload concentration; experimental conditions: 80.0 mL sample exposed for two hours, GC-MS in SIM mode. The response is the mean value of three measurements. Bars represent standard deviation.**

### 3.5. Conclusions

Non-covalent imprinted materials were prepared using toluene as a porogen and a template for selective uptake of the lighter more water soluble PAHs. In the synthesis

process the components were identified using previous available information and the optimum composition for a maximum selective uptake was established using factorial design. The resulting polymer showed linearity over several concentration ranges and remarkable percent recoveries of PAHs in clean and waste water samples. No prior sample pretreatment was necessary. These facts paired with sensitivities at trace level concentrations in complex matrices and a low variability demonstrate the potential of MIPs made with toluene as the pseudo-template and porogen for rapid extraction of PAHs from environmental aqueous media. This study could be taken a step further by incorporation of the imprinted materials into microfluidic devices and coupling to a sensor for on site on line monitoring of light PAHs.

### 3.6. Acknowledgements

This research project was undertaken and completed with the financial assistance of Petroleum Research Newfoundland & Labrador, Research and Development Corporation (RDC), Natural Science and Engineering Research Council of Canada (NSERC) and School of Graduate studies at Memorial University of Newfoundland. This project is supported by the Atlantic Canada Opportunities Agency (ACOA) under the Atlantic Innovation Fund (AIF) program.

## 3.7. References


1. F. Meier, B. Mizaikoff, Artificial receptors for chemical sensors, Wiley-VCH, 2011, pp 391-406
2. I. Yungerman, S. Srebnik, Chem. Matter 18 (2006) 657-663
3. X. Song, J. Li, S. Xu, R. Ying, J. Ma, C. Liao, D. Liu, J. Yu, L. Chen, Talanta 99 (2012) 75–82
4. G. Wulff, K. Knorr, Bioseparation 10 (2002) 257-276
5. F. Chapuis, V. Pichon, M.C. Hennion, LC-GC Europe 17 (2004) 408-417
6. D.A. Spivak, R. Simon, J. Campbell, Anal. Chim. Acta 504 (2004) 23-30
7. J. Svenson, J.G. Karlsson, I.A. Nicholls, J. Chromatogr. A 1024 (2004) 39-44
8. A. Ellwanger, C. Berggren, S. Bayoudh, C. Crecenzi, L. Karlsson, P.K. Owens, K. Ensing, P. Cormack, D. Sherrington, B. Sellergren, Analyst 126 (2001) 784-792
9. C. Baggiani, C. Giovanolli, L. Anfossi, C. Passini, P. Baravalle, G. Giraudi, J. Am. Chem. Soc. 134 (2012) 1513-1518
10. C. Rossi, K. Haupt, Anal. Bioanal. Chem 389 (2007) 455-460
11. H. Kempe, M. Kempe, Macromol. Rapid Comm. 25 (2004) 315- 320
12. B. Sellergren, K.J. Shea, J. Chromatogr. 635 (1993) 31-49
13. J. Zolgharnein, A. Shahmoradi, J.B. Ghasemi, J. Chemometr. 27 (2013) 12-20
14. F.L. Dickert, M. Tortschanoff, Anal. Chem. 71 (1999) 4559-4563
15. S.N. Egli, E.D. Butler, C.S. Bottaro - submitted
16. R.J. Krupadam, M.S. Khan, S.R. Wate, Water Res. 44 (2010) 681-688

17. D.M. Pampanin, M.O. Sydnes, Polycyclic Aromatic Hydrocarbons a Constituent of Petroleum: Presence and Influence in the Aquatic Environment, Dr. Vladimir Kutcherov Ed., 2013, pp 83- 118

18. Canadian Environmental Protection Act – Priority Substances List Assessment Report. Polycyclic Aromatic Hydrocarbons. http://www.hc-sc.gc.ca/ewh-semt/alt_formats/hecssesc/pdf/pubs/contaminants/psl1lsp1/hydrocarb_aromat_polycycl/hydrocarbons-hydrocarbures-eng.pdf-Accessed July 25th, 2013

19. D.C. Harris, Quantitative chemical analysis, 8th Ed, W.H. Freeman, 2010, pp 103-105

20. R.J. Krupadam, B. Bhagat, M.S. Khan, Anal. Bioanal. Chem. 397 (2010) 3097-3106; J.P. Lai, R. Niessner, D. Knopp, Anal. Chim. Acta 522 (2004) 137-144; M.J. Hwang, W.G. Shim, C.Y. Yang, H. Moon, J. Nanosci. Nanotechnol. 11 (2011) 7206- 7209

# Chapter 4. Microfabrication and surface treatment for microfluidic devices

## 4.1. Introduction

Microfluidic devices, microfluidics or lab-on-a chip systems have emerged in the early 1980s as miniaturized total chemical analysis systems, μ-TAS that could integrate the main functions carried out in a laboratory setting on to small-scale devices [1, 2]. For example, extraction from a sample, derivatization, separation and detection of analytes could be carried out on microchips smaller than one square centimetre [1]. The commercial potential of these systems was recognized only in the mid to late 1990s such that research was carried out to make these systems smaller, more compact and more economically viable from manufacturing and operational costs perspectives [3]. The performance has equally improved in terms of versatility, robustness, specificity, quantitative analysis and response time [4, 3]. The most popular applications of microfluidics are in bioanalysis for proteomics, peptides and genomics research and for routine use in blood analysis, such as the cholesterol and glucose home testing kits [1, 5].

The onsite, online capabilities have attracted interest for use in environmental analysis of contaminants present at trace and ultra-trace levels [6, 7]. Detection and quantification of compounds at these levels can be challenging in the context of a miniaturized device with mass limited analyte capacity. Therefore, solid phase extraction materials capable of enrichment from complex matrices are employed. These materials are

somewhat selective toward compounds carrying similar degrees of polarity, but highly specific targeted analysis for a specific non polar compound, e.g. for a single PAH that carries no distinctive functionality can be inconclusive. Selective materials such as thin-film molecularly imprinted polymers presented in the previous two chapters could overcome these limitations, by selectively extracting light PAHs from a complex matrix based on size and shape compatibility and π-π interaction capability. The thin-film format enables easy integration into a microfluidic device. Online detection techniques coupled to a microfluidic device reported so far are the UV spectrophotometric, chemiluminescence, fluorescence, electrochemical and mass spectrometry in electrospray ionization (ESI) and matrix-assisted laser desorption ionization (MALDI) [2]. Separation has been driven preferentially by capillary electrophoresis given the ease of initiating and handling flow using electrodes, in addition to the excellent resolution, versatility and robustness. Fewer applications of liquid chromatography on microfluidic devices have been recorded because of the difficulty in integrating bulky pumps, needles or valves to generate flow [2, 4, 8].

Separation of analytes occurs in microchannels that have been etched or otherwise patterned into the microfluidic material. The performance of a microfluidic device in a particular application relies greatly on the properties of the material used, such as the optical transparency, surface chemistry, thermal conductivity, porosity or biocompatibility as well as the type of micro fabrication techniques the material affords. Microfluidic devices are fabricated from glass, silicon and polymers, or a combination of these materials [9]. Silicon has good thermal conductivity which is useful in dissipating heat; however it is opaque which usually makes it unsuitable for online optical detection [9]. Glass whose basic

structure is shown in Figure 4.1.(a) is a very good optically transparent material with surface chemistry amenable to induction of electroosmotic flow. The techniques used to make microchannels on silica and glass include standard photolithography and wet etching using hydrofluoric acid, HF or KOH as the etching reagent [3]. These fabrication techniques are time-consuming, expensive and make use of toxic reagents. This has limited their use in research and commercialization.

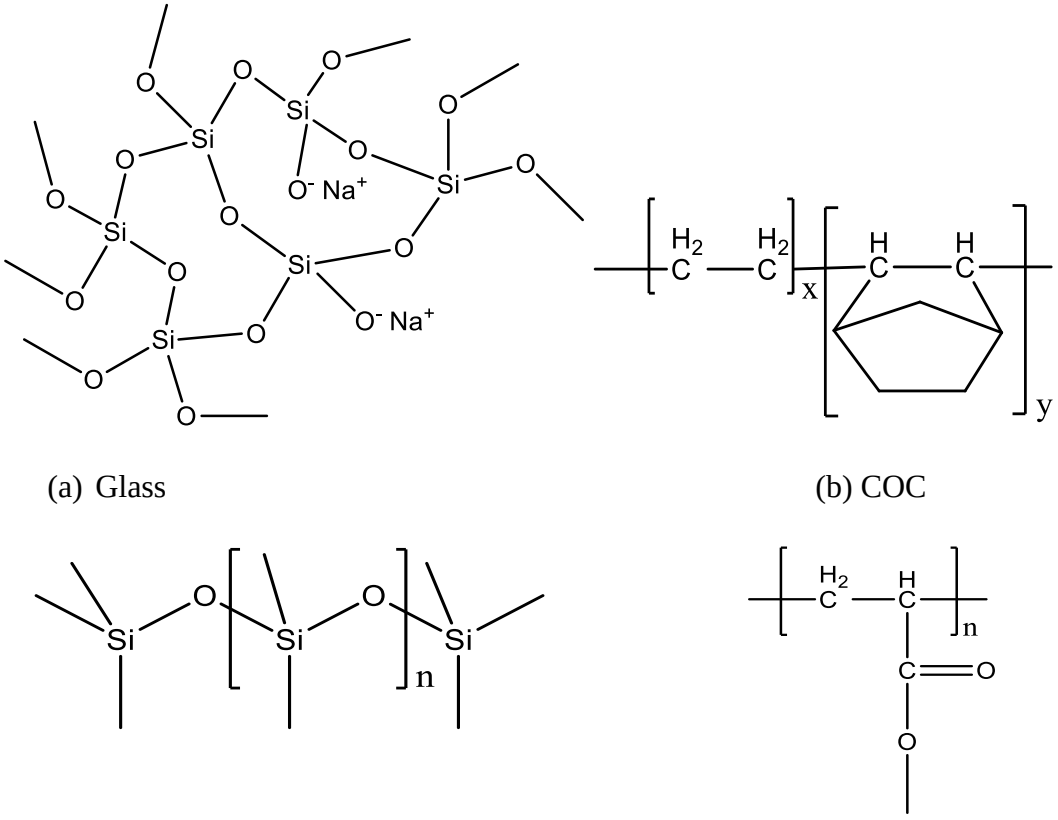


(a) Glass (b) COC

(c) PDMS (d) PMMA

**Fig. 4.1. Materials used in preparation of lab-on-a-chip devices: (a) glass (b) COC (c) PDMS (d) PMMA**

Over time, polydimethylsiloxane (PDMS), polymethylmethacrylate (PMMA) and cycloolefin (COC) polymers have gained more attention from microfluidic device manufacturers [9, 10].

The polymers illustrated in Figure 4.1 (b), (c) and (d) are easy to prepare, have low associated purchase and preparation costs and use low-tech technologies such as, soft lithography or nanoimprint lithography.

PDMS is the most used polymer in manufacturing of microfluidics because of chemical and physical properties, such as transparency in the UV-VIS region down to 280 nm, low polarity, low electrical conductivity (breakdown voltage of $2\times10^7$ $Vm^{-1}$), elasticity (thus easy release from a mould), thermal insulating properties (thermal conductivity of 0.2 $W(mK)^{-1}$), impermeability to liquid water and biocompatibility [10, 11]. The main limitations associated with this polymer are its hydrophobicity, which means that microchannels do not readily fill with aqueous solutions; a poor and often unstable electroosmotic flow and adsorption of hydrophobic compounds such as non-polar hydrocarbons, toluene and dichloromethane solvents into the polymer matrix, which causes swelling [9, 12]. Numerous reports outlining surface modification techniques to improve the PDMS surface wettability have been published over the past few years, which reflects the continuous interest in developing PDMS for a broad range of applications [9, 10, 13]. Limitations faced by lithography are primarily economic.

Microfluidic devices using PDMS can be made using microfabrication. Nanotechnology is the ensemble of technologies for fabrication of materials or systems with dimensions in the 1-100 nm range [14, 15]. The wide applicability of nanomaterials

and nanostructures in photonics, electronics, catalysis, and biotechnology fields has fuelled development of a large number of technologies [16]. These can be classified as conventional, such as electron beam or focused ion beam and nonconventional, depending on how well established techniques they are. Nonconventional nanofabrication techniques with high resolution and high throughput are soft lithography and nanoimprint lithography (NIL). In NIL, at temperatures above the glass transition point, hard master moulds made of metal, silicon or silica are pressed against a surface coated with a resist, to form a mould [17, 18]. Polymer residues around the patterned features are removed by dry etching or reactive ion etching steps. NIL is a simple low-cost technique, however long processing times and alignment issues when patterning on several levels, reduce wider adoption by industry [14, 19]. Soft lithography follows similar principles as NIL in creating channels but lacks the etching steps. The latest advances in soft lithography include the use of a 3D printer to prepare a microfluidic device starting from a computer/software designed prototype. In a paper published in 2013, Anderson *et al.* successfully used a 3D imprinted fluidic device to study cell transportation and to differentiate between living and dead cells in a sample, [20]. The device was reusable, allowed for high throughput and integration of commercially available membranes. The use of 3D printing technologies has not yet reached an affordability that would allow it to be used on a large scale in industrial manufacturing; however it holds great potential for use in academic research for optimization of fluidic device design or materials.

In the work presented here, a low-tech microfluidic device was prepared using indium tin oxide coated glass slides and a microchannel imprinted PDMS polymer slide is described. The manufacturing steps included soft lithography, NIL, photolithography and

wet etching steps, as well as chemical surface treatment - some of the most important PDMS surface treatment procedures proposed in literature. Throughout the manufacturing procedure the most simple and cost effective techniques were sought.

## 4.2. Materials and methods

### 4.2.1. Materials

To prepare the PDMS polymer, Sylgard 184 Silicone Elastomer base and Sylgard 184 Silicone Elastomer curing agent from Dow Corning, Midland, US were used. Silicone wafers of 3 inch Mechanical Grade Single Side Polished (SSP) Si were used for soft lithography. All organic solvents (methanol, isopropyl alcohol, ethyl acetate and acetone) were purchased from ACS Montreal Quebec with minimum 99% purity. To modify the surface of the PDMS, triethylamine and benzyl alcohol purchased from Sigma Aldrich, St. Louis, MO in 99.5% purity, were used. The indium tin oxide (ITO) covered glass slides were purchased from Corning, Delta Technologies, US with Rs of 4-8 Ω and 25 x 50 x 1.1 mm. To etch the ITO slides, the following compounds were used: tetraethyl ammonium hydroxide in 25 %wt. in $H_2O$ from Sigma Aldrich), sodium dodecyl sulfate (SDS) in a 99% assay from Fluka, Biochemika, Switzerland, hydrochloric acid (HCl) in 36.5-38% concentration from Caledon, Ontario, Canada and sodium carbonate ($Na_2CO_3$) in 99% from JT Baker Analyzed. All the chemicals needed in the preparation of the thin- film MIPs: ethylene glycol dimethacrylate (EGDMA) crosslinker, 4-vinyl pyridine (4-VP) monomer, 2,2-dimethoxy-2-phenyl acetophenone (DMPA) initiator, 2,4- dichlorophenoxyacetic acid

(2,4-D) template were purchased from Sigma Aldrich in the best available purity and were used with no further purification.

### 4.2.2. Preparation of PDMS

Following a conventional PDMS preparation method, Sylgard 184 Silicone Elastomer curing agent was added to the Sylgard 184 Silicone Elastomer base in a ratio of 1 to 10 (w/w). The mixture was cured in an oven over a mould for two hours at 60 °C.

### 4.2.3. Soft lithography with: (a) a printer, (b) silicon masks

(a) The features for channels and device elements were drawn using computer aided design (CAD) with the Inkscape or the Macromedia Freehand software and printed on clean acetate sheets using a laser jet printer (Samsung ML 2501). Different T-shape designs were printed, cropped and attached to a Petri dish, and PDMS was cured over the masks.

(b) Silicon wafers were cut into 2.5×2.5 $cm^2$ squares with a diamond pen and cleaned by sonication in ethanol, then dried and placed on the spin coater. A volume of 1 mL of negative SU8 photoresist was dispensed on the Silicone surface. The spin coater method was assigned as follows: the speed was increased from rest to 500 rpm with an acceleration of 100 rpm, left at 500 rpm for 30 s, then raised again to 1000 rpm using an acceleration of 300 rpm and left to spin for one min at the final speed. This method was used to ensure an average thickness of 20 μm of resist. The silicon wafer created with resist was then soft baked at 65 °C for one min and then hard baked at 95 °C for 2.5 min. Using the Maskless Patterning System (MPS), Intelligent Micro Patterning, LLC, SF-100, the substrate was

exposed to UV light for 60 s to polymerize the exposed areas of the resist and render them insoluble. The different patterns utilized are shown in Figure 4.2.

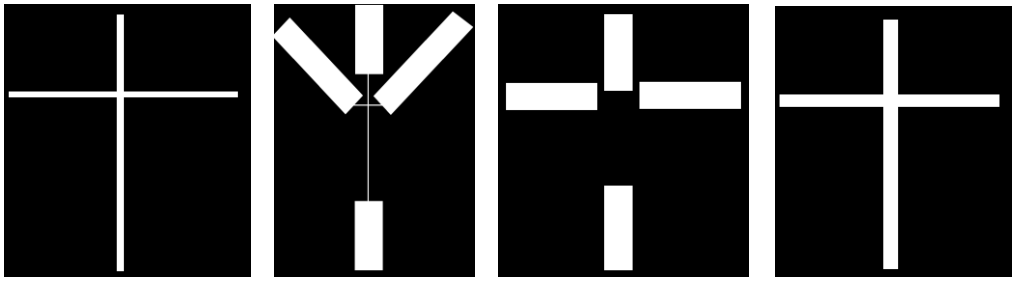

**(a)** **(b)** **(c)** **(d)**

**Fig. 4.2. Patterns for SI masks**

The substrate was again soft baked at 65 °C for one min and then hard baked at 95 °C for 2.5 min. The un-polymerized photoresist was removed by immersion into developer solution for 3 min followed by a rinse in isopropyl alcohol. A final bake at 95 °C for 5 to 10 min ensured a greater stability and longer life of the photoresist structure. The silica moulds were attached to the bottom of the Petri dish and the polymer was poured them over and left to cure in the oven at 60 °C for 2 hours.

### 4.2.4. Modification of the PDMS surface to increase wettability

(a) *Plasma treatment*

Squares of cured PDMS with an average area of 1 $cm^2$ were rinsed with methanol, dried under $N_2$ and then exposed to $O_2$ plasma in a Plasma Etch, Model PE-100 instrument at 50 W and 60 mTorr for 60 s.

(b) *Treatment in dilute HCl solution*

This procedure was modified from Chou *et al.*, [21]. Squares of 1 $cm^2$ of cured PDMS were placed in an aqueous solution of HCl with a pH of 2.48 in large Petri dishes at 47- 49 °C, under continuous stirring for 45 min.

(c) *Surface oligomer extraction*

Using an optimized procedure from Vickers *et al.* [22], PDMS squares of 1 $cm^2$ were immersed in 5.00 mL of triethylamine for two hours at 25 °C under continuous stirring. Under the same conditions the PDMS was exposed to 5.00 mL of ethyl acetate and then to 5.00 mL of acetone for two hours each, with the solvent refreshed every hour. The polymer was then dried under $N_2$, exposed to $O_2$ plasma at 50 W and 60 mTorr for 60 s and stored in water.

(d) *UV grafting polymers*

With a modified procedure from Hu *et al.*, [23], squares of PDMS of 1 $cm^2$ area were placed in 25.0 mL of an aqueous solution containing 0.5 mM sodium iodate, 0.5 % (wt) benzyl alcohol and 10 % (wt) methacrylic acid. The Petri dish was placed under a handheld UV lamp ($\lambda$= 254 nm, 6 W) at ambient temperature (~20 °C) for 3 h, then the material was rinsed with distilled water under overnight stirring. Alternatively a 400 W UV lamp was used for a total exposure time of 1 h ensuring that the Petri dish with the polymer is placed in an ice bath to prevent the sodium iodate, benzyl alcohol and methacrylic acid mixture from evaporating. Following UV treatment, the polymer was rinsed under stirring in water at 60 °C for 24 h. The graft density was measured by the

difference in weight of the PDMS squares before and after the treatment procedure. To verify the hydrophilicity of the PDMS surface visual observations of the contact angle of a drop of liquid of a constant volume on the PDMS surface were carried out.

### 4.2.5. Surface analysis studies by scanning electron microscope (SEM) studies

SEM images were recorded using a FEI MLA 650 F SEM, operating at an acceleration voltage of 10 kV and a magnification of ×50,000. All samples were sputtered with a thin layer of gold prior to analysis.

### 4.2.6. Developing electrodes on metal coated glass slides

Electrodes were developed on the ITO coated glass slides by patterning and acid etching. Several concepts were attempted but the one in Figure 4.3. was used in all further experiments.

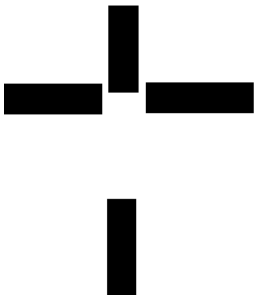

**Fig. 4.3. Transparency design for electrode pattern on ITO slides**

The ITO plates were cleaned by sonication in isopropyl alcohol for 15 min and dried under $N_2$. A volume of 1.00 mL S1813 positive photoresist was dispensed on the ITO surface. The plate was spin coated at 4000 rpm for 30 s for an even thickness of 10 µm. The ITO plate was soft baked at 105 °C for 1 min and then attached to an acetate

transparency and to a glass slide to ensure perfect alignment. With this fitting, the ITO was exposed to UV light from a UV 6 W handheld lamp for 25 min. A developer solution was prepared using a composition similar to that of Microposit MF-319 containing 8.8 mL of tetramethylammonium hydroxide (25% solution in $H_2O$), 1.8 mg of sodium dodecyl sulphate, SDS in 100 mL water (i.e. 1.8% surfactant). The exposed photoresist was removed by immersion in this solution and a red particulate appeared in solution during removal of the photoresist. The plates were rinsed with water, then immersed in boiling aqueous solution of 30% HCl for 8 s and neutralized in a 20% $Na_2CO_3$ solution. The residual photoresist was removed in the final step with a quick rinse with acetone. To confirm proper etching of the ITO, the electrodes and etched glass surface were tested for resistivity using a Hewlett Packard 34401 A Multimeter. The ITO patterned surface indicated a resistivity of 15-20 ohms while the glass slide indicated an overload.

### 4.2.7. Sealing by conformal contact of the PDMS and ITO surfaces

(a) *Plasma exposure*

Both PDMS and ITO slides were exposed to oxygen plasma for 60 s following the same method outlined in section 4.2.4 a), then the two surfaces were brought in contact and were left overnight.

(b) *Silanization*

The ITO slides were rinsed in a solution of 3-aminopropyldimethylethoxysilane, DMOAP following a method reported by Unni *et al.*, 2011 [24]. The ITO surface was then dried under $N_2$ and brought into conformal contact with the PDMS surface.

### 4.2.8. Surface functionalization with molecularly imprinted polymers, MIPs

(a) *On the etched ITO slides*

The etched ITO slides were derivatized overnight in a solution of 2.00% 3-(trimethoxysylil) propyl methacrylate in toluene. The resulting functionalized surface was dried under $N_2$ and stored in the dark. The composition of the MIP was based on the procedure developed by van Biesen *et al.*, [25] for the 2,4-D MIPs and later the toluene MIPs described in Chapter 3 [9]. The pre-polymerization mixture for the 2,4-D was prepared by adding into a 2 mL vial the template 2,4-D (0.04 mmol), the initiator DMPA (0.012 mmol), the crosslinking agent EGDMA (0.8 mmol), the monomer 4-VP (0.16 mmol) and 200 µL of MeOH:$H_2O$ (4:1) porogen. A volume of 8.0 µL aliquot of the pre-polymerization complex was dispensed on the derivatized glass surface, covered with a glass microscope cover-slide and placed directly under a UVP handheld UV lamp ($\lambda$ = 254 nm, 6 W) at ambient temperature (~20 °C) for 30 min.

(b) *On the PDMS surface*

Squares of 1 $cm^2$ of PDMS were first exposed to $O_2$ plasma for 1 min. Then, they were left overnight in a 2% (v/v) 3-(trimethoxysylil) propyl methacrylate in toluene in a covered Petri dish. Upon contact with the toluene solution, the polymer appeared to shrink and after leaving overnight it became sticky. Nevertheless, the procedure was used on this material. Fifteen hours later, 2 to 4 µL of pre-polymerization solution was applied on each plate and exposed to UV for 30 min. MIP formation was attempted on PDMS treated

according to the guidelines in Section 4.2.4.(c); however no satisfactory results were obtained.

### 4.2.9. Making a well on the ITO plate

Soft lithography using the positive S1813 or the negative SU8 photoresist were employed following the same procedures as described in Sections 4.2.6 and 4.2.3.(b) respectively to coat the surface of the ITO leaving uncovered the electrode pads and a square area for MIP formation. The range of shapes used with the SU8 photoresist shown in Figure 4.4 was drawn using the Inkscape software.

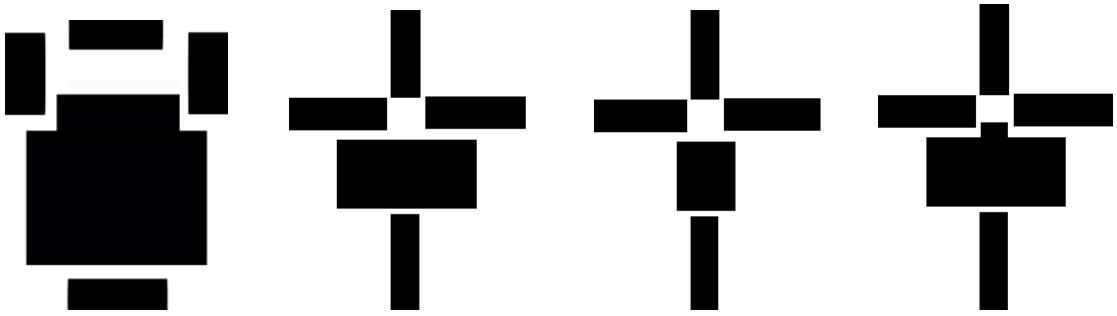

**Fig. 4.4. Well designs**

## 4.3. Results and discussion

### 4.3.1. Preparation of the PDMS and results

As described in the Materials and Methods, a very simple concept was used to generate masters for PDMS moulding. Features were patterned in PDMS by soft lithography using

CAD, a few acetate transparencies and an office laser printer. Several designs were used either to improve the channel length as described in Figure 4.5.(a) or the surface of the reservoirs, as shown in Figure 4.5.(b). This approach proved to be very simple, fast, inexpensive and with no need for extensive training.

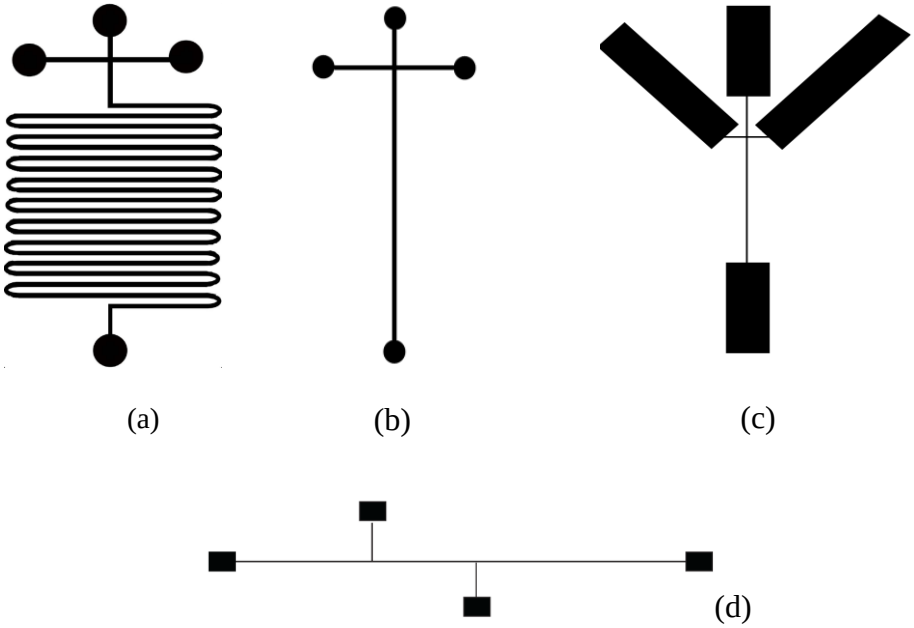


**Fig. 4.5. T-shape soft lithography masks for microchannels**

PDMS was cured over these masters and the features were analyzed by SEM. As shown in Figure 4.6., the patterns generated displayed a poor resolution of the features, which can be mainly attributed to the capacity of the printer to make high resolution, sharply delineated features. Given the poor results obtained, the printer – acetate was abandoned and nanoimprint lithography using silica rigid masks made by SU8 patterning and acid etch on silicon wafers were used to imprint channels in PDMS.

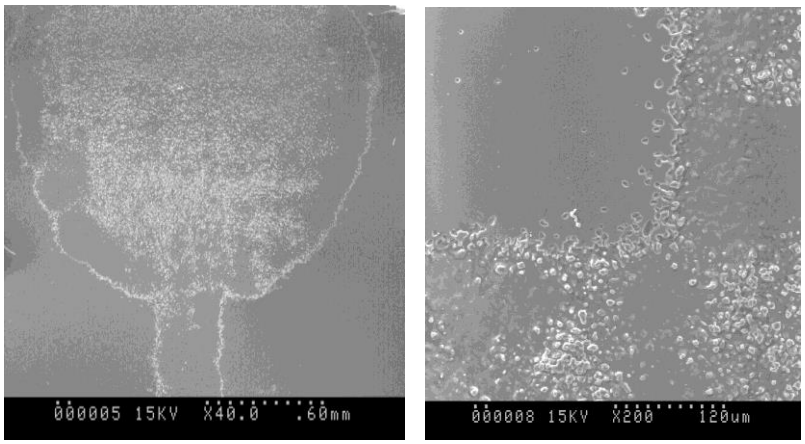


**Fig. 4.6. Reservoir and channel crossing- SEM analysis**

In making the Si masks, S1813 photoresist was used at first, but its low viscosity resulted in very thin, low depth features on the PDMS, thus it was replaced with the more viscous SU8 photoresist. SU8 is a negative photoresist therefore upon UV treatment the exposed area becomes insoluble to the developer. The pattern that remains is an epoxy that is very durable and hard to remove. The preparation of Si masks was time consuming and difficult to reproduce given the fragility of the Si wafers. However, excellent resolution and reproducibility of features and larger channel depth were made possible.

### 4.3.2. Modification of the surface of the PDMS to increase wettability and surface studies

Given the high hydrophobicity of PDMS surface, several procedures were used to increase its hydrophilicity. For a more reliable measurement of the degree of hydrophilicity acquired during the treatment procedures described above, attenuated total reflectance-Fourier transform infrared spectroscopy (ATR-FTIR) studies were used.

(a) *Plasma treatment*

Hydrophilicity not only makes the surface more wettable, but it improves the electroosmotic flow. The procedures to modify PDMS are key to make these systems robust and hydrophilic. Oxygen plasma treatment with $O_2$ can render the PDMS surface hydrophilic by oxidizing the dangling polymer bonds as shown in Figure 4.7., however this technique is reversible, though when joined together two plasma treated PDMS surfaces can be sealed irreversibly. Hydrophobic recovery occurs within less than half an hour from exposure to plasma. Ren *et al.* argued that this may be due to reorientation of hydroxyl groups about sigma bonds from the surface into the bulk [8].

It is not always possible to carefully control plasma treatment efficiency and the effects on the polymer surface have not been studied extensively. As such this technique will only be used to seal PDMS to ITO.

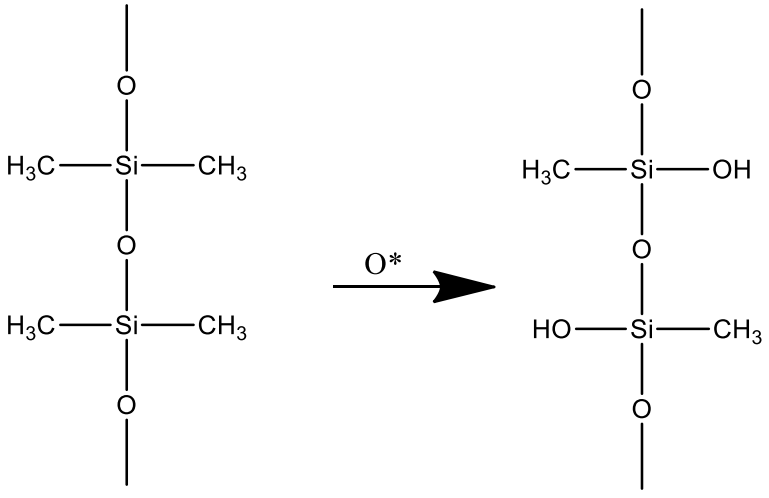


**Fig. 4.7. Oxidation of the PDMS surface as a result of oxygen plasma treatment**

(b) *Treatment in dilute HCl solution*

The contact angle was estimated visually by comparison with an untreated PDMS surface by placing a drop of 0.05 mL $H_2O$ on each surface. No difference between the untreated and the treated surface was observed, so the procedure was abandoned.

(c) *Surface oligomer extraction*

Visual comparison of the contact angle of a drop of 0.05 mL water on the surface of native and treated polymers showed that the treated surface has a much lower contact angle and therefore had become hydrophilic.

Table 4.1. The percent extracted polymer

| PDMS square no | Initial weight, g | Final weight, g | % extracted oligomer* |
|---|---|---|---|
| 1 | 0.5359 | 0.5109 | 4.665% |
| 2 | 0.5800 | 0.5508 | 5.034% |
| 3 | 0.4750 | 0.4509 | 5.074% |
| 4 | 0.5246 | 0.4979 | 5.090% |

* The following formula was applied: $\%\ extracted\ polymer = \frac{M_{native\ polymer} - M_{extracted}}{M_{native\ polymer}} x\ 100$

(d) *UV grafting polymers*

Upon treatment, the PDMS squares lost their transparency and shine, and acquired a matte look. This may be the only disadvantage when compared with the surface oligomer extraction technique.

Each of the additives in the UV grafting solution has a specific role. The $NaIO_3$ is there to scavenge $O_2$. Benzyl alcohol is used as a chain transfer agent to increase the grafting surface while the methacrylic acid is the hydrophilic moiety that attaches to the surface of PDMS as shown in Figure 4.8 below:

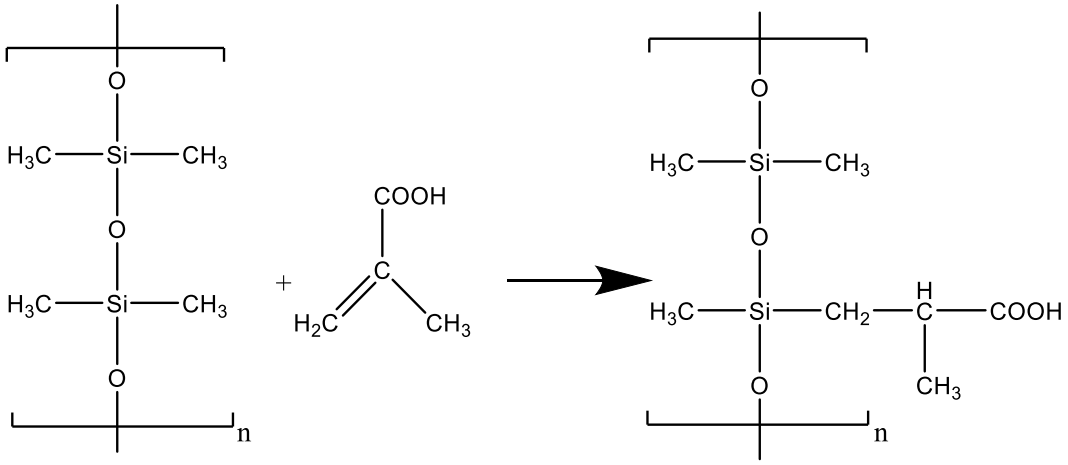


**Fig. 4.8. PDMS surface modification by UV grafting**

Scanning electron microscopy (SEM) studies, in Figure 4.9. showed a channel depth and feature resolutions that were considered insufficient for the purpose of this study. Regardless of the surface chemistry of PDMS, the same poor resolution of features was observed in all cases. The depth of the channels was too small to be measured. The best results were obtained with UV grafting polymers and surface oligomer extractions.

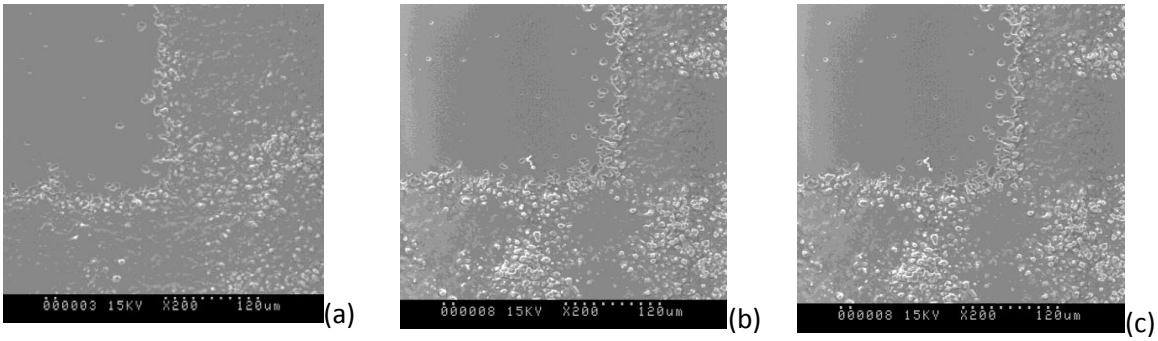


**Fig. 4.9. SEM micrographs of channel crossing on PDMS surfaces, (a) non-treated, (b) treated with UV, (c) surface oligomer extraction**

### 4.3.3. Etching the electrode pads on the ITO surface

In the process of determining the optimum method to etch electrodes on the ITO plates, several difficulties were encountered. The results using the initial developer recipe suggested that NaOH was not efficient in removing the S1813 photoresist. The exposure to UV light was optimized in terms of the lamp power and the exposure time to the lamp. The metal etch procedure was optimized in terms of the acid concentration used and exposure time. When left too long in acid, metal was etched even under the polymerized photoresist which lead to poorly defined features.

### 4.3.4. ITO and PDMS surface functionalization

Polymerization of a MIP was attempted on the PDMS surface, but the results were poor. The coating had a semitransparent white appearance; therefore it was concluded that polymer did not form on the polymer surface.

The idea of a well formed directly on the ITO plate was based on the need to prepare the MIP within a delimited perimeter and surface area as to control the number of absorbing sites, the MIP surface formation and the MIP thickness and render them reproducible. Initially S1813 was used because of the ease in developing this photoresist.

The reasoning for using a MIP well lies in the need to accurately control the MIP surface formation and the thickness of the MIP. Initially the positive S1813 photoresist was sought because of its higher tolerance to organic solvents that are used in the prior steps in MIP formation. However, since it has a low viscosity, a very thin layer and thus shallow cavity was obtained. The walls of the well were too short to hold the pre-polymerization solution within a defined space. Consequently, S1813 was replaced with another photoresist, the negative resist SU8, a more viscous polymer that would ensure a thicker layer, deeper cavity and thus thicker MIP film. The SU8 is easily removed when using organic solvents. Because the preparation of the 2,4-D MIPs implies use of organic solvents and acids, the glass surface could not be prepared by washing in ethanol, and mixing overnight in a toluene solution. MIP formation was attempted within these well with no success. The MIP polymerized but did not attach to the surface during polymerization. Further trials should be done to further the aim of generating wells on ITO plates. Thin-film MIPs for 2,4-D were obtained but were not tested for upload with standard solutions, upon conformal sealing of the ITO and PDMS surfaces.

## 4.4. Conclusions and future work

### 4.4.1. Coupling to detection techniques

One advantage of microchips is that minimal sample volume is required for analysis, thus detectors with high resolution and sensitivity are necessary. Laser induced fluorescence (LIF) was the first and most common detector coupled to microfluidic devices due to its simplicity and high sensitivity [1, 8]. However this detector is limited to naturally fluorescent analytes or subsequent derivatization pre- or post- separation is required. For non-fluorophores, this implies that the number of sample preparation steps integrated on the microchip increases, which increases the complexity of the microfabrication process and overall decreases repeatability of analysis [1, 8, 26]. Absorption spectrophotometric detectors (with a path length of 20 μm or less) and electrochemical detectors (with platinum electrodes) have also been successfully interfaced to microfluidic devices [4, 8].

An attractive alternative to these detectors has been mass spectrometry (MS). MS is one of the most versatile analytical tools because using specific mass-to-charge ratios (m/z) and if necessary fragmentation patterns can provide information about the nature of a sample, its composition in terms of organic and inorganic compounds or the isotope ratio of the atoms [27]. Despite the large instrumental footprint of traditional instruments, mass spectrometry is highly suitable for off-chip detection from microfluidic devices because it easily accommodates the low flow rates associated with these devices [1]. For portability reasons, attempts to reduce interfaced microchips-MS for *in situ* analysis started in the early 1990s [30]. Although the attempts to build ion traps, quadrupole, time of flight and electrostatic sector mass analyzers have been successful, their performance is not yet at the

level of conventional instruments [1, 3, 28]. The success of a microchip-MS analysis relies on how well the microchip is interfaced to the MS, that is how effectively the samples leaving the micro capillary are ionized and introduced into the mass analyzer, sometimes under vacuum conditions. Depending on the nature of the sample, various ionization techniques exist and many were interfaced to microchip-MS analysis [1]. Electrospray ionization (ESI), atmospheric pressure chemical ionization (APCI) and atmospheric pressure photoionization (APPI) have been developed for coupling to lab-on-a-chip liquid chromatography (LC) based when working at low flow rates; however APCI and APPI have been successfully coupled to gas chromatography (GC) too. Matrix assisted laser desorption ionization (MALDI) is another technique successfully interfaced to microchip-MS for high throughput ionization of very large non volatile biomolecules.

## 4.5. References


1. R. D. Oleschuk, D.J. Harrison, Trends in Anal. Chem. 19 (2000) 379- 388
2. D. Gao, H. Liu, Y. Jiang, J.M. Lin, Lab Chip 13 (2013) 3309- 3322
3. T. Sikanen, S. Franssila, T.J. Kauppila, R. Kostiainen, T. Kotiaho, R.A. Ketola, Mass Spec. Rev. 29 (2010) 351-391
4. F.E. Regnier, B. He, S. Lin, J. Busse, TIBTECH 17 (1999) 101-106
5. F. Foret, P. Kusý, Eur. J. Mass. Spectrom. 13 (2007) 41-44
6. A.D. Beaton, C.L. Cardwell, R.S. Thomas, V.J. Sieben, F.E. Legiret, E.M. Waugh, P.J. Statham, M.C. Mowlem, H. Morgan, Environ. Sci. Technol. 46 (2012) 9548-9556
7. C.D.M. Campos, J.A.F. da Silva, RSC Advances 3 (2013) 18216-18227
8. F.C. Poole, The essence of Chromatography, 1st Edition, Elsevier, 2003, pp 703-705
9. J. Zhou, A.V. Ellis, N.H. Voelcker, Electrophoresis 31 (2010) 2-16
10. J.C. McDonald, G.M. Whitesides, Accounts Chem. Res. 35 (2002) 491- 499
11. X. Ren, M. Bachman, C. Sims, G.P. Li, N. Allbritton, J. Chromatogr. B 762 (2001) 117-125
12. J.N. Lee, C. Park, G.M. Whitesides, Anal. Chem. 75 (2003) 6544- 6554
13. T. Li, W. Lei, W. Wei, L. Xlaowei, Key Eng. Mater. 562-565 (2013) 131- 135
14. http://www.nanoscience.at/aboutnano_en.html -accessed on March 3rd, 2011
15. H.S. Kim, C.H. Lee, P.K. Sudeep, T. Emrick, A.J. Crosby, Adv. Mater. 22 (2010) 4600-4604

16. G. Cao, Nanostructures and nanomaterials- synthesis, properties and applications, Imperial College Press, 2004, pp 312-328
17. H.P. Chou, Proc. Natl. Acad. Sci. USA 96 (1999) 11-13
18. C. Pina-Hernandez, P.F. Fu, L.J. Guo, ACS Nano 5 (2011) 923-931
19. S. Hu, X. Ren, M. Bachman, C.E. Sims, G.P. Li, N. Allbritton, Anal. Chem. 74 (2002) 4117-4123
20. K.B. Anderson, S.Y. Lockwood, R.S. Martin, D.M. Spence, Anal. Chem. 85 (2013) 5622-5626
21. S.Y. Chou, P.R. Krauss, P.J. Renstrom, J. Vac. Sci. Technol. B 14 (1996) 4129-4133
22. J.A. Vickers, M.M. Caulum, C.S. Henry, Anal. Chem. 78 (2006) 7446-7452
23. S. Hu, X. Ren, M. Bachman, C.E. Sims, G.P. Li, N.L. Allbritton, Anal. Chem. 76 (2004) 1865- 1870
24. H.N. Unni, D. Hartono, K.M. Lim, Adv. Mat. Res. 254 (2011) 191- 194
25. G. Van Biesen, J.M. Wiseman, J. Li, C.S. Bottaro, Analyst 135 (2010) 2237-2240
26. M. Haapala, V. Saarela, J. Pól, K. Kolari, T. Kotiaho, S. Franssila, R. Kostiainen, Anal. Chim. Acta 662 (2010) 163- 169
27. C.S. Bottaro, CHEM 6151-Lecture notes- Jan 2011
28. R.R. Boyd, C. Basic, A. Bethem, Trace quantitative analysis by Mass Spectrometry, Wiley, England , 2008, pp 195-196

# Chapter 5. Conclusions and future work

Molecular imprinting has garnered interest for applications in many chemistry fields as reflected by the number of articles and reviews published every year and enumerated in a MIP database, [1]. The potential for commercialization has long been recognized with over 180 patents filled in 2012 [1]. For reasons relating to the response reproducibility, sensitivity in *in situ* conditions and ruggedness, the transition to a marketable prototype has been more challenging [2- 4]. The aim of this thesis has been to generate a simple, sensitive, rugged, low-tech MIP product for the detection and monitoring of light PAHs indicating crude oil discharges in environmental water bodies.

In the second chapter, a detailed account of the development of a novel thin-film MIP using toluene pseudo-template and octanol solvent for the uptake of a group of four light PAHs is given. An initial evaluation of the imprinted and non-imprinted polymers in aqueous standard solutions suggested a sensitive imprinted material capable of a linear response over an upload concentration range of 10 to 100 μg $L^{-1}$ with a good degree of selectivity relative to the response of the non-imprinted polymer. Applicability to complex matrices was then verified by MIP analysis for spiked PAHs in wastewater and seawater. The linearity of response was excellent in all matrices and at very low spiked concentrations considering the low mass of polymer used for adsorption, the lack of sample preparation or conditioning steps prior to analysis and the use of a simple GC-MS equipped with a single quad.

The third chapter described the preparation of another novel imprinted polymer with toluene as a porogen and a template. The interest was to determine whether this approach will result in more sensitive and selective materials. Optimization of the MIP composition was carried out by trial-and-error and experimental design approaches. These new MIPs were evaluated in increasing upload concentration conditions and in presence of other possible inhibiting compounds in various matrices to conclude that they can be used for real time analysis although they are not as selective at low concentrations as the previously designed materials.

In the fourth chapter, all the preliminary steps to manufacture a microfluidic device from ITO coated glass slides with etched electrode pads and PDMS micro patterned surfaces have been described. Surface modification of the PDMS to achieve a better surface hydrophilicity was attempted using different methods from the literature. Various approaches using soft lithography, photolithography and etching techniques were tested to build the most efficient and low-tech method possible.

To summarize, two types of thin-film MIPs targeting PAHs were prepared and evaluated as very sensitive and selective materials capable of reliable response in simple and complex matrices. The studies carried out in environmental samples suggested that the MIPs could be used *in situ* for immediate upload useful in screening studies or for longer time upload suitable to monitoring, and then coupled offline to GC-MS for detection of the PAHs adsorbed. To add the *online* analysis feature to these materials, the MIPs can be integrated into the microfluidic device, using the preliminary microfabrication methods proposed in Chapter 4. Consequently the separation can be carried out with the aid of electroosmotic or hydrodynamic flow (capillary electrochromatography or liquid

chromatography, respectively) with detection by UV. The optimum conditions to fabricate a microfluidic device would require a clean room to ensure minimum interference of particulates in the sealing or the curing process. Comparison to US-EPA standard methods for detection in industrial wastewater (EPA-610) or drinking water (EPA-8270-D) will be necessary to give a better picture of the excellent performance of these MIPs [5]. Taking this work one step closer to a commercial prototype would imply a life cycle cost analysis to outline all the costs involved in the preparation, utilization, maintenance and disposal of a MIP, as well as an evaluation of the market demand for such a product and a comparison to the current products on the market.

As concluded in Chapters 2 and 3, excellent sensitivity for low concentrations in the μg $L^{-1}$ were obtained with a simple GC-MS with a quadrupole analyzer. However, surface analysis could equally be carried out by DESI-MS. The advantages are numerous. DESI is an advanced ionization technique that was developed in 2000 by Cooks and co-workers [6]. Once the analyte is adsorbed from the environmental matrix using the MIP it could be analyzed directly on the substrate, without any further sample preparation: separation of the different PAHs and detection. This would increase throughput, limit the use of solvents and provide a more representative value of the environmental concentration [6]. DESI was reported for sensing of PAHs in 2008, when Chen *et al*. detected all the 16 priority PAHs in aerosols from burning of rice straws with LODs of 10 pg for 5 s of sampling. The observed dynamic range spanned over 3 orders of magnitude [7]. Coupling DESI with MIPs would enable sample pre-concentration and analysis in one step. To our knowledge, the only account of such an application comes from our group. Van Biesen *et*

*al.* prepared a thin-film MIP for selective uptake of 2, 4-D and detected the pesticide by direct DESI analysis on the MIP [8].

The whole process of developing thin-film MIPs that covered the literature review, the material preparation, optimization and characterization in Chapters 2 and 3 not only served to make the final two MIP products, but also provided insightful and valuable information on the type of interactions, mechanisms of adsorption and chemistry of the MIP composition necessary for analysis of pollutants in water. This knowledge is applicable now to designing MIPs for different applications. An example that does not range far from the MIPs already described is the preparation of MIPs with a deuterated phenanthrene (phenanthrene-$d_{10}$) template. Preliminary optimization studies were carried out and very good results for uptake in seawater were obtained, as will be described further. The phenanthrene-$d_{10}$ were prepared following the same ratio of template to monomer to crosslinking agent as in Chapter 2 and are listed in Table 5.1.

Table 5.1. MIP composition

| Pre-polymer component | MIP | NIP |
|---|---|---|
| phenanthrene-$d_{10}$ | 7.6 mg (0.0405 mmol) | _ |
| 4-VP | 17.0 µL (0.158 mmol) | 17.0 µL (0.158 mmol) |
| EGDMA | 151 µL (0.801 mmol) | 151 µL (0.801 mmol) |
| DMPA | 3.20 mg (0.0125 mmol) | 3.20 mg (0.0125 mmol) |
| 1-octanol | 200 µL (1.26 mmol) | 200 µL (1.26 mmol) |

The optimization procedure was limited to determining the optimum polymerization temperature at ~20 °C the room temperature and at 4 °C and the optimum porogen between octanol and a ternary azeotropic mixture (DCM:$H_2O$:MeOH =1:1:5, v/v). Binding assays were carried out in aqueous multi standard solutions. The highest binding response was observed for polymerization at room temperature. This does not agree with previous reports where a higher number of binding sites and thus higher binding capacity were observed when polymerization was carried out at lower temperature [9, 10], However, Hosoya *et al*. [11] had similar observations to those in this thesis for a MIP prepared from anthracene and EDMA and based on their explanation, the observed behavior could be attributed to the lack of polarity in the template and the weak interactions governing the assembly of the pre-polymerization complex in the Phen-$d_{10}$-4VP system, [11]. The phenanthrene-$d_{10}$ MIPs showed similar binding characteristics when the ternary azeotrope and octanol were used as porogens, however, when octanol was used a visibly more porous material was obtained.

No method validation studies were carried out given the short timeframe of the project; however, the applicability to environmental samples was tested by binding studies in seawater spiked with different amounts of PAHs to reach a final concentration of 0.5, 1, 3, 6, 10, 50, 80 and 120 µg $L^{-1}$. The seawater samples were collected in the morning from the same sampling point in the St. John's harbor area and were stored at 4 °C overnight and analyzed within 24 h after collection. Multi-standard PAH solutions were prepared in a range from 0 to 1200 µg $L^{-1}$ and samples prepared in a number of 4 replicates were analyzed by GC-MS in SIM mode. The fragments corresponding to phenanthrene-$d_{10}$ with m/z of

160 and 189 did not interfere with determination of the phenanthrene analyte fragments with m/z of 152 and 178.

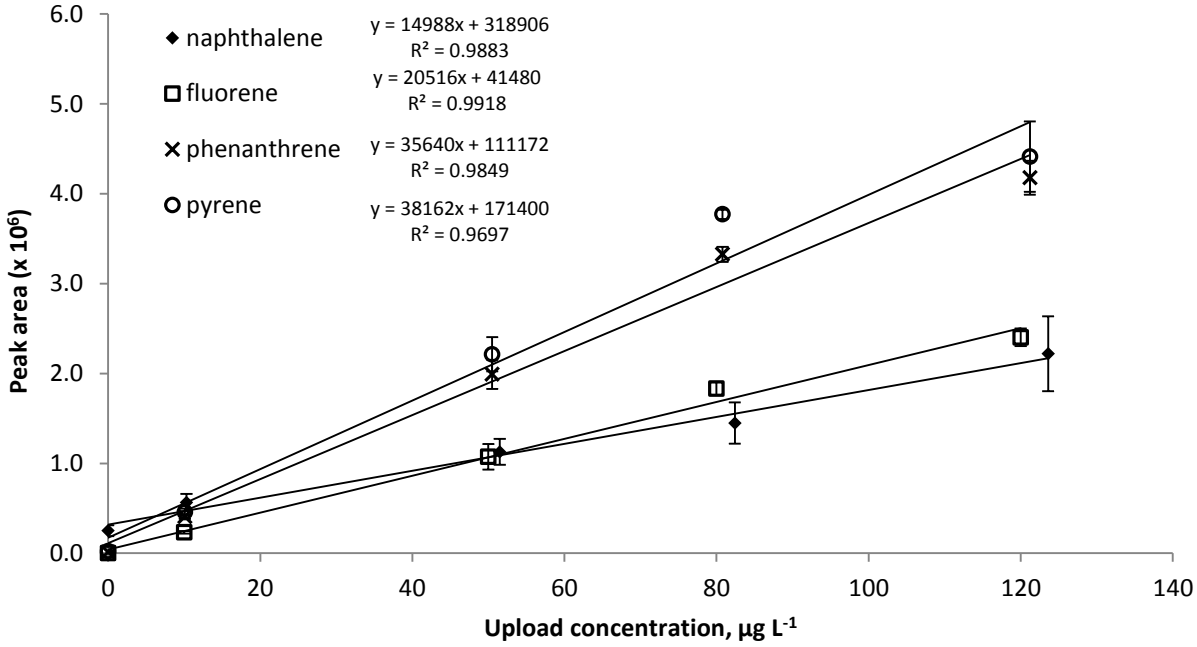


**Fig. 5.1. Increase in response of MIPs with increase in the spiked concentration of PAHs in raw seawater samples; experimental conditions of 80.0 mL sample for two hours, GC-MS in SIM mode. The response is the mean value of three measurements. Bars represent standard deviation.**

The binding curves (Figure 5.1) show an excellent linear response with the lowest variation coefficient of $R^2$ = 0.97 for pyrene. The MIPs preference for pyrene and phenanthrene followed by naphthalene and fluorene can be explained using the same arguments as in the previous chapters (please refer to Chapter 2, Section 2.3.2). At lower

spiked concentrations, similar linear responses were obtained as seen in Figure 5.2, except for naphthalene.

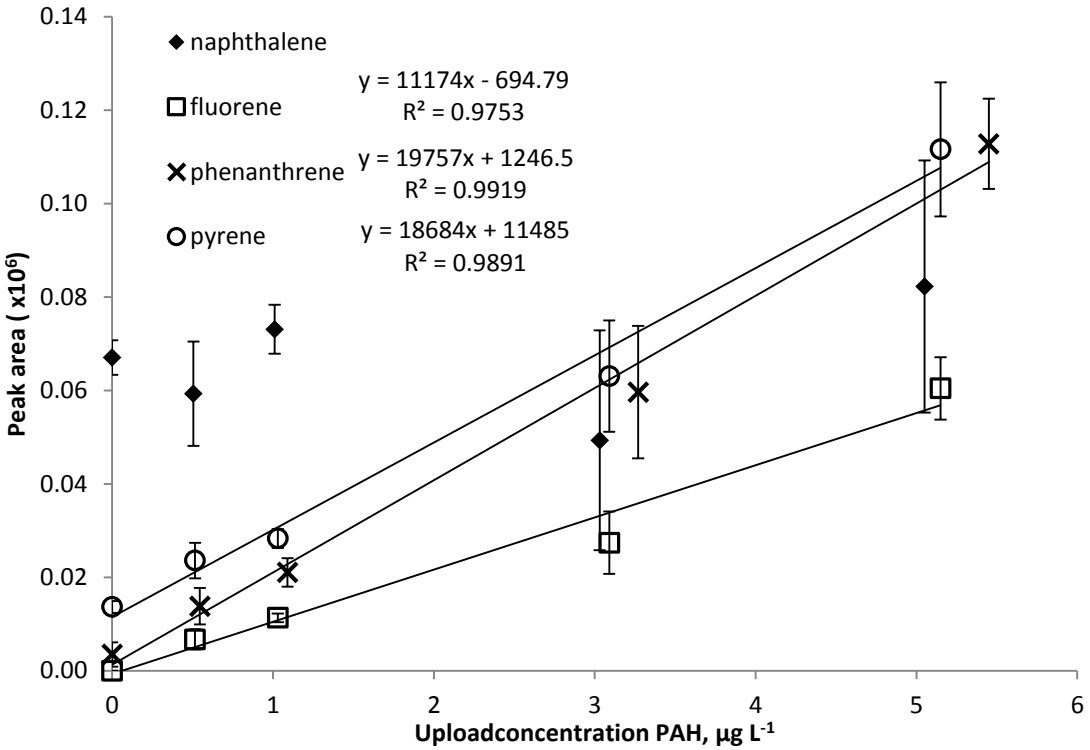


**Fig. 5.2. Increase in response of MIPs with increase in the spiked concentration of PAHs in raw seawater samples; experimental conditions of 80.0 mL sample for two hours, GC-MS in SIM mode. The response is the mean value of three measurements. Bars represent standard deviation.**

The results obtained for naphthalene cannot be fully explained and repetition of the binding experiment would be necessary to confirm the results obtained for this particular analyte. For fluorene, phenanthrene and pyrene, the sensitivity and linearity of response are very good.

The binding capacity for the individual PAHs as suggested by the peak area does not surpass the performance of the MIPs prepared using the toluene pseudo-template in Chapter 2, though the larger phenanthrene-$d_{10}$ template opens new opportunities in targeting larger, more complex PAHs. Given the excellent sensitivity proven in seawater matrices achieving this should be easy and application could be extended for example to specific industrial waste samples.

Finally, other supports for thin-film MIPs could be experimented with. Good results were already obtained using polymethylmethacrylate (PMMA) with no prior surface derivatization required. Another advantageous step is that microfabrication techniques can be more easily applied to PMMA to build microchannels than to silica glass, which could open an opportunity for generating microfluidics with patterned MIPs.

To conclude, this thesis has reached its goals by providing a MIP material for easy selective and sensitive detection of light PAHs in complex water samples and has laid the foundation for preparing a competitive prototype for *in situ* real time environmental analysis. A great achievement is that the work described here does not end when closing this book, but has the potential to expand in many possible ways as a platform technology for other environmental water analysis applications.

## 5.1. References


1. www.mipdatabase.com- accessed on 18/07/2013
2. A. Ellwanger, C. Berggren, S. Bayoudh, C. Crecenzi, L. Karlsson, P.K. Owens, K. Ensing, P. Cormack, D. Sherrington, B. Sellergren Analyst 126 (2001) 784- 792
3. N. Iqbal, P.A. Lieberzeit, Molecularly Imprinted Sensors, 1st Edition, Elsevier, 2012, pp 195-235
4. P.P. Fu, Q. Xia, X. Sun, H. Yu, J. Env. Sci. Health 30 (2012) 1-41
5. D.M. Pampanin, M.O. Sydnes, Polycyclic Aromatic Hydrocarbons a Constituent of Petroleum: Presence and Influence in the Aquatic Environment, Hydrocarbon, Dr. Vladimir Kutcherov, 2013, pp 83-118
6. J.M. Wiseman, D.R. Ifa, Q. Song, R.G. Cooks, Angew. Chem. Int. Ed. 43 (2006) 7188-7192
7. H. Chen, M. Li, Y.P. Zhang, X. Yang, J.J. Lian, J.M. Chen, J. Am. Soc. Mass Spectrom. 19 (2008) 450-454
8. G. Van Biesen, J.M. Wiseman, J. Li, C.S. Bottaro, Analyst 135 (2010) 2237-2240
9. B. Sellergren, M. Lepisto, K.J. Mosbach, J. Am. Chem. Soc. 110 (1988) 5853-5860
10. E.V. Piletska, A.R. Guerreiro, M.J. Whitcombe, S.A. Piletsky, Macromol. 42 (2009) 4921-4928
11. K. Hosoya, Y. Iwakoshi, K. Yoshizako, K. Kimata, N. Tanaka, J. High Resol. Chromatogr. 22 (1999) 256–260

## Appendix 1

## Toluene octanol MIPs

### GC-MS data

- Analysis of a 3.0 µg $L^{-1}$ PAH multi standard prepared in ACN
- Analysis of 10.0 µg $L^{-1}$ PAH multi standard prepared in ACN
- Analysis of a DCM rinse in the roto vap prior to reducing the PAH containing solutions to extracts
- Analysis of PAH extract from the upload of 0.5 µg $L^{-1}$ PAH multi standard in distilled water on a MIP over two hours
- Analysis of PAH extract from the upload of 30 µg $L^{-1}$ PAH multi standard in wastewater on an NIP over two hours
- GC-MS of PAH extract from the upload of 3.0 µg $L^{-1}$ PAH multi standard in seawater on a MIP over two hours

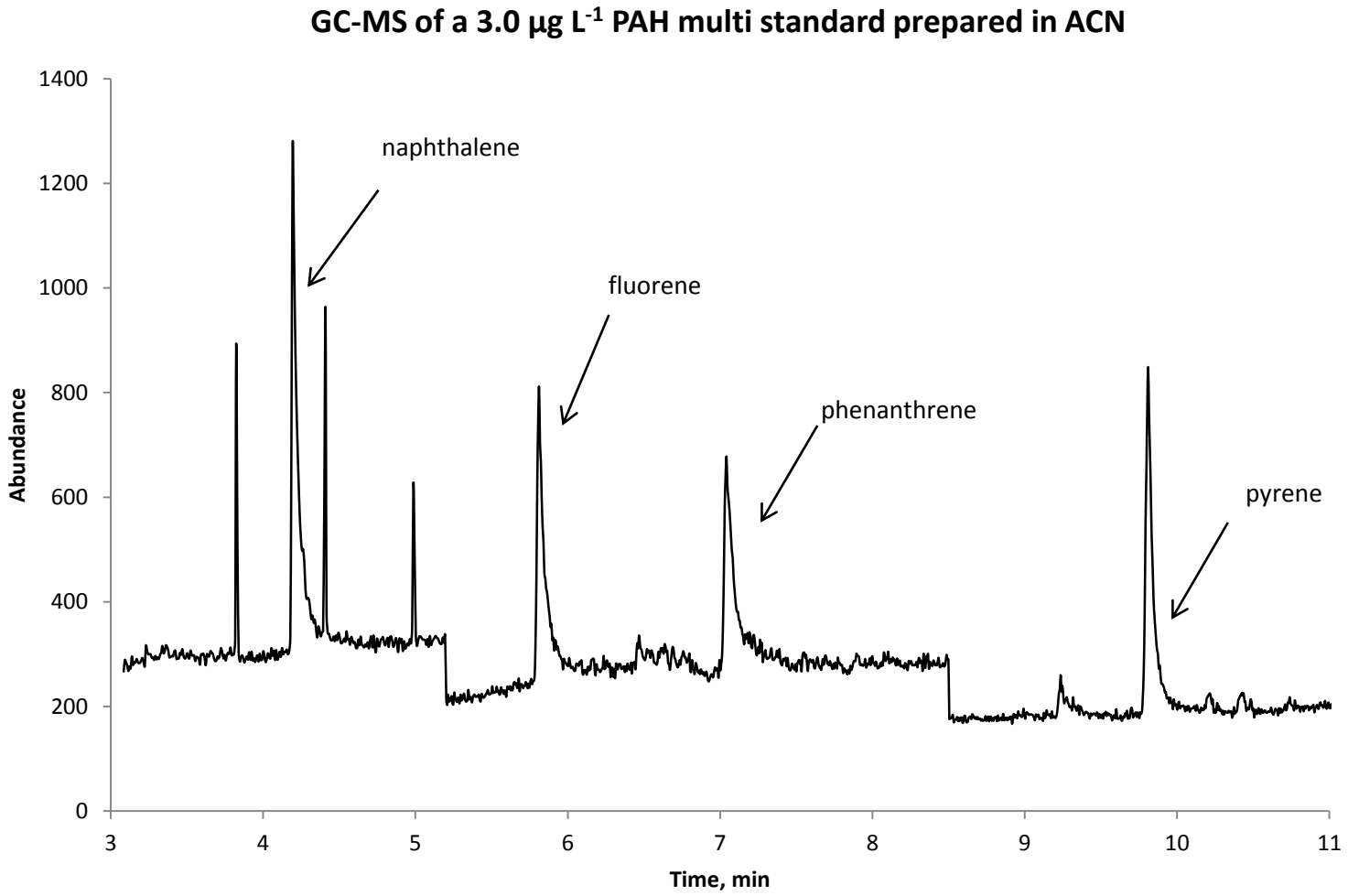
GC-MS of a 3.0 µg L-1 PAH multi standard prepared in ACN
Abundance
Time, min
naphthalene
fluorene
phenanthrene
pyrene
0
200
400
600
800
1000
1200
1400
3
4
5
6
7
8
9
10
11

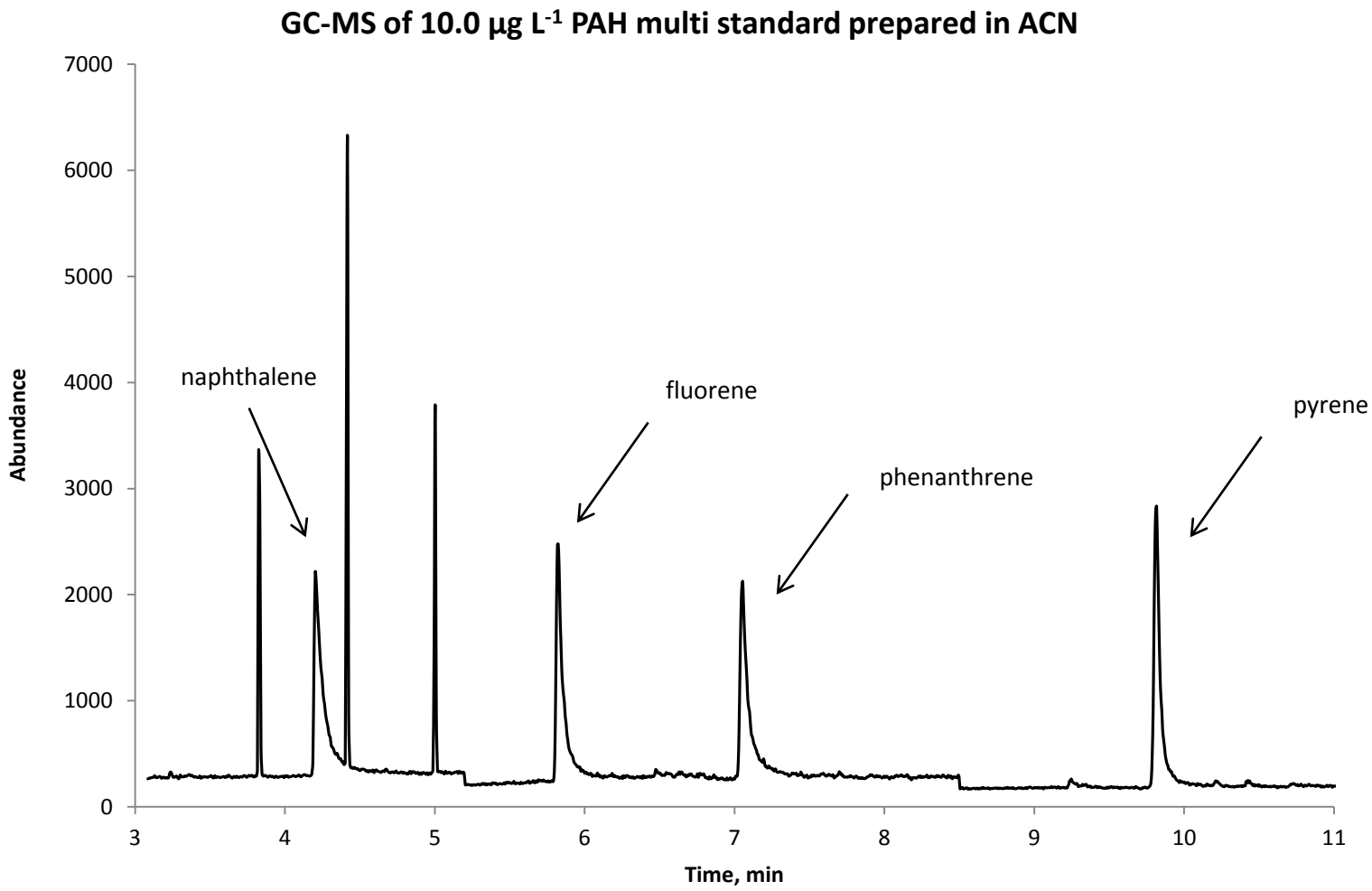
GC-MS of 10.0 µg L-1 PAH multi standard prepared in ACN
Abundance
7000
6000
5000
4000
3000
2000
1000
0
naphthalene
fluorene
phenanthrene
pyrene
3
4
5
6
7
8
9
10
11
Time, min

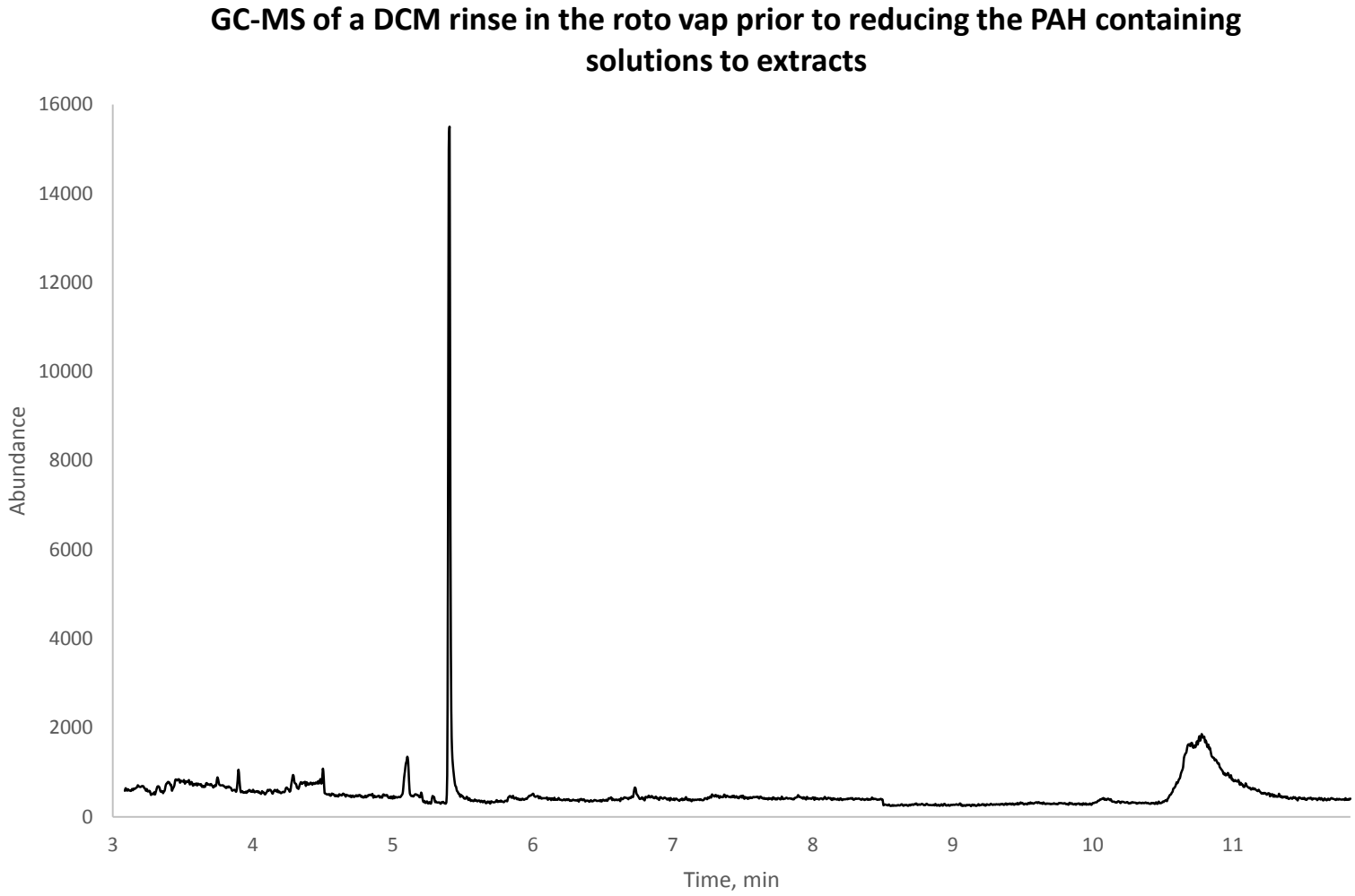
GC-MS of a DCM rinse in the roto vap prior to reducing the PAH containing solutions to extracts
16000
14000
12000
10000
8000
6000
4000
2000
0
Abundance
3
4
5
6
7
8
9
10
11
Time, min

**GC-MS of PAH extract from the upload of 0.5 µg $L^{-1}$ PAH multi standandard in distilled water on a MIP over two hours**

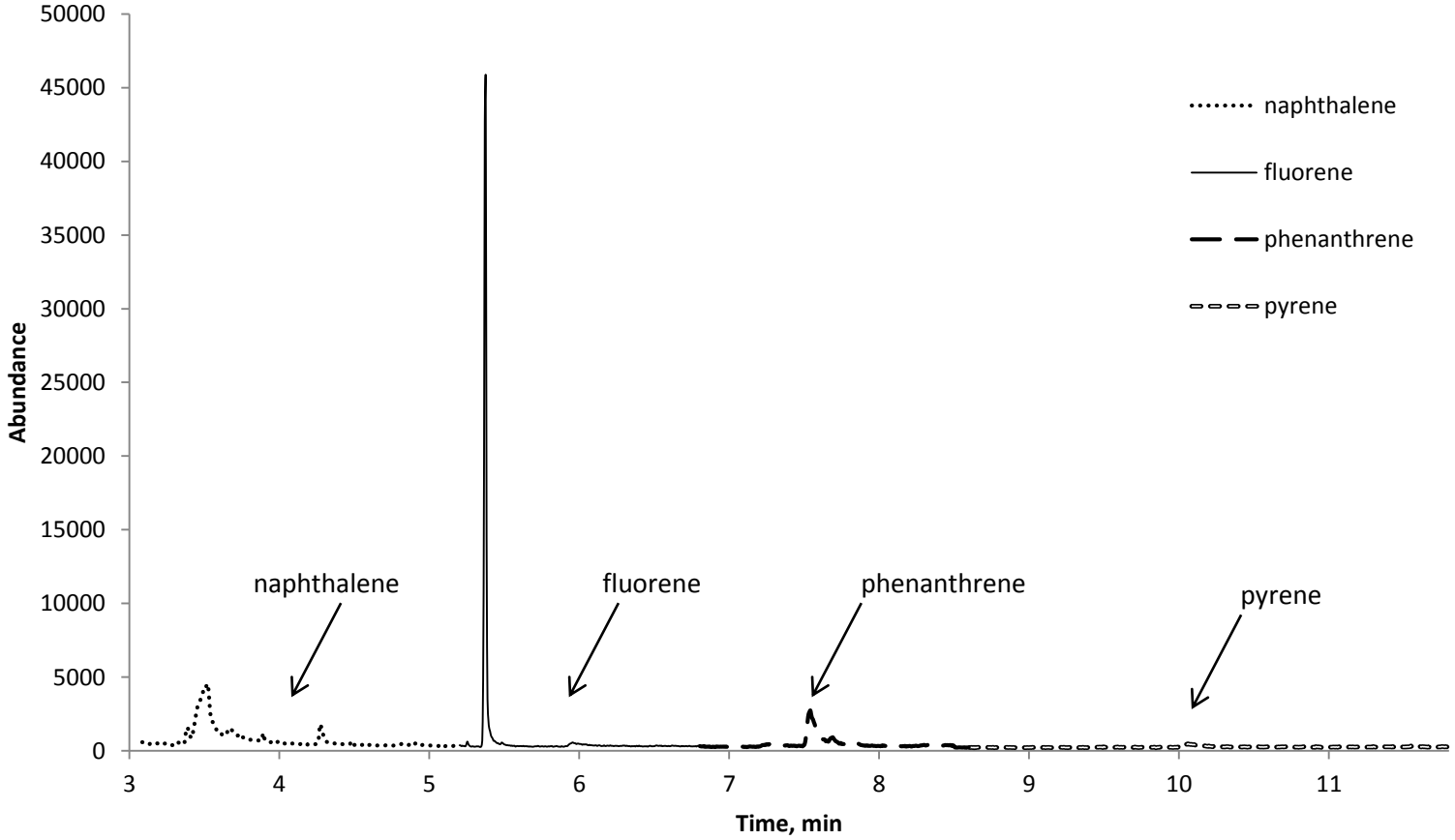

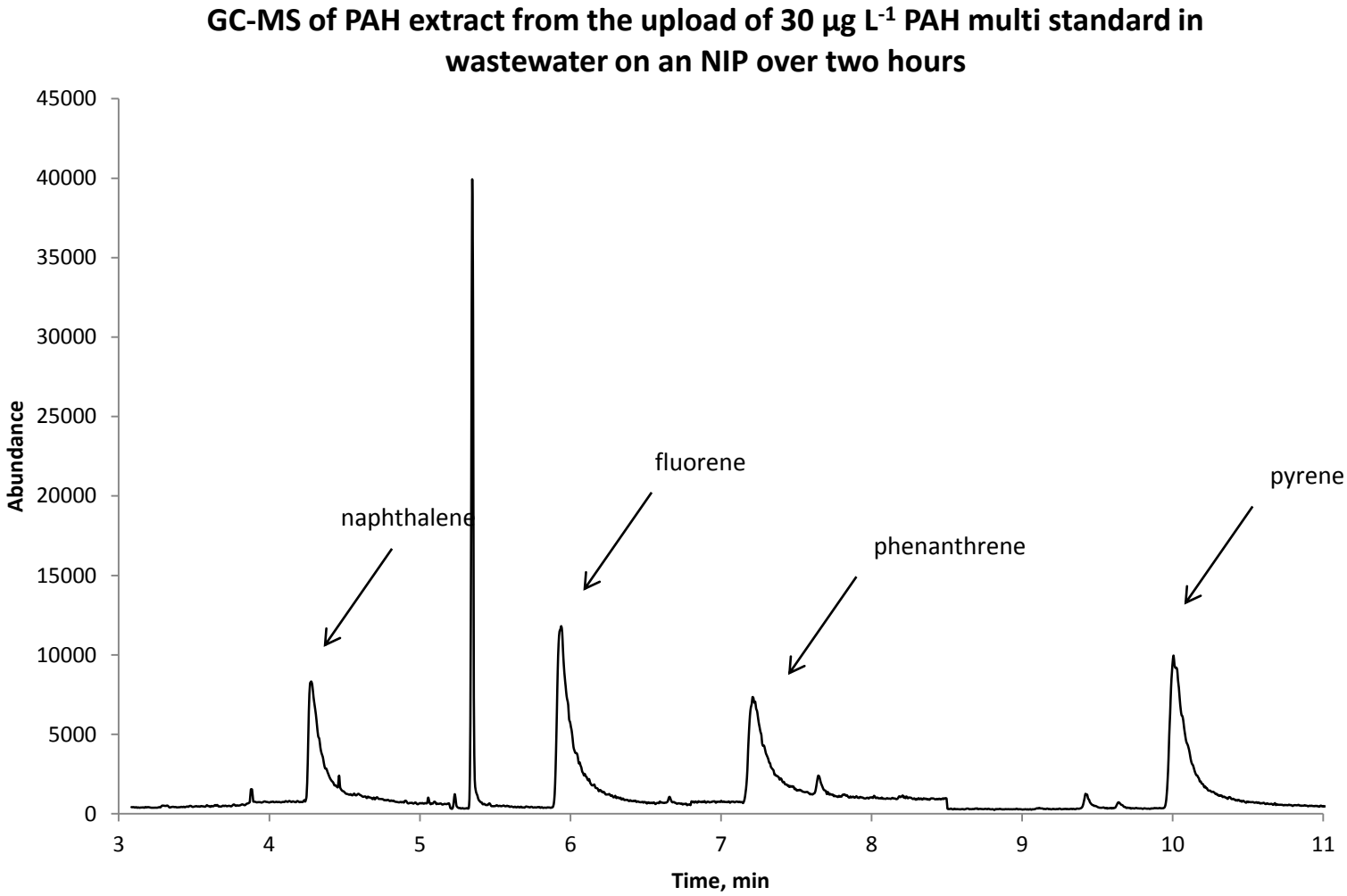
GC-MS of PAH extract from the upload of 30 µg L-1 PAH multi standard in wastewater on an NIP over two hours
Abundance
45000
40000
35000
30000
25000
20000
15000
10000
5000
0
3
4
5
6
7
8
9
10
11
Time, min
naphthalene
fluorene
phenanthrene
pyrene

**GC-MS of PAH extract from the upload of 3.0 µg $L^{-1}$ PAH multi standard in seawater on a MIP over two hours**

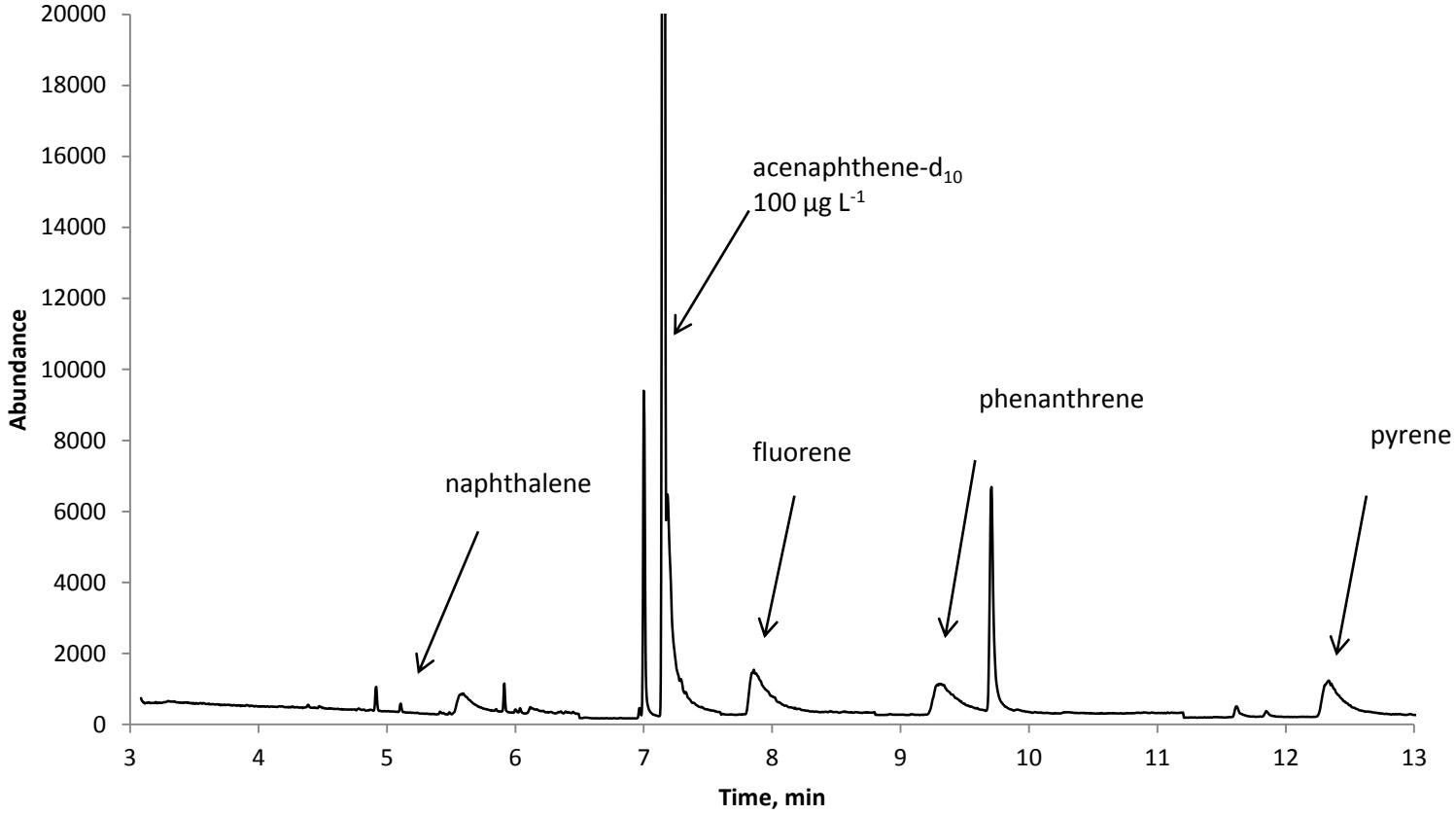

# Fluorescence data

PAH standards:

- Fluorescence analysis of residual concentration for naphthalene at various concentrations from a PAH multistandard
- Fluorescence analysis of residual concentration for fluorene at various concentrations from a PAH multistandard
- Fluorescence analysis of residual concentration for phenanthrene at various concentrations from a PAH multistandard
- Fluorescence analysis of residual concentration for pyrene at various concentrations from a PAH multistandard

Binding assay after upload of 10 ug $L^{-1}$ PAH multistandard in distilled water (done in four replicates)

- Analysis of the residual concentration for 0.5 h upload
- Analysis of the residual concentration for 2 h upload
- Analysis of the residual concentration for 3 h upload
- Analysis of the residual concentration for 5 h upload
- Analysis of the residual concentration for 7 h upload
- Analysis of the residual concentration for 9 h upload

**Fluorescence analysis of residual concentration for naphthalene at various concentrations from a PAH multistandard**

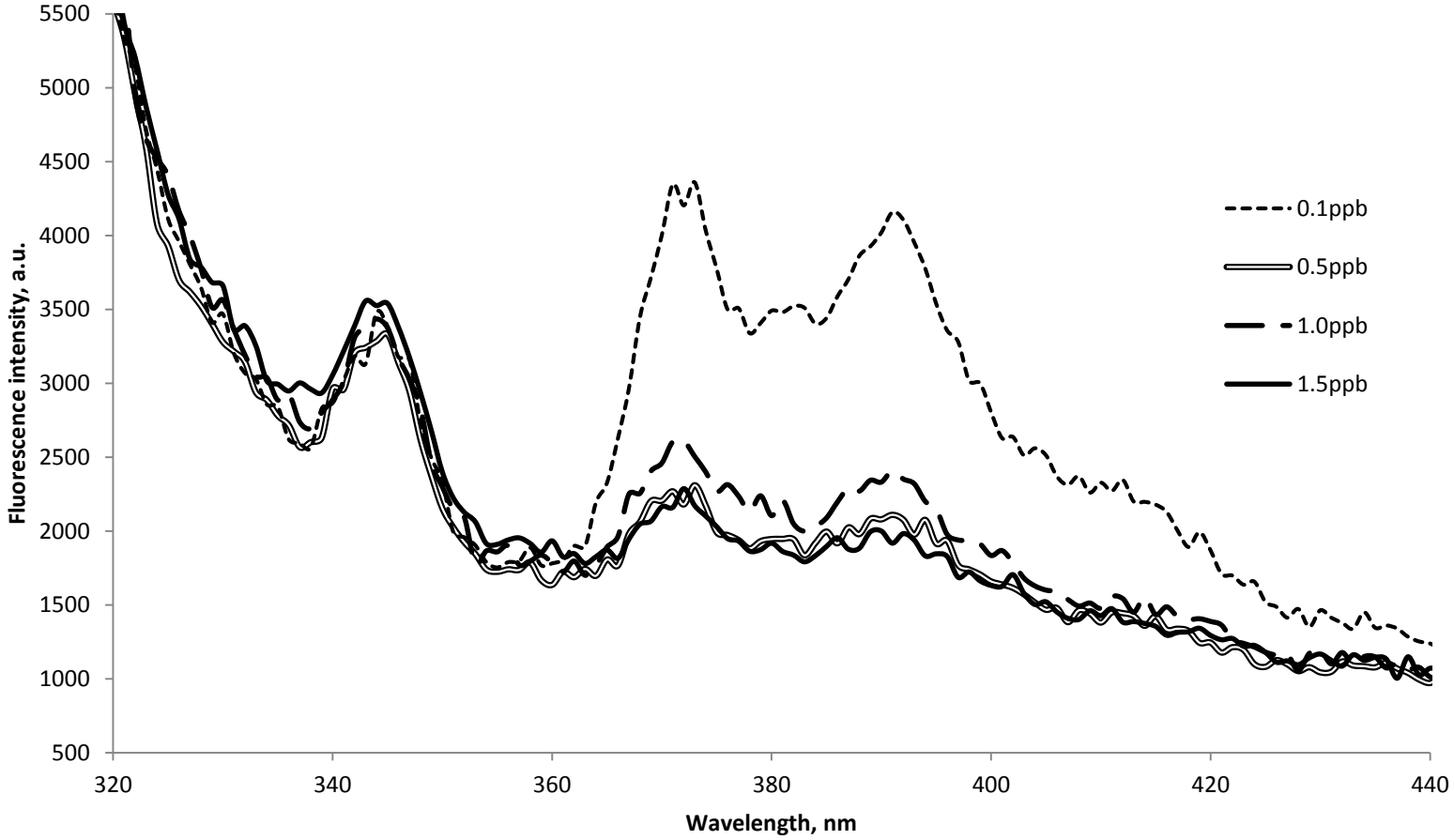

**Fluorescence analysis of residual concentration for fluorene at various concentrations from a PAH multistandard**

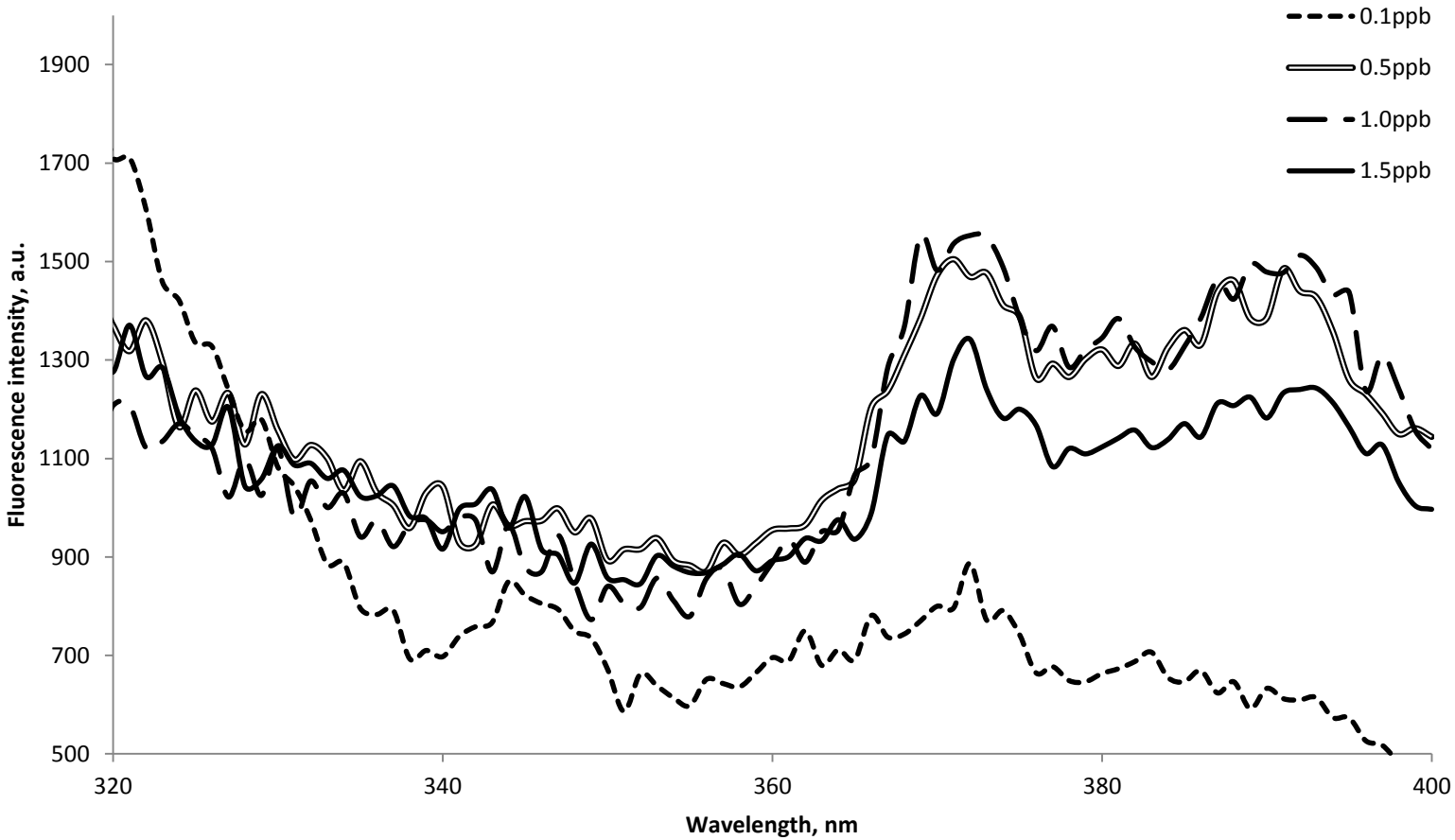

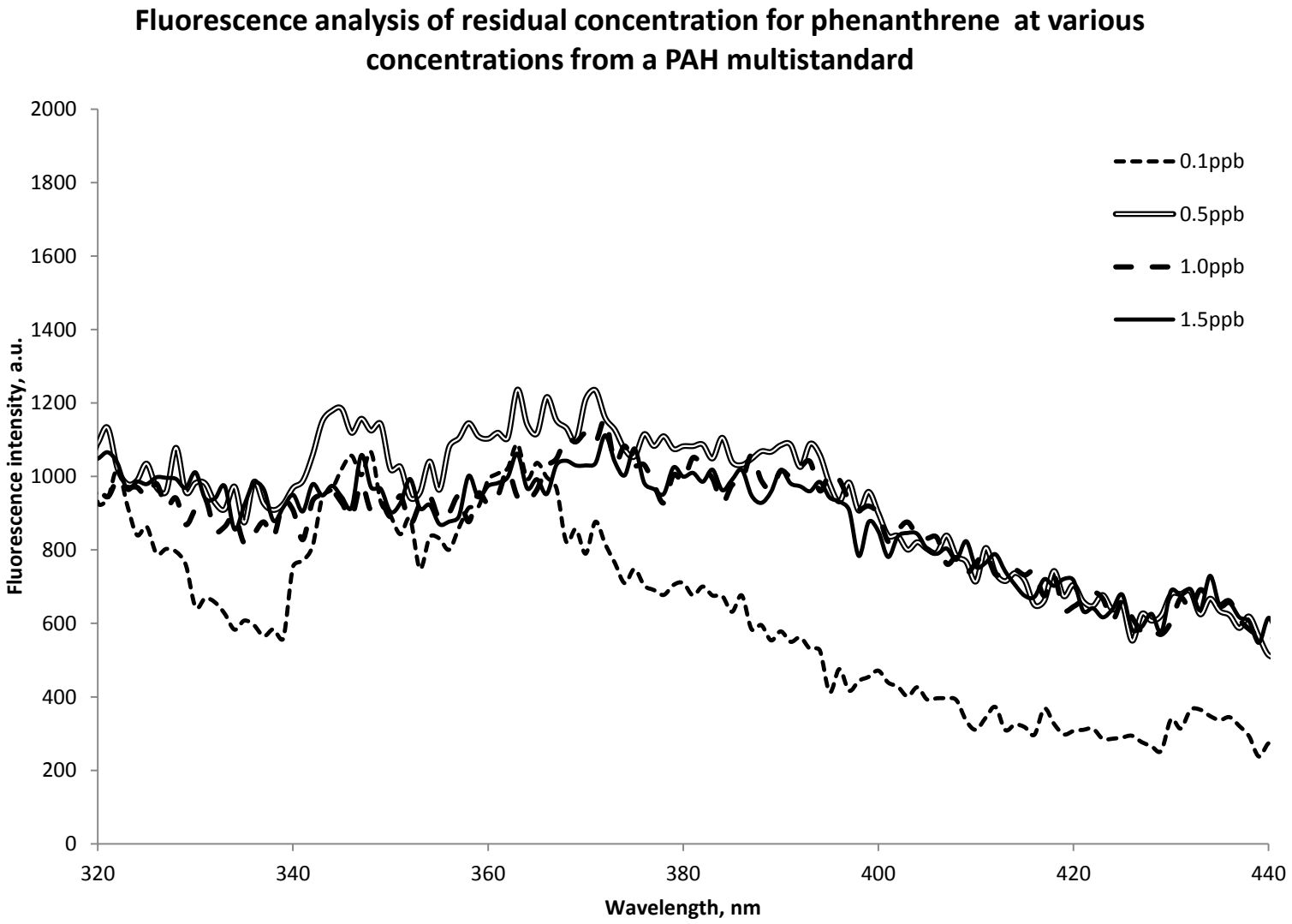
Fluorescence analysis of residual concentration for phenanthrene at various concentrations from a PAH multistandard
Fluorescence intensity, a.u.
Wavelength, nm
0.1ppb
0.5ppb
1.0ppb
1.5ppb
2000
1800
1600
1400
1200
1000
800
600
400
200
0
320
340
360
380
400
420
440

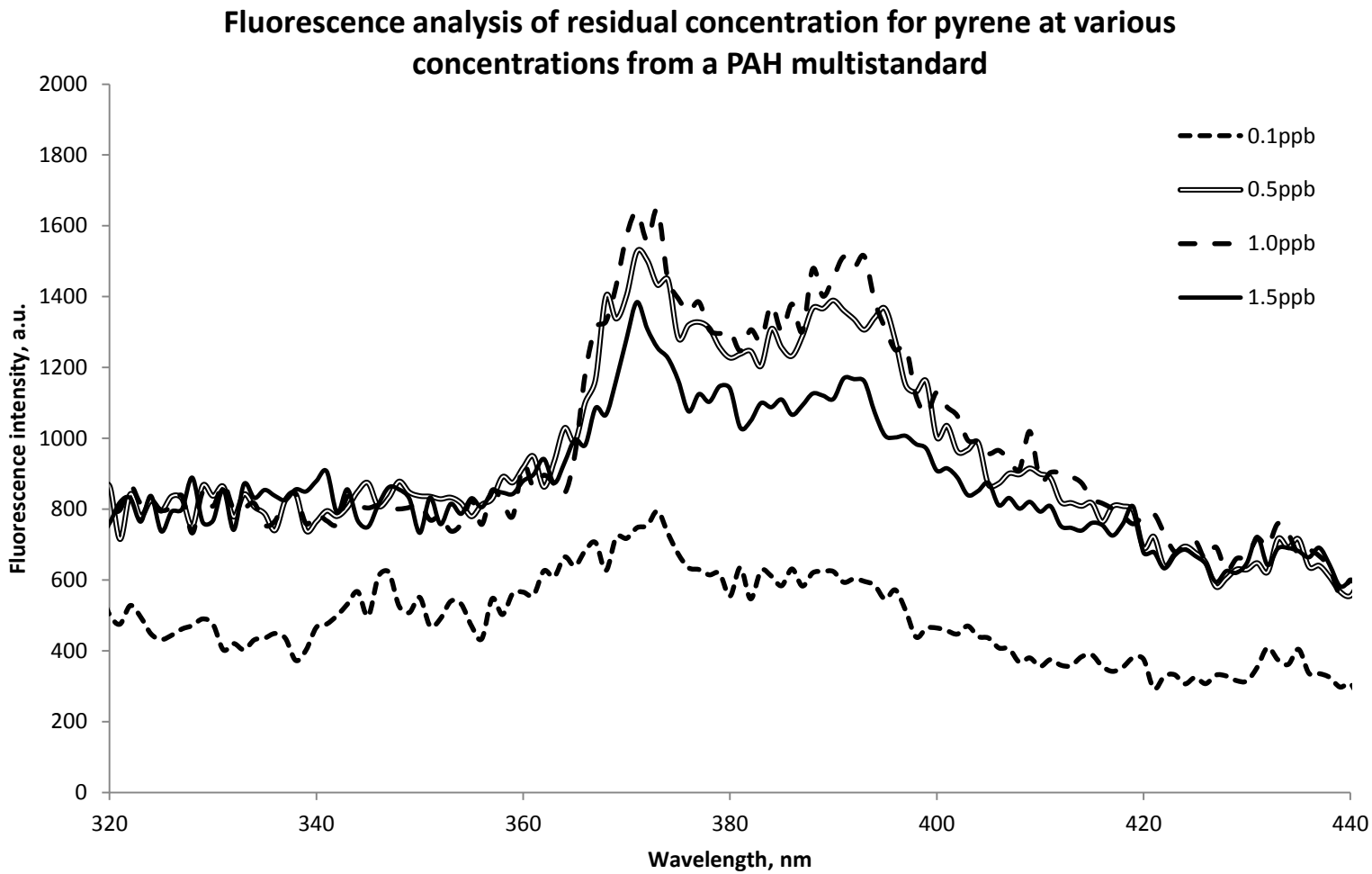
Fluorescence analysis of residual concentration for pyrene at various concentrations from a PAH multistandard
Fluorescence intensity, a.u.
2000
1800
1600
1400
1200
1000
800
600
400
200
0
320
340
360
380
400
420
440
Wavelength, nm
0.1ppb
0.5ppb
1.0ppb
1.5ppb

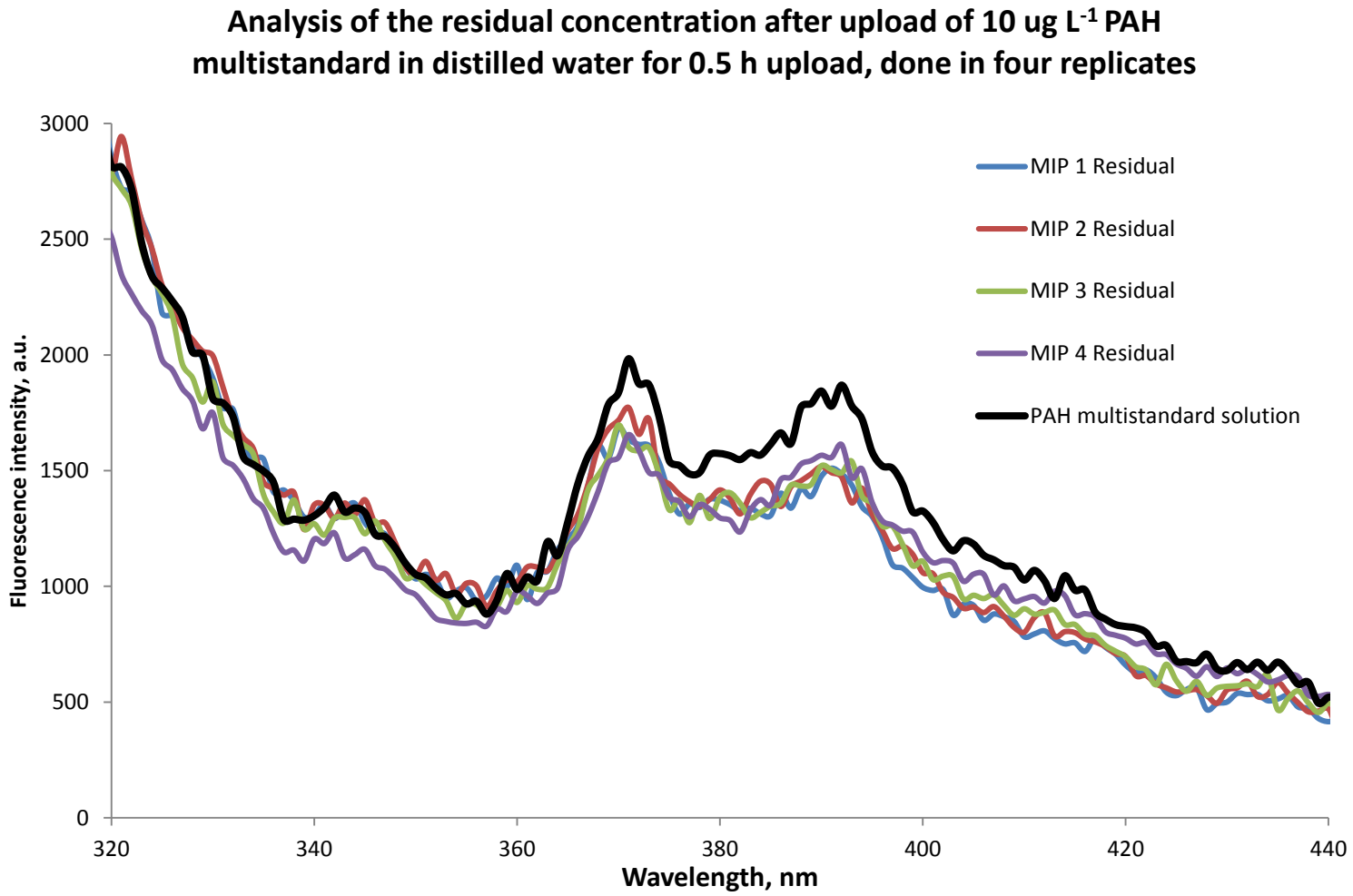
Analysis of the residual concentration after upload of 10 ug L-1 PAH multistandard in distilled water for 0.5 h upload, done in four replicates
Fluorescence intensity, a.u.
3000
2500
2000
1500
1000
500
0
320
340
360
380
400
420
440
Wavelength, nm
MIP 1 Residual
MIP 2 Residual
MIP 3 Residual
MIP 4 Residual
PAH multistandard solution

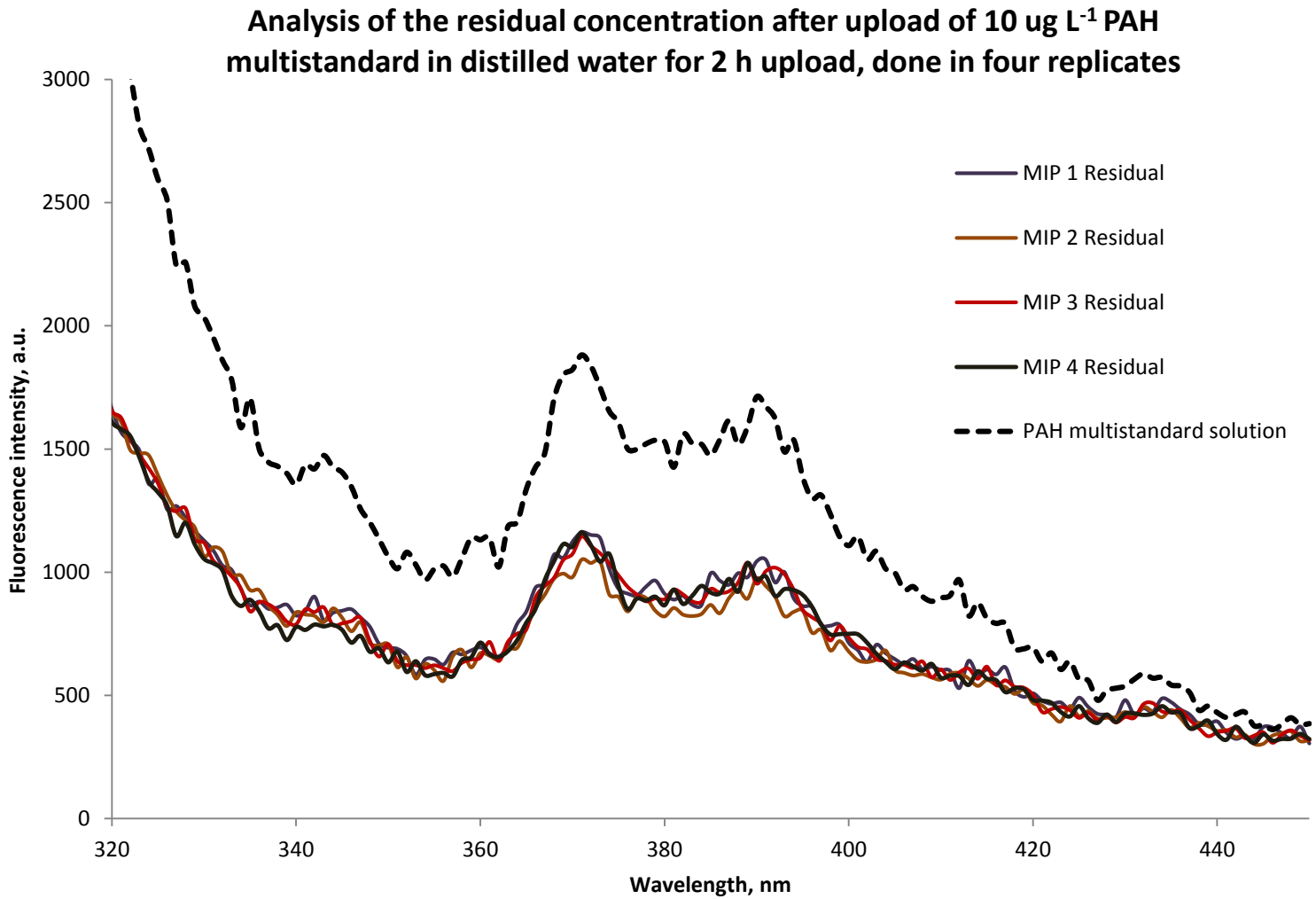
Analysis of the residual concentration after upload of 10 ug L-1 PAH multistandard in distilled water for 2 h upload, done in four replicates
Fluorescence intensity, a.u.
3000
2500
2000
1500
1000
500
0
320
340
360
380
400
420
440
Wavelength, nm
MIP 1 Residual
MIP 2 Residual
MIP 3 Residual
MIP 4 Residual
PAH multistandard solution

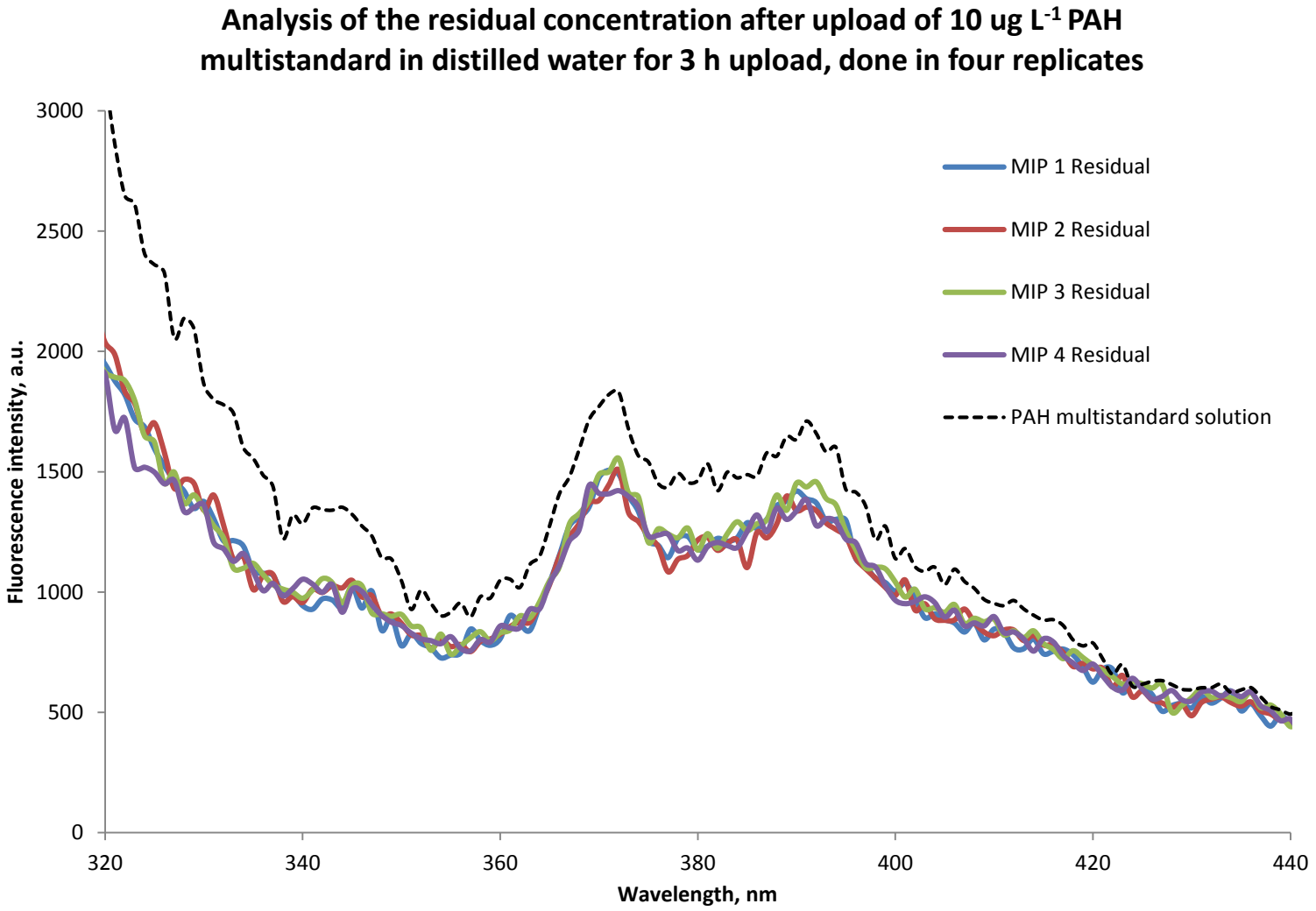
Analysis of the residual concentration after upload of 10 ug L-1 PAH multistandard in distilled water for 3 h upload, done in four replicates
Fluorescence intensity, a.u.
3000
2500
2000
1500
1000
500
0
320
340
360
380
400
420
440
Wavelength, nm
MIP 1 Residual
MIP 2 Residual
MIP 3 Residual
MIP 4 Residual
PAH multistandard solution

**Analysis of the residual concentration after upload of 10 ug $L^{-1}$ PAH multistandard in distilled water for 5 h upload, done in four replicates**

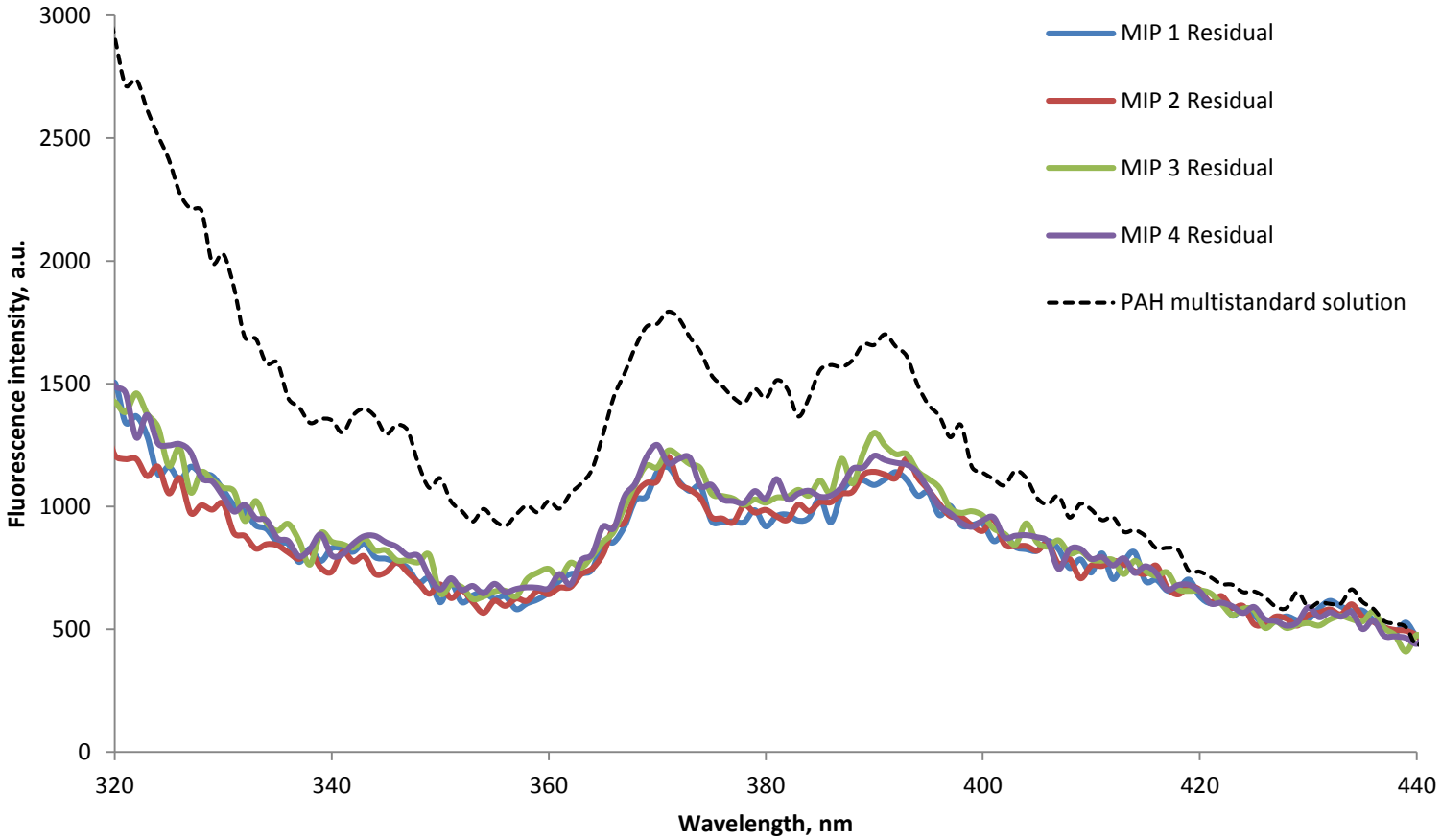

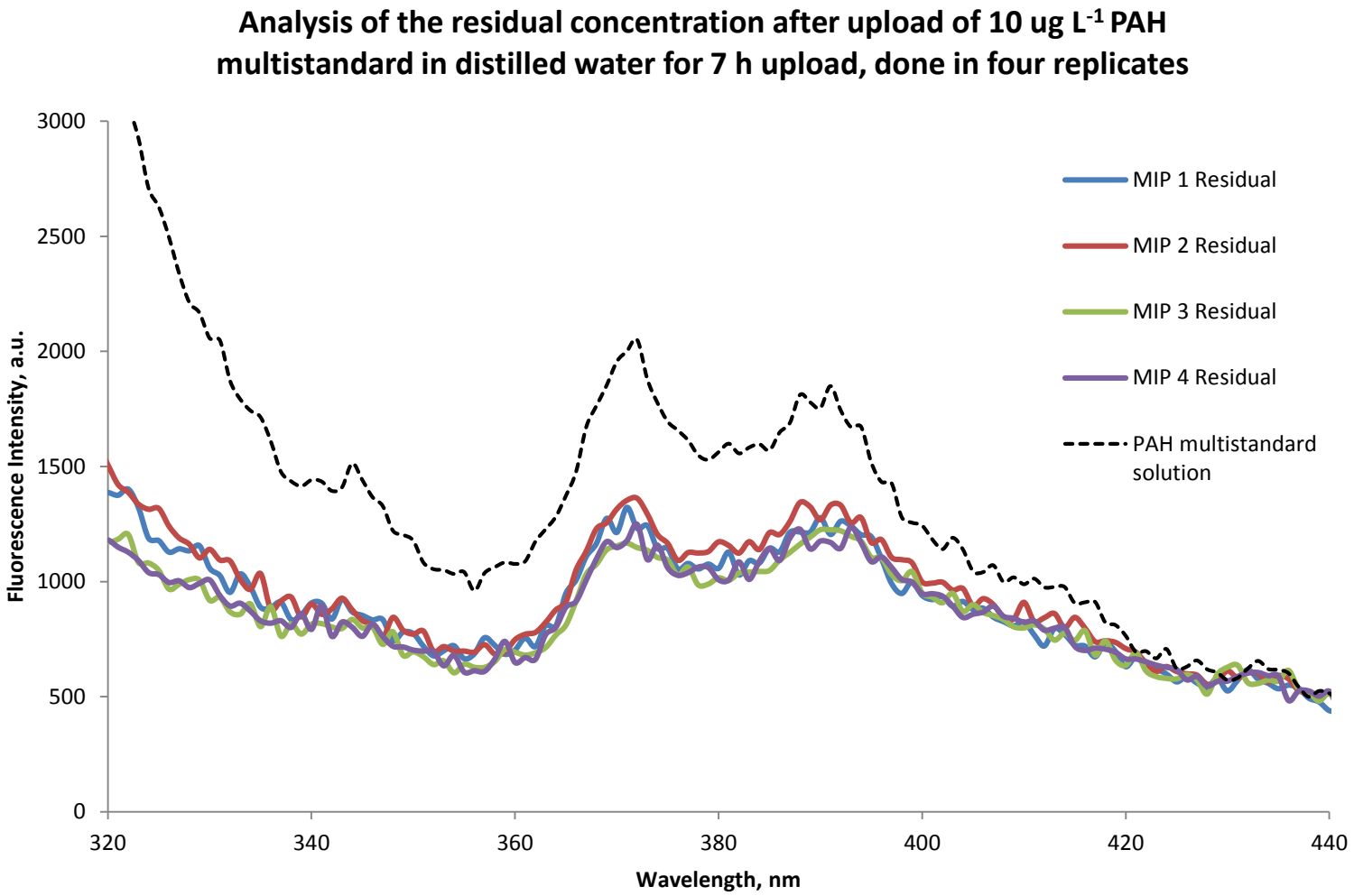
Analysis of the residual concentration after upload of 10 ug L-1 PAH multistandard in distilled water for 7 h upload, done in four replicates
Fluorescence Intensity, a.u.
3000
2500
2000
1500
1000
500
0
320
340
360
380
400
420
440
Wavelength, nm
MIP 1 Residual
MIP 2 Residual
MIP 3 Residual
MIP 4 Residual
PAH multistandard solution

**Analysis of the residual concentration after upload of 10 ug $L^{-1}$ PAH multistandard in distilled water for 9 h upload, done in four replicates**

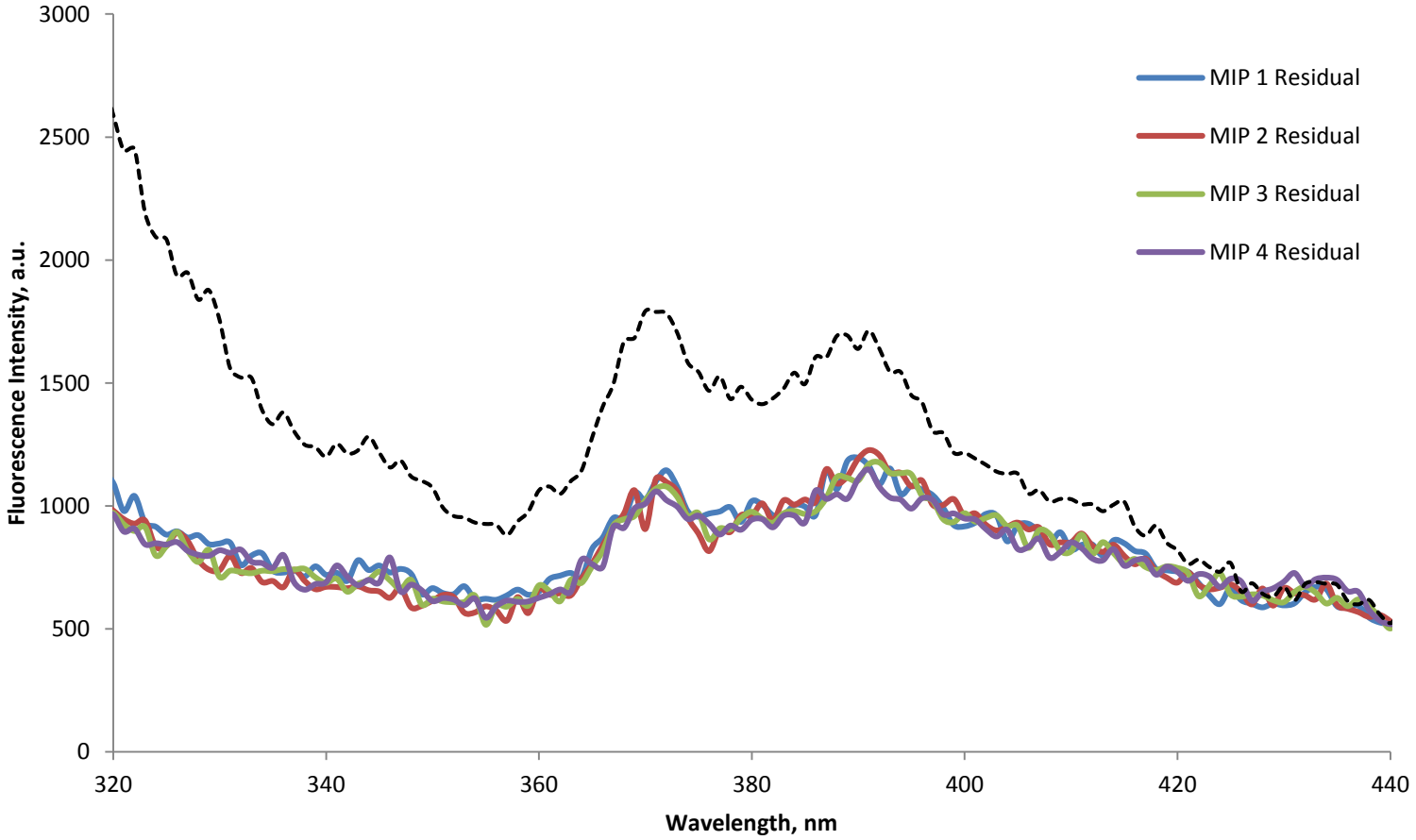

## Appendix 2

## Toluene toluene MIPs

- GC-MS of PAH extract from the upload of 10.0 µg $L^{-1}$ PAH multi standard in distilled water on a MIP over two hours
- GC-MS of PAH extract from the upload of 10.0 µg $L^{-1}$ PAH multi standard in waste water on an NIP over two hours
- GC-MS of PAH extract from the upload of 10.0 µg $L^{-1}$ PAH multi standard in waste water on a MIP over two hours

**GC-MS of PAH extract from the upload of 10.0 µg $L^{-1}$ PAH multi standard in distilled water on a MIP over two hours**

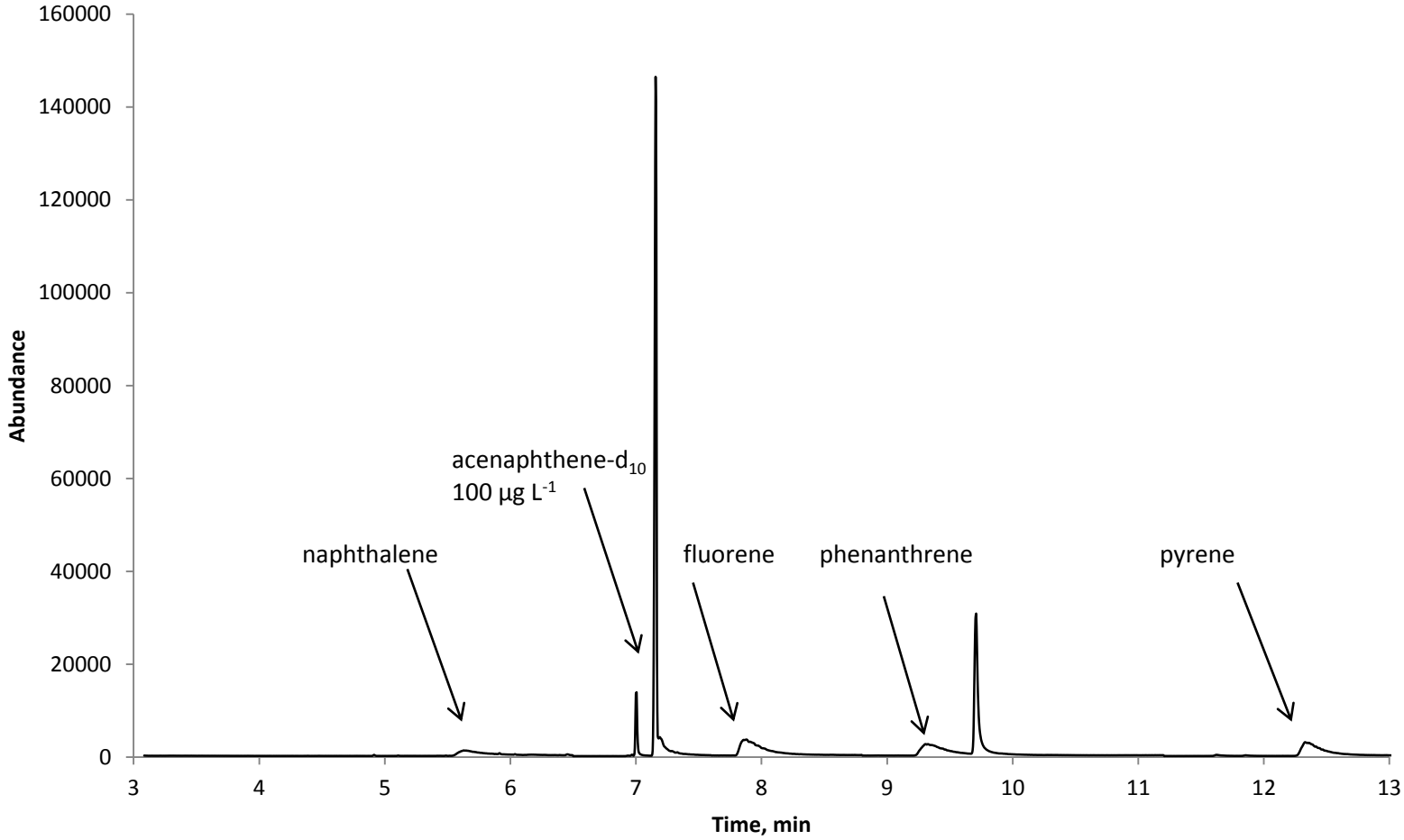

**GC-MS of PAH extract from the upload of 10.0 µg $L^{-1}$ PAH multi standard in waste water on an NIP over two hours**

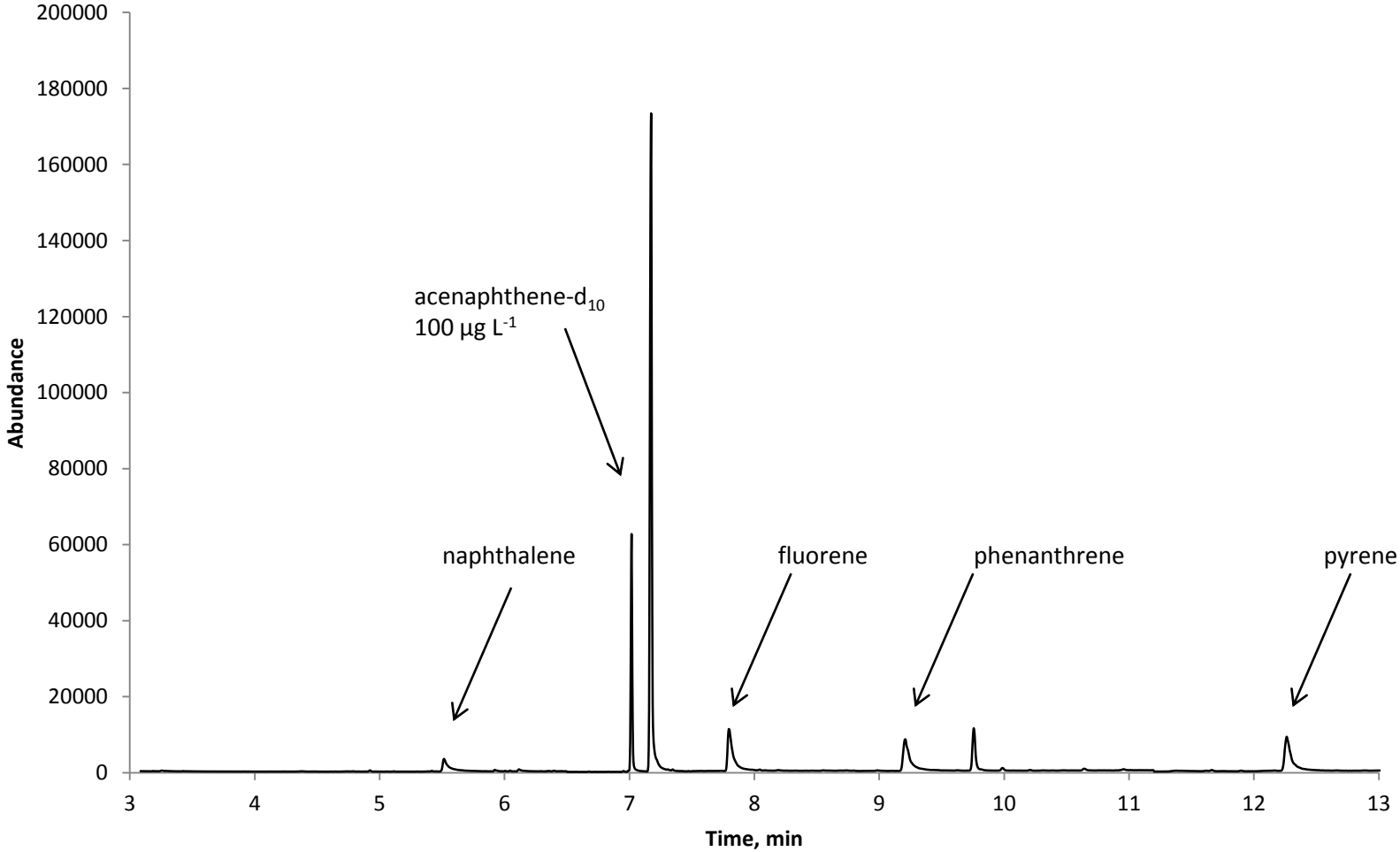

**GC-MS of PAH extract from the upload of 10.0 µg $L^{-1}$ PAH multi standard in waste water on a MIP over two hours**

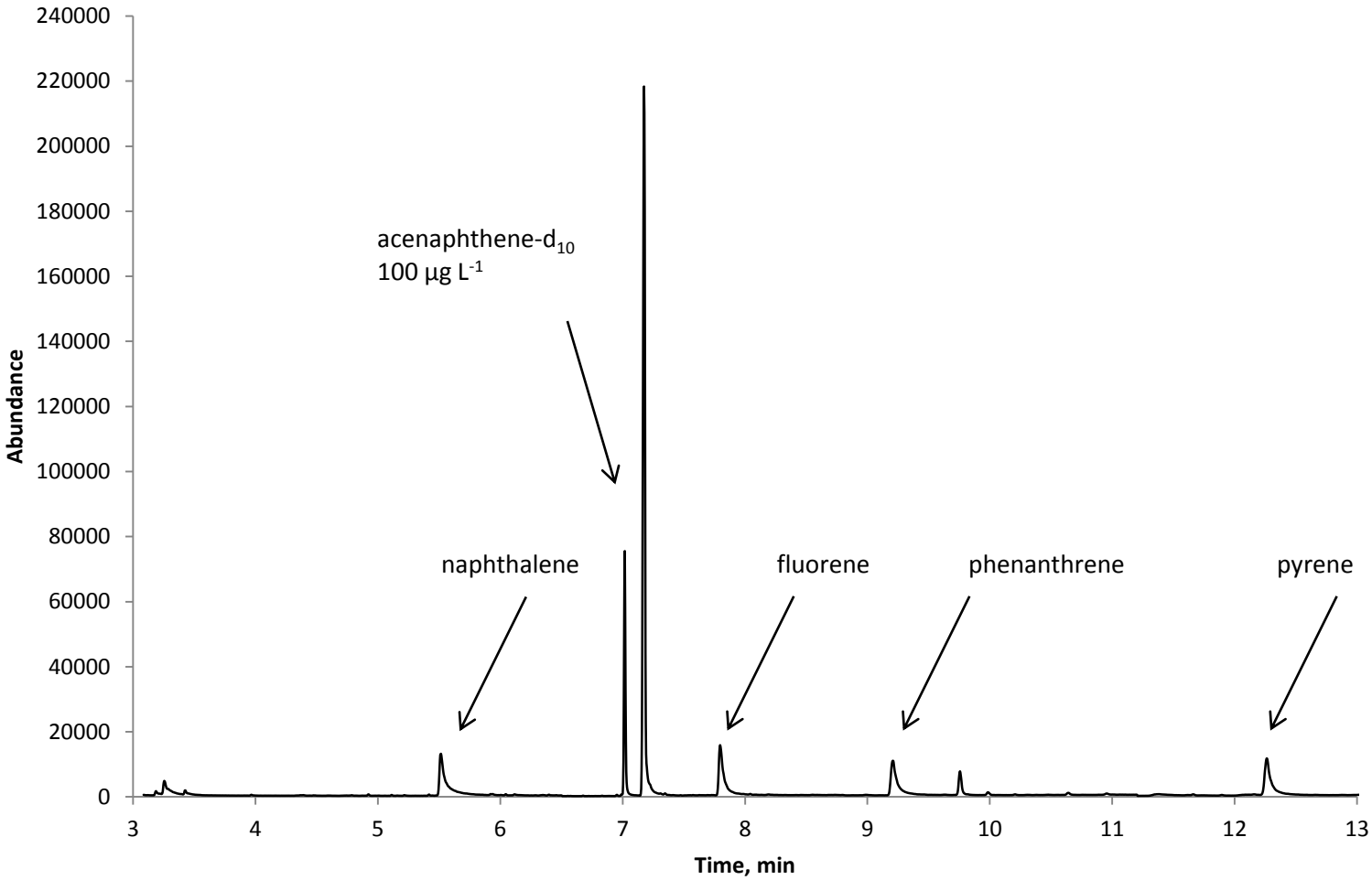

Appendix 3

**Phenanthrene-$d_{10}$ MIPs**

GC-MS of PAH extract from the upload of 3.0 µg $L^{-1}$ PAH multi standard in seawater on a MIP over two hours

**GC-MS of PAH extract from the upload of 3.0 µg $L^{-1}$ PAH multi standard in seawater on a MIP over two hours**